Numerical Ground-Water Flow Modelling Of the

Awassa Catchment

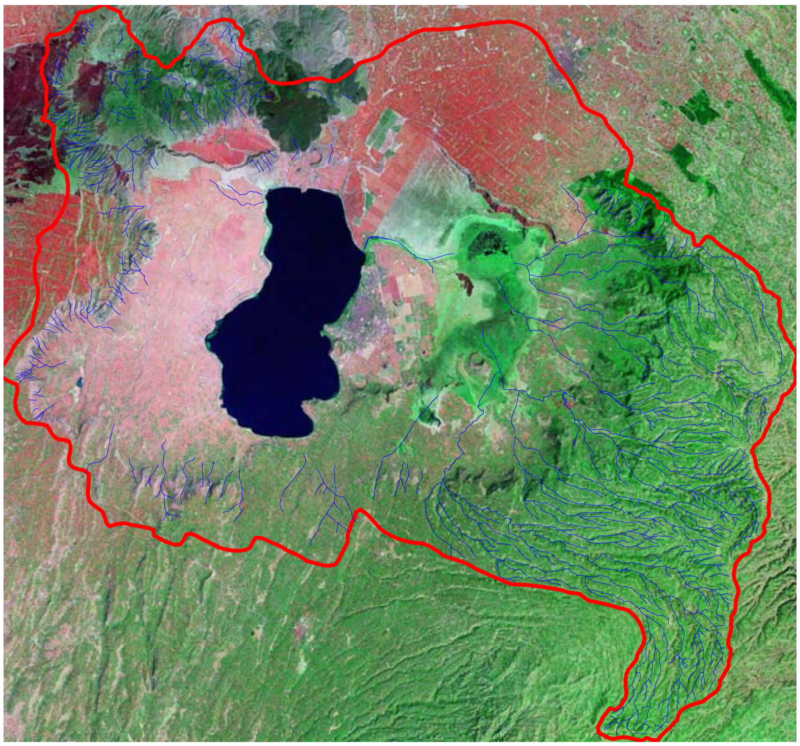

By

Nardos Tilahun Abebe

A thesis submitted to the School of Graduate Studies of Addis Ababa University in partial fulfillment of the requirements for the Degree of *Master of Science* in Hydrogeology

June 2006.

Acknowledgements

I am deeply grateful to my advisor Dr. Tenalem Ayenew for his supervision, support and guidance he has provided me throughout my research and most importantly for his recommendation for modeling training, which was a base for this study. His critical comments and helpful guidance gives me an opportunity to explore further. Further more, I sincerely appreciate his cooperation in sharing his knowledge and in giving reference materials for the best outcome of the research. I would like to extend my acknowledgment to the Department of Earth Sciences, AAU with its staff members for their help during my two years stay in the university.

I gratefully acknowledge all organizations and individuals who directly or indirectly supported me in my study. First I would like to thank Wondwosen Mekonnen, for all his help and reference material for supporting my study. I would also like to thank Zenaw Tessema, Geological Survey of Ethiopia, for all the data he has given me. I am very grateful to Japan International Cooperation Agency (JICA) and Ministry of Water Resources for giving me the opportunity to participate in Groundwater Modeling training. I greatly acknowledge Water Works Design and Supervision Enterprise, Ministry of Water Resources, National Meteorological Service Agency and Southern Nation and Nationalities People Water Resources for allowing me to use their data.

My earnest thanks go to my beloved family. My father Tilahun Abebe, I would like to thank him for all the support and inspiration he gave me. My mother Fetlework Eshete, I would like to thank her for being my mother and for being there whenever I needed her, you are everything to me and the reason for everything I am. I would like to thank my two sisters Hiwot Tilahun and Meron Tilahun, my big brother Samson Tilahun who are always supportive and encouragement for my work. I would also like to be grateful for the remaining part of my family for their support and endless love.

Last but not least, I would like to thank my colleagues and friends in and outside the University and those who helped me in my research and forgotten to be mentioned.

Table of Contents

List of Tables

.

List of Figures

List of Appendices

Abstract

Groundwater is of major importance to civilization, because it is the largest reserve of drinkable water in regions where humans can live, so it is very important to calculate the quantity and quality of this resource for better protection and management. Groundwater modeling is a result of careful understanding of hydrology, hydrogeology and dynamics of groundwater flow in and around the study area.

The modeled aquifer is important water resource in the study area and is used extensively for irrigation, municipal, and domestic water supplies. This thesis describes a conceptual model of groundwater flow in the aquifer and documents the development and calibration of a numerical model to simulate groundwater flow. Data for a two year period (from 2004 to 2006) and other source without specified time were analyzed for the conceptual model. Regional steady state groundwater model was calibrated to average conditions from 2004 to 2006. A three-dimensional groundwater flow model, with one unconfined layer, was used to simulate groundwater flow in the Lake Awassa Basin. The study area was divided into uniform grid size of 200m by 200m, with 230 rows and 250 columns.

Arial recharge to the Lake Awassa basin aquifer occurs from precipitation and initial recharge rates were given in five different zones ranging from 1.195×10^{-4} m^2/day to 2.787×10^{-4} m^2/day. Discharge from the aquifer occurs through discharge to perennial streams, well withdrawals and springs, and groundwater outflow to the next Ziway-Shalla Basin. Discharge rates in million cubic meters per year (MCM/year) for the steady state simulation were 111 for base flow including Tikur Wuha River and 3.03 for outflow through wells and springs. Outflow to the neighboring catchment is simulated using general-head boundary. Estimated horizontal hydraulic conductivity used for the numerical model ranged from 0.05 to 100 m/d, which were adjusted during model calibration.

Model calibration was accomplished by varying parameters within plausible ranges to produce the best fit between simulated and observed hydraulic heads. The root mean square error for simulated hydraulic heads for all wells was 4.42 meter. Simulated hydraulic heads were within ±10 meter of observed values for all observation wells.

A sensitivity analysis was used to examine the response of the calibrated steady state model to changes in model parameters including horizontal hydraulic conductivity, recharge, and pumpage. The model was most sensitive to recharge and relatively less sensitive to horizontal hydraulic conductivity. Three different scenarios were simulated to see the response of aquifer. Increased withdrawals decrease the groundwater outflow through river leakage and general-head boundary. Complete disappearance of Lake Shallo result in an increase in water level particularly in wells found around this lake, while decreased recharge result in more inflow from constant-head boundaries as well as lower streamflow and groundwater discharge through the general-head boundary.

CHAPTER ONE

Introduction

1.1 Background

Lake Awassa Catchment is part of the Main Ethiopian Rift containing Lake Awassa, which is one of the better documented lakes in the Rift Valley. Lake Awassa is like an engine for Awassa city and the region with respect to its fishery production, recreation, agricultural production and residence for different species, fauna and flora. The region has also high geothermal potential areas where six were productive out of eight boreholes which were used for electric production. Awassa town, which is the capital city of the Southern Regional State, is found adjacent to the lake which put it at risk of flooding during wet seasons due to the rise of the lake level.

Lake Awassa, including Lake Ziway, Langano and Abiata, are of tectonic origin aligning themselves in the NNE – SSW direction which is the main tectonic trend of the rift. An enormous single lake, during late Pleistocene wet climate period, seems to occupy the Lake District, from Lake Ziway to Lake Awassa, which then severely dry. Outcrop of lacustrine diatomite deposits in Bulbula can be one explanation.

Regardless of its high documentation, modeling studies related to the lake and its catchment is quite recent and little experience has been accrued in this context for the area. Groundwater modeling is a result of careful understanding of hydrology, hydrogeology and dynamics of groundwater flow in and around the study area. The final model can be used as a tool to help understand the flow system, to confirm that previous estimates of aquifer properties are reasonable, to estimate aquifer properties in areas without data and also to see the response of the system for different scenarios which help us to better understand the system. These days it is becoming the most important means of groundwater exploitation, protection and remediation.

1.2 Problem Identification

Groundwater studies in Awassa catchment is more difficult compared to surface water studies because of its complex geological conditions. The area consists mainly of volcanic strata and lake sediments derived from this volcanic material. The catchment is also affected by at least three types of faults, based on their strike direction we can see NNE-SSW, N-S running, NW-SE and E-W running faults/fracture zones (Wondwosen Mekonnen, 2005).

The hydrogeological condition of the catchment is controlled mainly by these two systems, especially by the fault systems. A regional groundwater model may give insight to the hydrogeological conditions of the catchment as well as provide a better understanding of other hydrological processes, such as recharge, lake and aquifer water balance, groundwater-surface water interactions, etc.

1.3 Objectives

- The general objective of this study is to understand the regional groundwater flow systems and develop groundwater management schemes through simulation of regional ground water flow in the aquifer as single layer system under water table, steady state conditions.

And the Specific Objectives include:

- Organization of adequate database based on the available information from previous works done by different government and private organizations and data collected during field work.

- Construction of a GIS database, based on MODFLOW input file type, for the construction of the numerical model.
- To build a regional hydrogeological numerical model.
- Steady state model calibration using observed water level points and map of the study area.
- Sensitivity analysis of the aquifer system based on different values of aquifer parameters.
- To evaluate the behavior of the groundwater system under possible future utilization scenarios.
- To make groundwater flow calculation using the calibrated model in order to determine the amount of flow into or out of the system.

1.4 Methodology

- Collect and organize appropriate secondary data from all possible sources and asses previous studies conducted on the area.
- Collect primary data from the field such as groundwater level measurement, reading coordinates of water points, measuring river length, width, head and estimate river bed thickness to divide a river in different zones for the river package, and ground verification of gathered data on geology, structure, hydrogeology and hydrology.
- Select the appropriate computer code, MODFLOW.
- Thoroughly analyze the conceptual model to develop the numerical model for the study area, which is done by designing the grid, selecting time steps, setting boundary and initial conditions, and inputting reasonable aquifer parameters.
- Calibration of the model, using the field measured heads, by adjusting parameters based on trial and error method.
- Presentation of modeling design and results.
- Interpretation of results and conclusions.

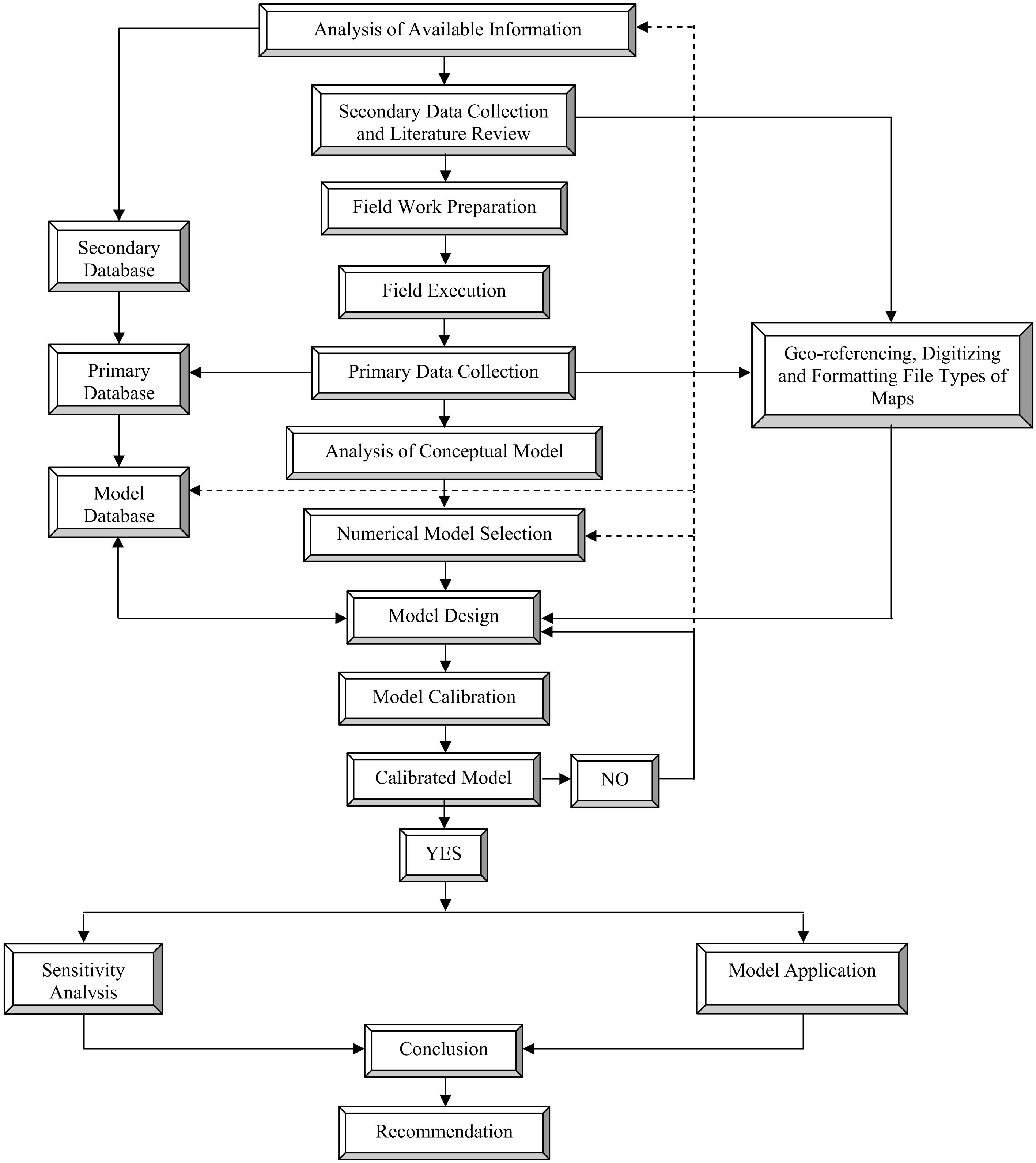

Fig.1.1 Flow chart showing the general modeling processes.

CHAPTER TWO

General Overview of the Area

2.1 Location

The study area is located with in the geographical co-ordinates of $6^0 45^1$ to $7^0 15^1$ north and $38^0 15^1$ to $38^0 45^1$ east latitude and longitude (UTM: 419485-470099E and 752392-799477N, Zone 37, Northern Hemisphere) respectively. It is found 275km south of Addis Ababa, it has an elevation generally ranging from 1680 to 2997 m.a.s.l Lake Awassa occupies the lowest elevation in the catchment, which is located in the main Ethiopian Rift (MER) called Lake District.

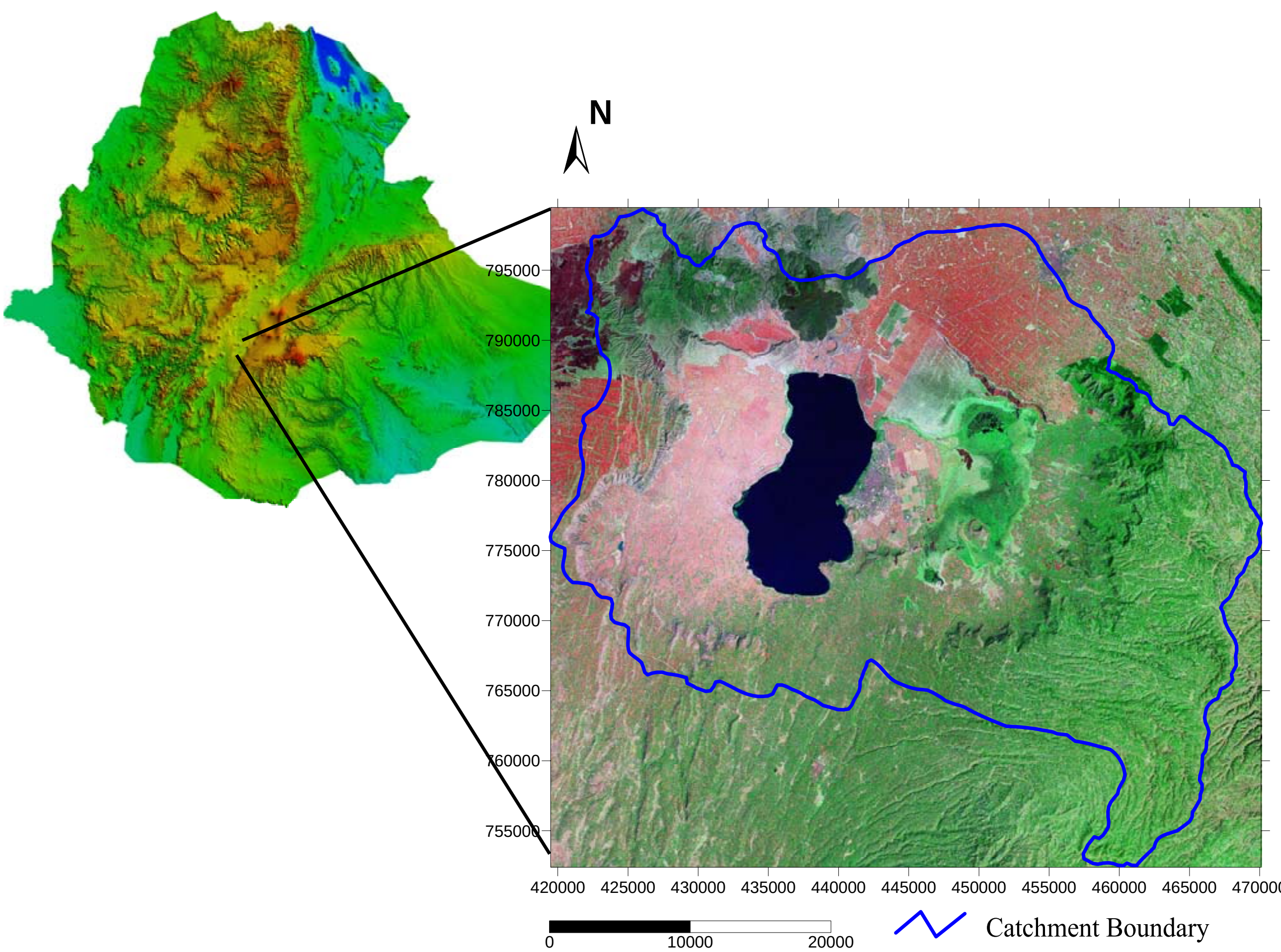

Fig. 2.1 Location Map with TM Image of the Study Area

The study area can be accessed through an asphalt road connecting Addis Ababa to Moyala, which is a border town on the way to Kenya. The catchment can be accessed in different direction using quite a lot of weathered roads. The total area of the catchment is about 1376km^2, where 100km^2 is taken by the lake and the rest 1284 km^2 of the catchment is occupied by surface land.

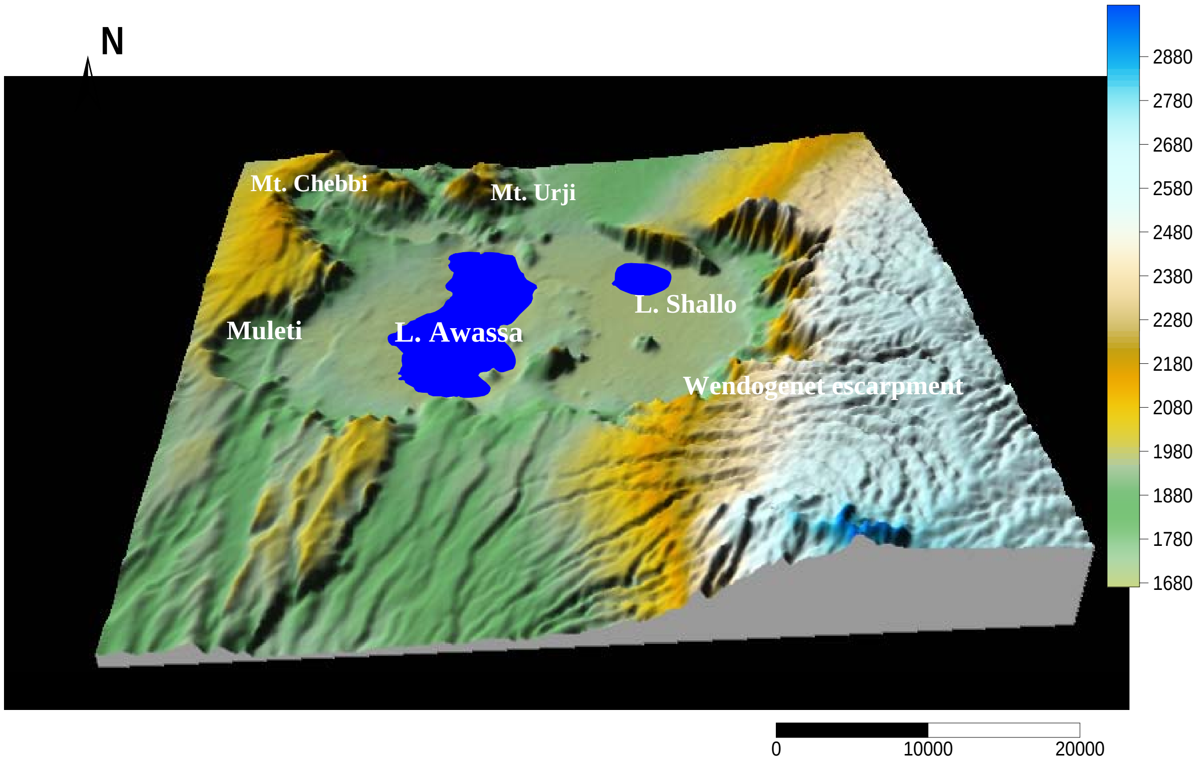

Fig. 2.2 Digital Elevation Model of the Study Area

2.2 Physiography and Drainage

Lake Awassa, which is positioned within a nested caldera complex, is the smallest in size and highest in elevation of the major MER lakes, which makes it possible for groundwater to flow from Lake Awassa to other lakes. Including Lake Awassa the catchment area consists of escarpments, ridges and plateau, undulating to rolling and dissected plains, depressions and swamps, and recent cracks. Eastern boarder of the catchment overlaps with the eastern escarpment of the Main Ethiopian Rift, where its average through is about 500m and maximum elevation goes up to 2997 m.a.s.l., which is the maximum in the catchment.

As long as surface water is concerned, there is none going out of the lake which makes it a Closed-catchment Lake. Lake Awassa is fed by Tikur Wuha River, which is the main perennial river in the catchment, joins the lake passing through Cheleleka swamp found on the east side of the lake. High discharge springs at the upstream feeds Cheleleka swamp in addition to the runoff from the eastern escarpments of the rift.

Out of the perennial streams originating from the eastern highland, Wodesa stream drains swampy area of Cheleleka with higher discharge to join Tikur Wuha River. Tikur Wuha River having 625 km^2 catchment area and 45% of the lake catchment area is the only perennial and gauged river flowing into Lake Awassa. The western part of the catchment has no significant drainage system due to the flat laying thick and fertile agricultural land infiltrating the dispersed overland flow from the highlands.

Lake Awassa Catchment is a result of volcano-tectonic depression (caldera) as a result its drainage pattern is radial, where rivers flow in all directions away from a raised feature, which is volcano. Surface and sub-surface fracture intensities, rock and soil formation, topography and climate are the governing factors for the drainage density and pattern.

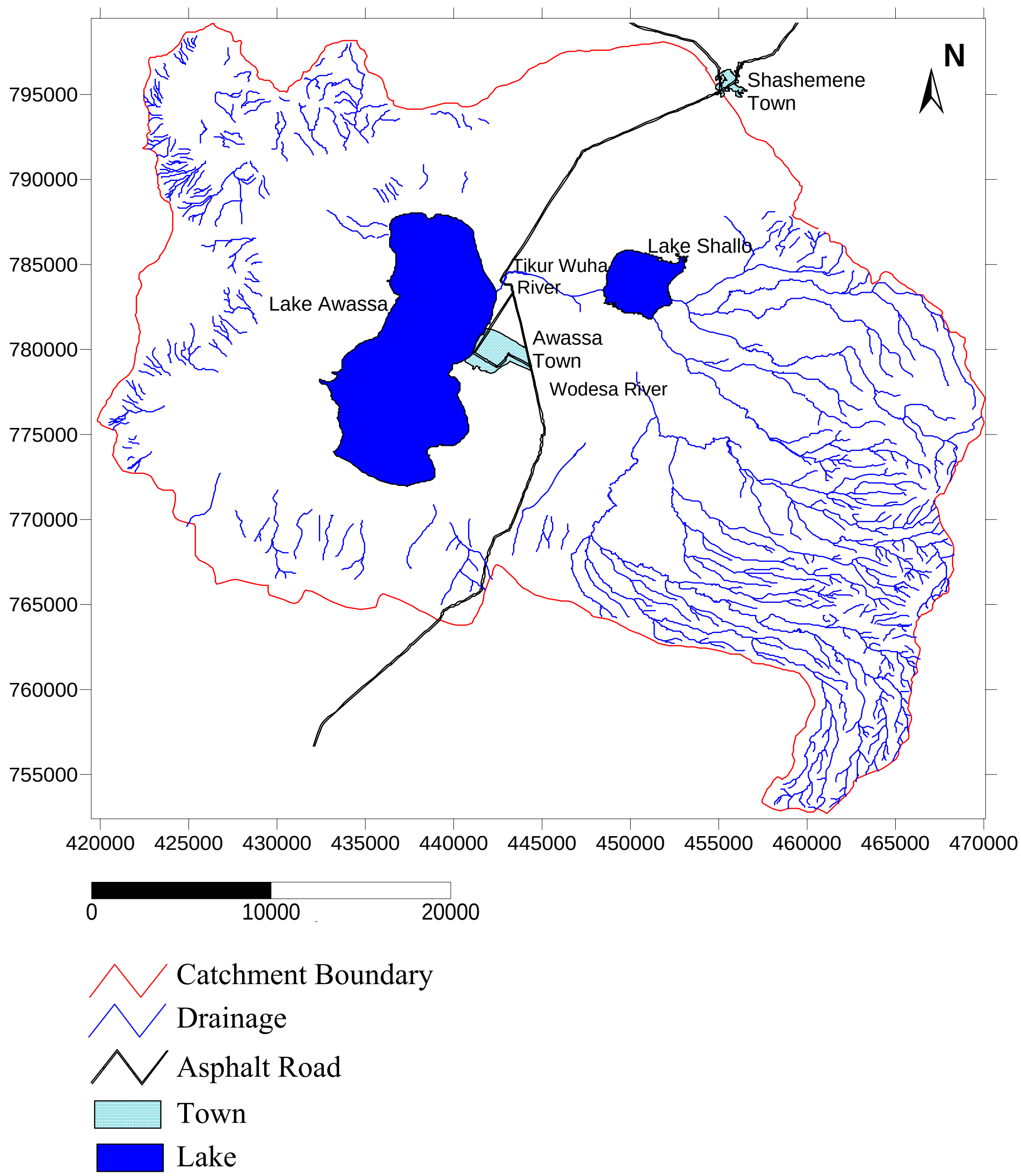

Fig. 2.3 Drainage map of the study Area

2.3 Soil and Land use

Water Works Design and Supervision Enterprise have classified the soil based on the physical and chemical characteristics. Depth, color, structural development, texture and evidence of profile development such as presence of diagnostic horizons, reaction to 10%HCl and ph value are some of the classification criteria based on which soil map has been produced.

Cambisols, Andosols, Vertic cambisols, Vertic luviosols, Regosols, Gleysols, Alisols, and Leptosols are some of the soil types described by W.W.D.S.E with respect to their position in a different relief intensity and slope. Generally based on their dominant characteristics these soils of the study area are classified in to four groups as clay loam, fine sand, fine sandy loam and silty loam (Wondwosen Mekonnen, 2005).

The land use of Lake Awassa catchment has been changed progressively due to extreme deforestation as a result of increase in population which results in replacement of vegetation cover by cultivation land. Agriculture is the main land use practice in the catchment and occupies most of the floor of the catchment. Open bushy woodland with cultivated land found on the floor and southern part of the area; Cultivated land with exposed bare rock and soil found on southwest corner of the area; Open grassland with bare soil covering the eastern escarpment western caldera rims; Open grassland with open bushy woodland on the volcanic hills are Landuse/Landcover condition of the area (as of 1998 surveyed by WWDSE)

As the deforestation of the natural vegetation cover continues soil loss due to erosion will result and it is aggravated where the slope is higher especially on the escarpments. This erosion could be one of the reasons for the rise of Lake Awassa water level.

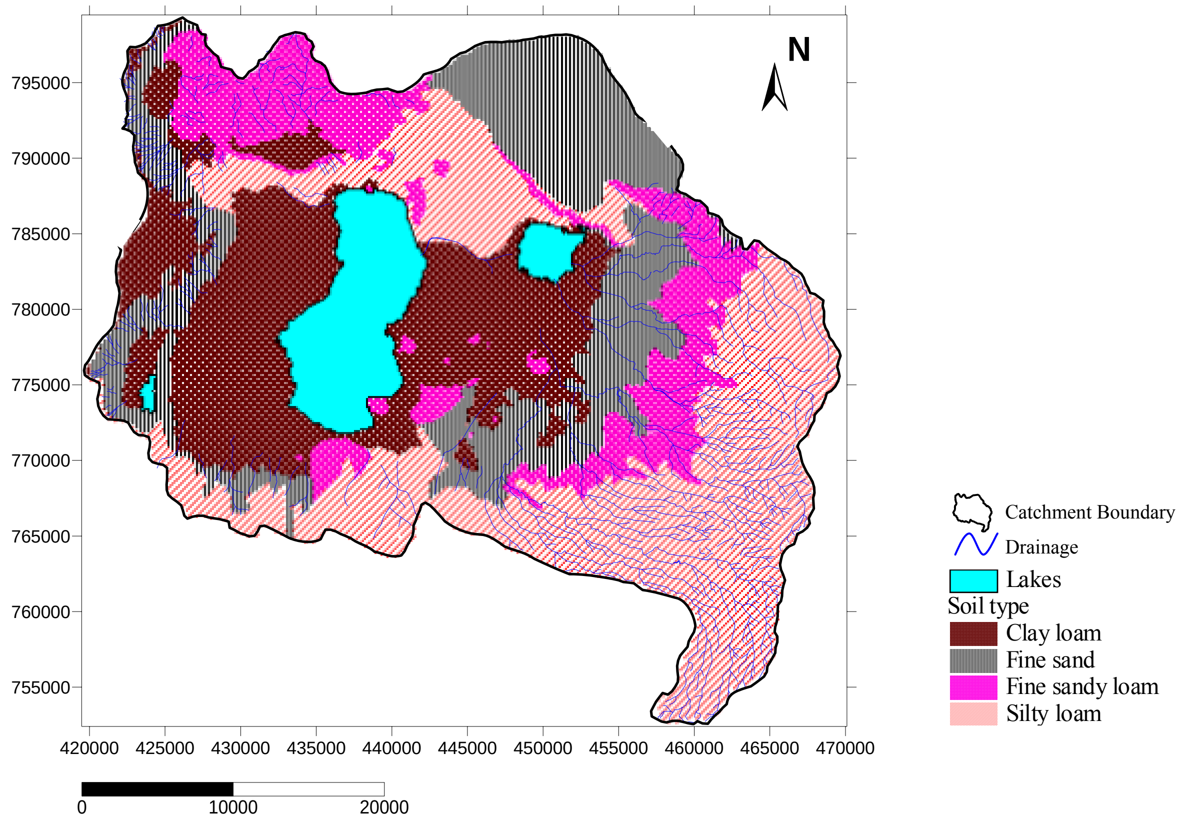

Fig. 2.4 Simplified Soil Map of the Study Area (after WWDSE, 1999)

2.4 Climate

The climate of Awassa area is characterized as sub-humid climate (FAO, 1984) and has extended period of wet season from March to October, in addition to the main rainy season taking place from July to September (Fig. 2.5). The maximum amount of mean annual rainfall goes up to 1150mm at Wendogenet on the wall of the caldera and Shashemene has the minimum 918mm. The study area has 19.5^{0}C mean annual temperature where March and April have the highest and November and December have the lowest (Fig. 2.6). The mean monthly wind speed varies from 0.74-1.26m/s as measured 2m above ground surface, June and July have the peak wind speed where as October and November have the least (Fig. 2.7).

The mean monthly sunshine hours vary from 4.81hrs to 9.14hrs where minimum sunshine hours occur in June, July and August and maximum in November, December and January (Fig. 2.8). Relative humidity at three different hours at Awassa station shows that the mean monthly relative humidity ranges from 54.4-76.3%. February has the highest relative humidity and September with the least (Fig. 2.9). Long term pan evaporation data at Awassa Station, using Class A pan, is used to show the highest evaporation in dry month and least in summer time. Pan coefficient of 0.8 is used for correction and result in 1581mm of mean annual lake evaporation at Lake Awassa (Fig. 2.10). Long-term mean monthly Hydro-meteorological variables at Awassa Station are presented in the following figures.

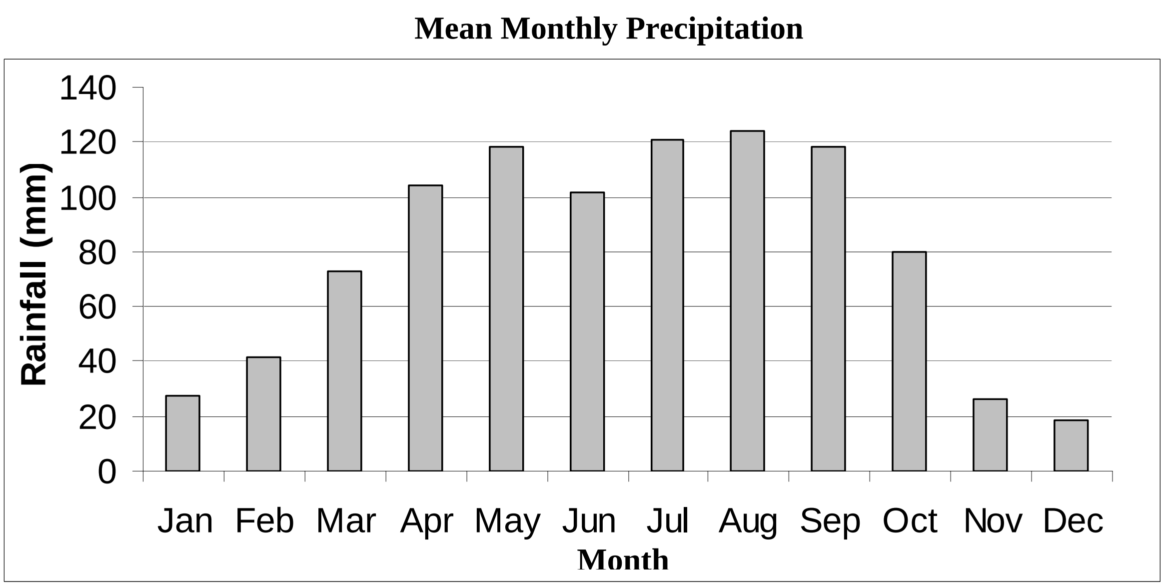

Fig. 2.5 Long-term mean monthly precipitation at Awassa Station

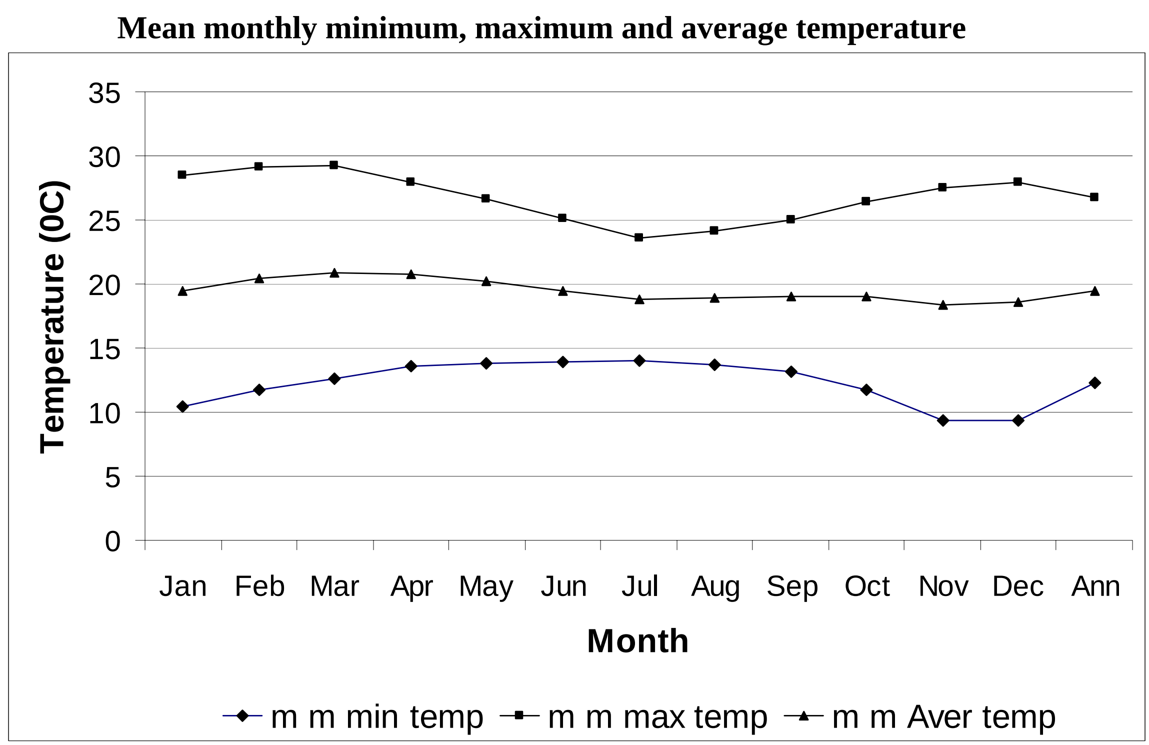

Fig. 2.6 Mean monthly minimum, maximum and average temperature at Awassa (1988 - 2003).

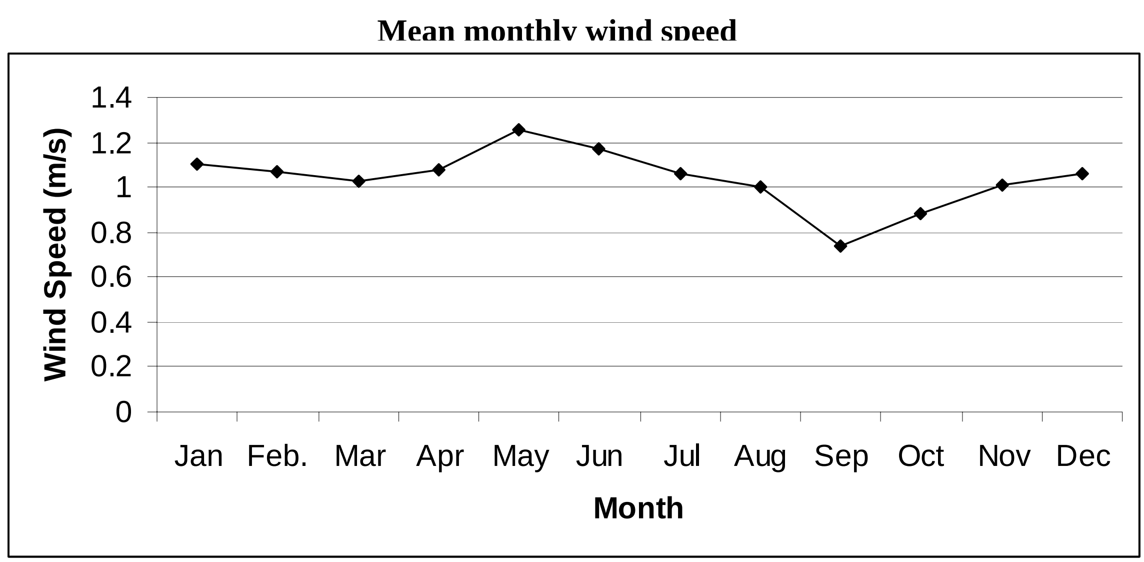

Fig. 2.7 Mean monthly wind speed (m/s) (1973 - 2003).

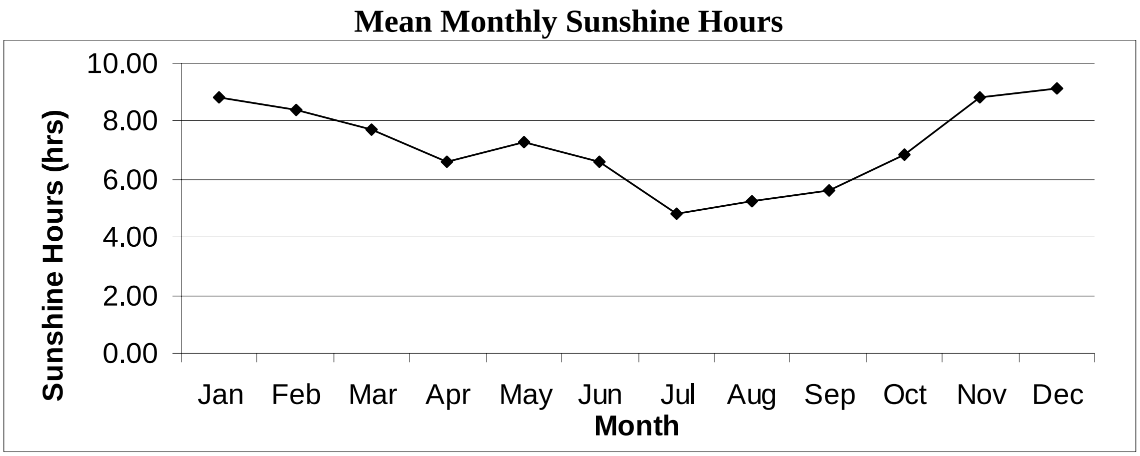

Fig. 2.8 Mean monthly sunshine hours (hrs) (1975 - 2003).

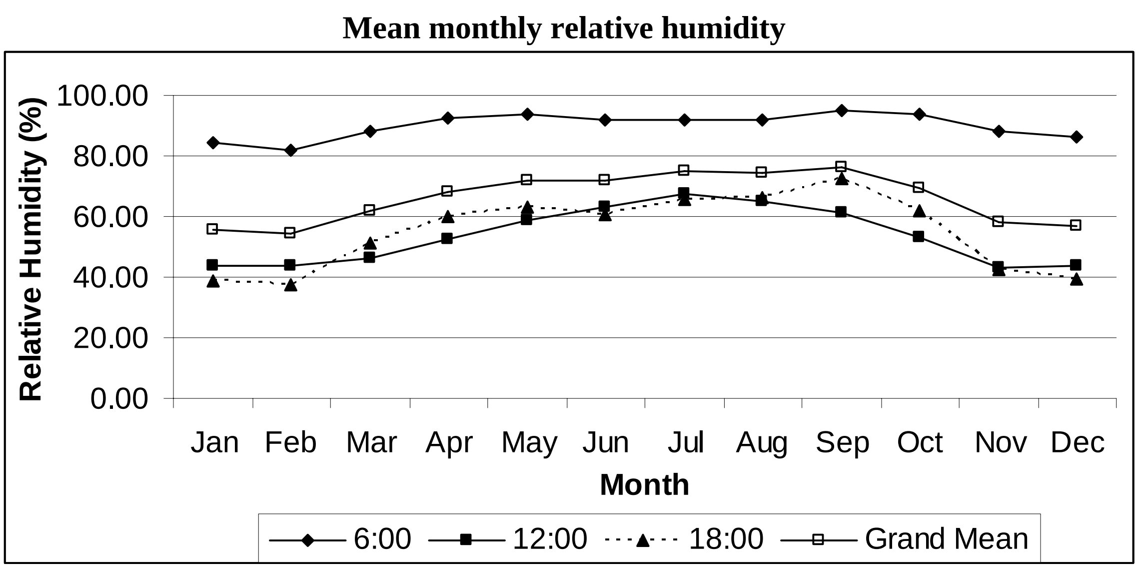

Fig. 2.9 Mean monthly relative humidity (%) at different hours (1988 - 2003).

Mean Monthly Pan and Lake Evaporation (mm)

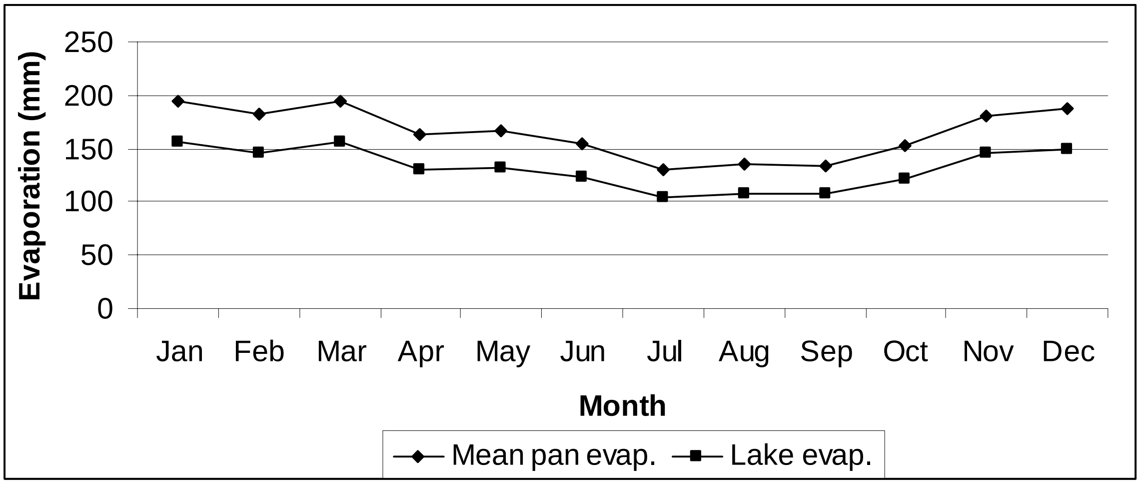

Fig. 2.10 Mean Monthly Pan Evaporation and Lake Evaporation (mm) (1986-2003)

CHAPTER THREE

Geology and Structures

3.1 Geology

3.1.1 General

The Great East African rift system is one the most remarkable features of the earth's crust. The rift, rather than just a single valley, forms a more or less continuous scar from Israel and Jordan in southwestern Asia to Mozambique in southeastern Africa (Ase et al., 1986). The study area is part of the central sector of the Main Ethiopian rift (MER), which is the northern segment of the Great East African rift system running NNE-SSW direction. The main part of the Rift Valley faulting took place during the Middle Pleistocene times (Wiberg, 1974), possibly along older fault lines and continued into Upper Pleistocene. Some investigations suggest that the development of the fault system continues at the present time. The MER is 80km wide and 700km long extending from Lake Abe, Afar-triple junction and fade away southward into Lake Turkana and Lake Stifane rifts south of Lake Chamo

Based on structural features the main Ethiopian Rift System is divided into three geographic areas where the Awassa lake basin belongs to the Central (Nazret Awassa) Sector, which is a symmetric rift basin where both sides of the rift margins are fully defined with the exception of the regions between Gurage and Sodo of the western escarpment and the Shashemene area of the eastern margin. The rest two are Northern (Fentale Nazret) and Southern (Awassa-Konso) sectors.

The oldest volcanic rocks, which are the plateau trap series are exposed on the western escarpment and consists of about 1000m of basaltic lava flows, with interbedded ignimbritic beds, overlaid by massive rhyolites and intervening tuffs and basalts (Di Paola, 1972; Merla et al., 1979; Woldegebriel et al., 1990). Radiometric age of the basalts range from 40-25Ma and the rhyolites 37-27Ma (Merla et al., 1979; Woldegebriel et al., 1990).

The eastern plateau is constituted by Pliocene to early Pleistocene (4.6-1.6Ma) shield volcanoes such as Chillalo, Kecha and Badda). It is characterized by trachayte with subordinate basalts and mugearites (Di Paola, 1972; Merla et al., 1979; Woldegebriel et al., 1990), Miocene phonolites.

Most parts of the floor of the MER are covered by silicic pyroclastic materials, mainly per alkaline rhyolitic ignimbrites, interlayered with basalts and tuffs associated with unwelded pumice (Mohr, 1962; Di Paola, 1972; Woldegebreil, et al., 1990). They are early to middle Pliocene. Alkaline and Per alkaline rhyolitic lava flows associated with pumice and ash represent the late silicic volcanic events (Di Paola, 1972).

A more recent volcanic rock occur along the Wonji Fault Belt, which is made up of basaltic lava flows, associated with Hayaloclastites and Scoria cones (Di paola, 1972.). It is very recent and localized, with a radiometric age of 0.13Ma (Woldegebriel et al., 1990). The Bora Bericco complex, the Aluto volcano, Ficke, and Corbetti calderas are the youngest volcanoes & calderas in the region started to be active from middle Pleistocene (about 0.25Ma) (Di Paola, 1972; Woldegebriel et al., 1990). They are made up of rhyolitic lava flows, unwelded pumice flows & falls and ashes with obsidian, the obsidian flow represent the final product of the volcanic activity. Obsidian flows and pumices were dated 2000yBP (Gianelli, et al., 1993).

The Late Quaternary fluvio-lacustrine sediments cover the large part of the floor of the MER (the Lakes region) where the lakes in this region, they were in a very wide lake in the past occupying most of the rift floor (Merla et al., 1979).

3.1.2 Local Geology

(Wondwosen Mekonnen, 2005), stated the main geologic units in the area subdivided into five geologic units as follow, starting from the oldest.

1. Basalts of the Plateau Trap Series (Late Miocene), these are found on the eastern and southeastern part of the caldera wall and geo-chronologically grouped under Gurage Basalts, which are the oldest rocks of the area.

2. Old Alkaline and Peralkaline Silicic Rocks (Late Pliocene-Middle Pleistocene), which covers most eastern wall of the caldera, south and southeast of Lake Awassa (Dulecha Ridge), northeastern, southern, southwestern and northwestern part of the catchment, also forms ridge at Wendogenet.

3. Recent Basaltic Lava Flows, Hayaloclastites and Scoria Cones (Recent Pleistocene), it is found east, west and northeast of Lake Awassa and contains Basaltic Lava Flows associated with Scoria Cones and Hayaloclastites forming smaller scattered relief on the floor of the caldera with thickness of a few dozen meters.

4. Recent Acidic Volcanics (< 1.6Ma), this covers north and northwest of Lake Awassa around Corbetti Volcano in addition to eastern and western caldera wall, which are product of Chebbi Volcano (Mt. Chebbi and Urji). It is the youngest volcanic product in the catchment.

5. Volcano-Lacustrine Deposits (Pleistocene to Recent), which covers most part of the floor of the catchment and are volcanic in origin, with small amount of diatomite. These lacustrine deposits have variable lithology which is related with their mode of origin (Tenalem Ayenew, 1998) and it is the only non-volcanic formation in the catchment.

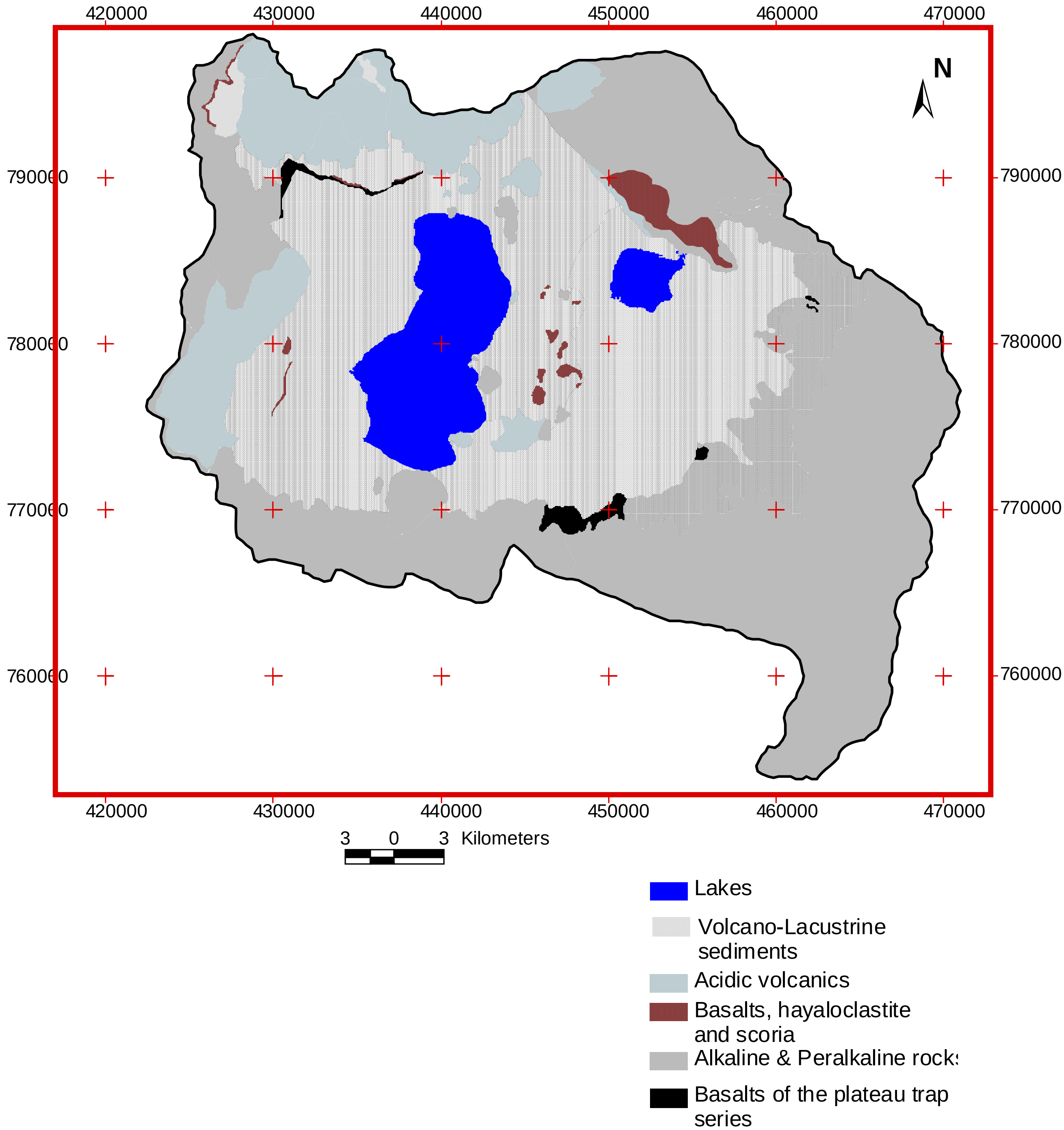

Fig. 3.1 Generalized geological units of the area (modified after Wondwosen Mekonnen 2005)

3.2 Structure

3.2.1 Geologic Structures

The study area has normal faults, fracture zones and faults, volcanic domes and cones, lineaments and collapse structures interpreted using enhanced Landsat TM Colour Composite (741) Image and Digital Elevation Model (DEM) derived from a 90m-resolution Shuttle Radar Terrain Model (SRTM) Image. In the study area there are normal faults forming step faults and volcanic collapse structure (caldera) shifting these faults, which imply that the caldera is a letter event when compared to the rifting.

There are at least three types of faults, which are present in the area based on their strike directions, NNE-SSW, N-S running, NW-SE and E-W running faults/fracture zones (Wondwosen Mekonnen, 2005). The rift floor is affected by several young faults resulting into a number of relatively small horst and grabens.

The NNE-SSW and N-S running faults are the dominant in the study area where the longest axis of Lake Awassa is aligned in this direction and are mainly found in the southern and eastern part of the catchment. The E-W running faults control rivers/streams in the southern part of the catchment. The NW-SE transfer faults are not common in the area.

Recent ground cracks are formed in Muleti, southwest of Lake Awassa, most of them formed in one night and after heavy rainfall. The cracks approximately strike NNE-SSW, which could convey water from the Muleti sub-catchment to Lake Awassa when intercepted by east-west running faults (Fig. 3.2 and Fig. 3.3). The cracks dimension ranges from 2.5 to12 meter wide and 150 meter to 2.4 km length, have no vertical or horizontal displacement. These are important hydrological features increasing recharge to groundwater by facilitating easy passage of surface water into the aquifer.

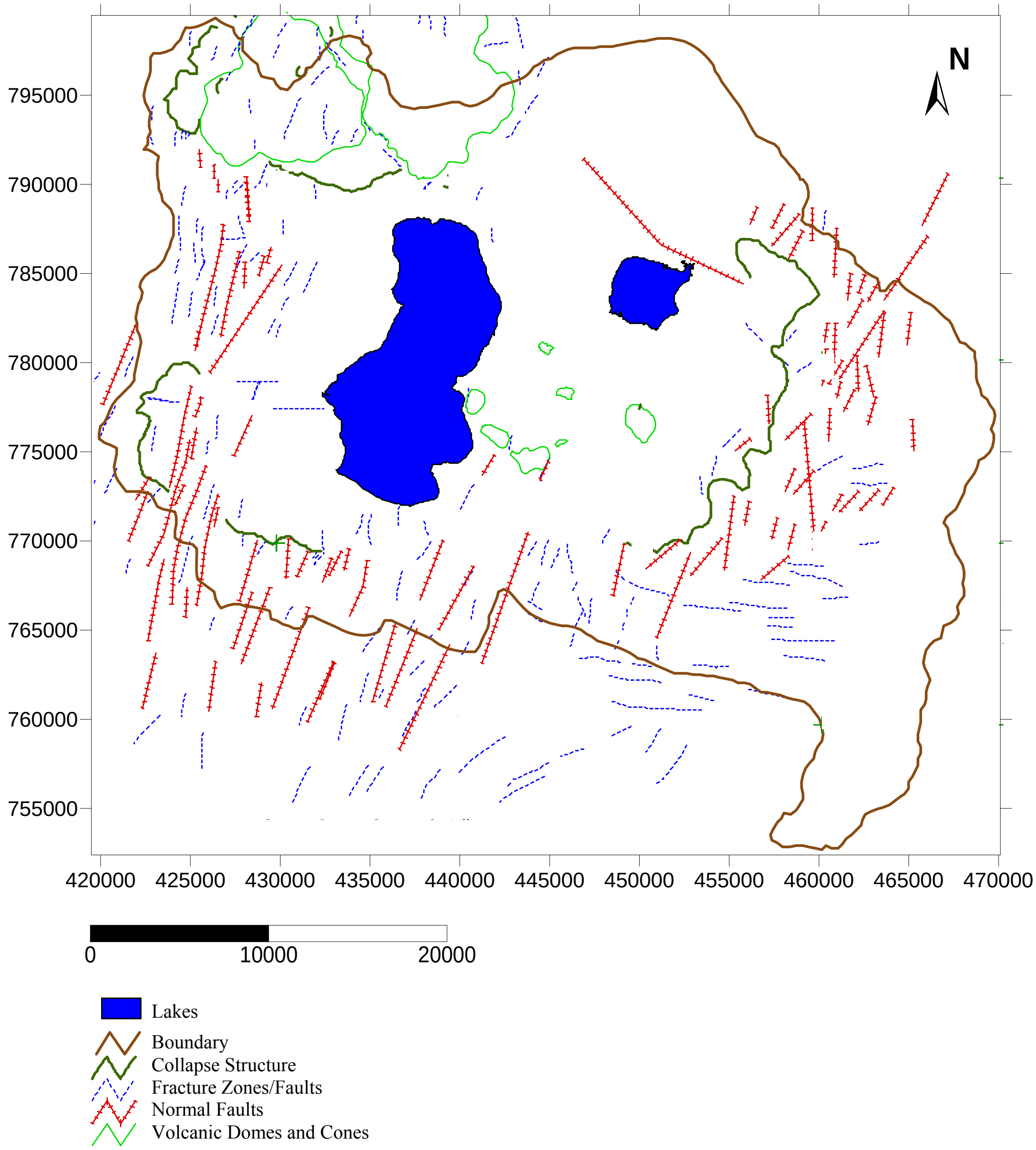

Fig. 3.2 Structural Map of the Study Area.

3.2.2 Effect of Faulting System on the Modeled Zone

In the study area groundwater flow is highly controlled by geologic structures, which also smooth the progress of the recharge and discharge processes. The effect of faults and fractures can be simulated using increased hydraulic conductivity since it facilitates easy passage of surface water into the aquifer.

Figure 3.3 shows two recent ground cracks west of Lake Awassa formed since 1996 with similar trend of propagation with the adjacent fault scarps and mountain ridges. These are found around Muleti village (with average width of 2.5m, depth of 8-12m and maximum length of 2.4km) and further south of Muleti on Derba area (with ranging width of 2-8m and observable depth up to 5m). The Derba Pond, which was previously in Derba area disappeared through these cracks in 2002 after their formation.

Inside the modeled area there is a predominance of sedimentary material composed by fluvial and lacustrine deposits and pyroclastic material. The effect of tectonic activities upon these types of formations will be suppressed and the influence of faults and fractures on the modeled area can be safely discarded using the hydraulic conductivity.

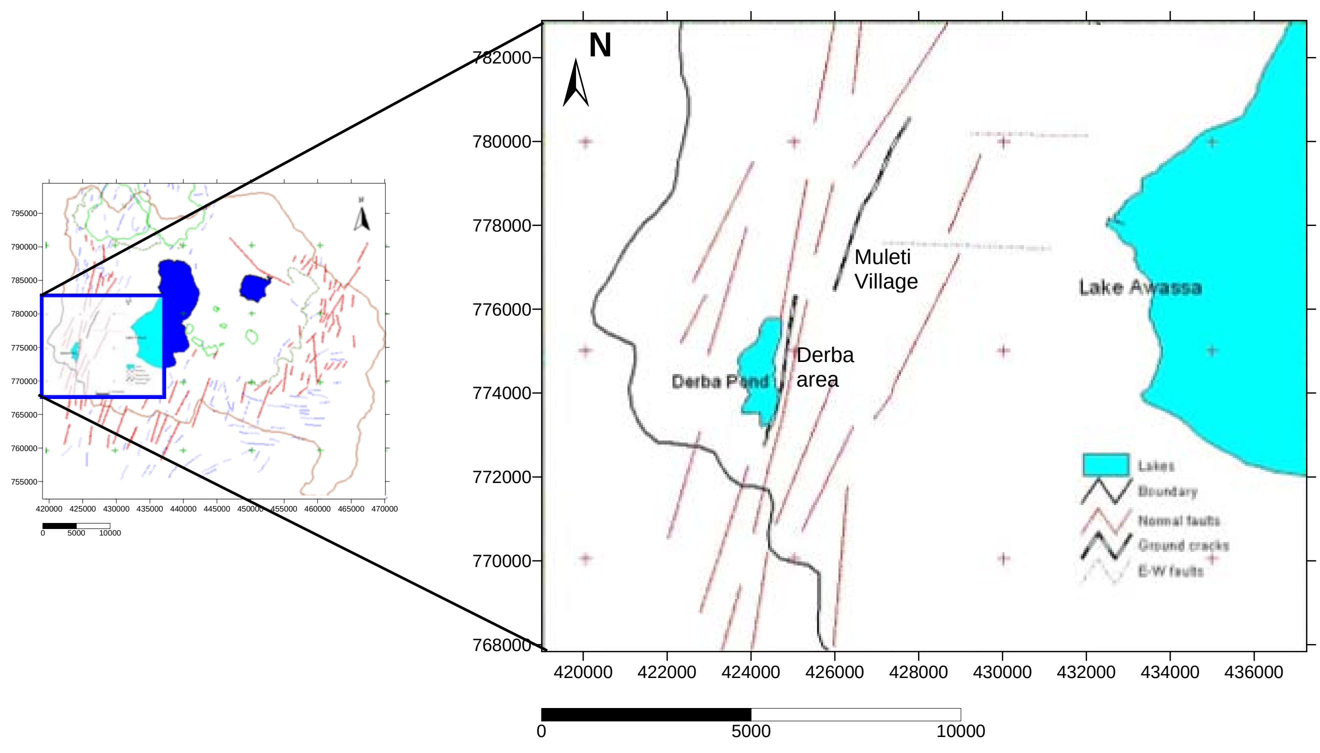

Fig. 3.3 Ground Cracks and Faults west of Lake Awassa, Muleti Village and Derba Area (modified after Wondwosen Mekonnen 2005).

CHAPTER FOUR

Conceptual Model

4.1 Introduction

The construction of a conceptual model is determined in some extent by the amount of information available, the model scale, the purposes of the model and the complexity of the zone under study. The conceptual model is a representation of the understanding of the real physical system of the study area. In general the following aspects define the conceptual model:

- Type of aquifers.
- Number of aquifers considered during modeling.
- Relation among aquifers.
- Aquifer geometry.
- Location, magnitude and spatial distribution of the aquifers.
- Location and distribution of surface water bodies.
- Boundary conditions.
- Hydraulic properties of aquifers. This topic includes transmissivity, hydraulic conductivity, storativity, leakage coefficient, etc.
- Natural and/or artificial recharge zones.
- Pollution sources.

4.2 Geometric Characteristics

The aquifer has average length in the east-west direction about 46 km, around 32 km in the north-south direction and about 58 km in the diagonal direction, NW-SE direction, which is the longest direction. Figure 4.1 shows three dimensional view of the modeled area.

Previous study conducted in the north east of Lake Awassa, around Shallo farm area, reveals that the main aquifer, which is unconfined lacustrine sands, has a thickness ranging from slightly more than 10m to over 60m. The underlying ignimbrite has an estimated thickness of 200m; similar to the lithology the aquifer thickness is highly variable.

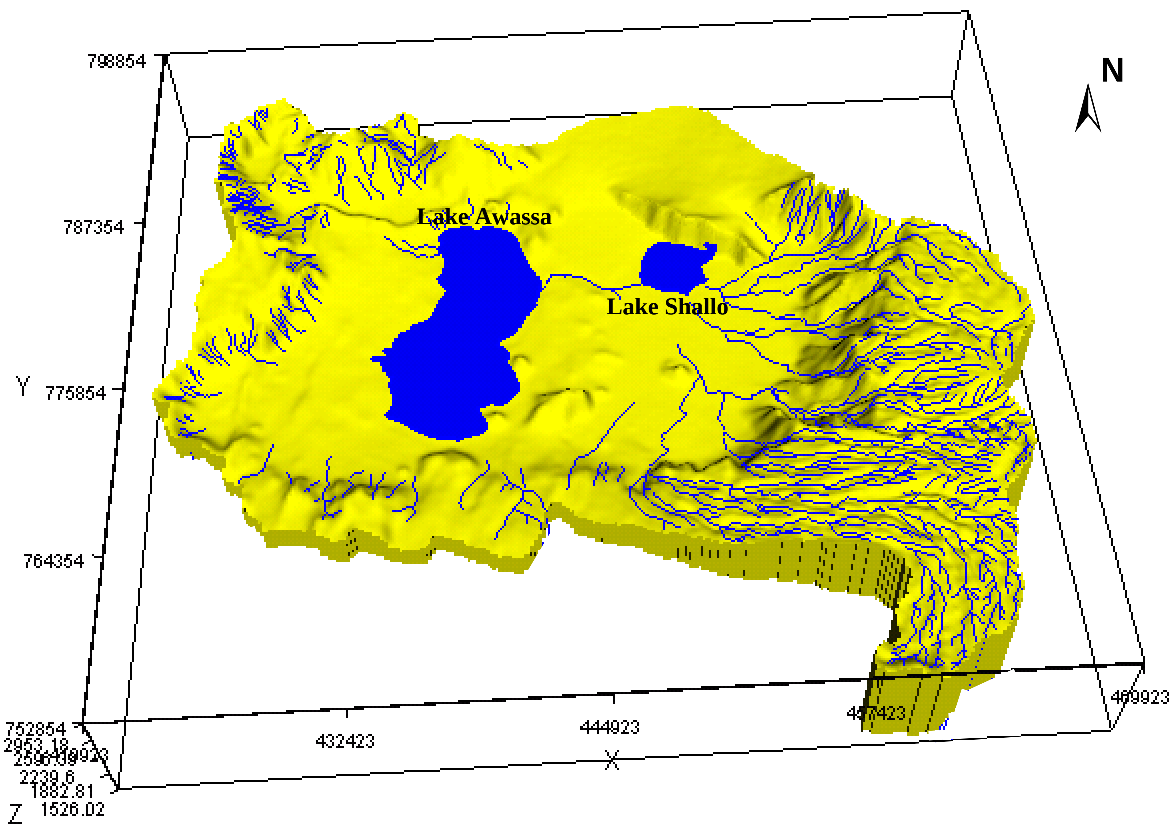

Fig. 4.1 Geospatial Model of the Aquifer.

4.3 Rivers and Lakes

In the study area groundwater level is affected by fluctuation of perennial river stages originating from the eastern highland and flowing to the west to join Tikur Wuha River which finally goes to Lake Awassa. Lake Awassa, Lake Shallo (Cheleleka) and other small ponds also affect groundwater levels. Groundwater table map, unconfined aquifer, prepared during a study conducted to assess the groundwater potential and quality at Shallo farm area, (North east of Lake Awassa) showed that the groundwater flow feeds the Tikur Wuha River (the main river that brings water to the lake from the sub-catchment) and lake Awassa evidencing an interaction between surface water and groundwater (Water Works Design & Supervision Enterprise, W.W.D.S.E 2001).

Water flows from the river into the aquifer and the groundwater becomes elevated when there is an increase in river stage with respect to the altitude of the groundwater level. A decrease in river stage with respect to the groundwater level causes water to flow from the aquifer into the river and result in the decrease of groundwater level. The extent of the change in the groundwater level elevation in response to river stage fluctuations depends on the magnitude of the change in the river stage, the length of time the river remains at the current river stage, the hydraulic properties of the aquifer material, and the distance from the river to the point of interest.

Due to the time required for the change to propagate into and through the aquifer the groundwater level increase or decrease in response to increase or decrease in river stage is more obvious in areas closer to the river. Therefore, the area of the aquifer that is affected by an increase or decrease in river stage depends on the length of time that the river stage remains at the new altitude. Changes in the groundwater level at distant locations from the river are the result of long term river-stage changes typically caused by seasonal high and low flows or long-term river-stage management.

Tikur Wuha River has high streambed hydraulic conductivity, the bottom of the river channel is below the top of the groundwater surface and therefore river stage changes have a large effect on groundwater flow. Tikur Wuha River streambed deposits are typically composed of Lacustrine with Alluvium and Volcano-Lacustrine Sediments, thus it is well connected hydraulically to the underlying lacustrine sand aquifer.

The other small steams have smaller streambed hydraulic conductivities and have less effect on groundwater flow than the larger Tikur Wuha River, locally the bottoms of the river channels can be above the top of the groundwater level. In the study area there are numerous smaller streams and drainage channels, mainly in the eastern part of the catchment.

Seasonal streams of the catchment, which carry a lot of water and sediment during rainy seasons to Lake Awassa, may affect groundwater flow locally during floods when they supply recharge to the aquifer or when the groundwater level rises above stream bed and aquifer drains into the stream.

In general, lake recharges an aquifer when the groundwater surface is below the bottom of the lake, but drain the aquifer when the groundwater surface is above the bottom of the lake. The total groundwater outflow to the lake is less than 100l/s (3.2 MCM /Year), which is very small with regard to the total volume of the lake and total surface water inflow to the lake per year. In the northern and western side of the lake, the lake recharges the aquifer annually with an average amount of 71.5 MCM per year. The main inflow to the lake is surface runoff; however, the major groundwater inflow to the lake is from the southern side of the lake and along Tikur Wuha River (cited in Tadesse Dessie and Zenaw Tessema, 2003).

4.4 Hydrogeology

4.4.1 Hydraulic Properties of the Aquifer

The hydraulic properties of the aquifer used in the conceptual model and for the first run of the numerical model were obtained from the existing data, fieldwork, indirect and direct, qualitative and quantitative approach. In previous studies made by Wondwosen Mekonnen, characterization of hydraulic properties of the aquifer involves use of existing pumping test data, geologic map, hydrogeologic map, soil map, lithology obtained from well logs, aquifer thickness, water table depth, structures and surface water features, etc so as to see the lateral distribution and nature of the aquifer. The spatial distribution and magnitude of hydraulic properties of the aquifer are not well-known for the study area. The aquifer hydraulic conductivities were adjusted during model calibration.

.

4.4.1.1 Horizontal Hydraulic Conductivity

Hydraulic conductivity of the area is highly variable due to the presence of different geologic structures and it is demonstrated on the results of the analysis of pumping test data. Ignimbrites and tuffs have the least in the area which is 0.24 m/day and goes up to 442 m/day in the lacustrine sediment, which has wide range of values. Transmissivity ranges from 13m^2/day to 4010 m^2/day, which is the characteristics of the fractured volcanic rocks and the variability in lithology of the lacustrine sediments, more or less similar variations are also found in Ziway-Shalla basin (Tenalem Ayenew, 1998).

Aquifer characteristics are determined using aquifer testes conducted in open holes and wells, and laboratory analysis of rock samples collected from outcrops and drill cores. Aquifer test data of pumping wells conducted for the past seven years were used to determine hydraulic conductivity and transmissivity.

No	Borehole Id	X(m)	Y(m)	Total depth(m)	T(m2/day)	K(m/day)	Drawdown(m)	Q(l/s)	Aquifer type
1	BH1	455189	775583	40					Lacustrine sediment
2	BH2	444891	775368						Lacustrine sediment
3	BH3	455372	795074	145	13	0.24	24	2.17	Ignimbrite
4	BH4	455631	795769	36					Ignimbrite
5	BH5	447033	791288	157				2.7	Lacustrine sediment
6	BH6	444932	778774	120				2.2	Lacustrine sediment
7	BH9	445781	777224						Lacustrine sediment
8	BH11	443273	779488		2080	71.72	0.3	2.5	Lacustrine sediment
9	BH12	443521	779636	46	81.8	3.2		5.25	Lacustrine sediment
10	BH13	442779	781335	50	52.18	1.5		4.67	
11	BH14	444761	777655	62	1980	185		5	Volcanic sand
12	BH15	444725	777839	60	3801.6	442.6		6	Volcanic sand
13	BH16	433850	790246	83				1.5	Volcanic sand
14	BH17	439497	770573	119				4.4	
15	BH18	443836	786728	30	96.8	12.3			Lacustrine sand & tuff
16	BH19	444389	787557	33	158	20.5			Lacustrine sand
17	BH20	444329	788916	29					Lacustrine sand
18	BH21	443190	785010	18					Lacustrine sand
19	BH22	443342	784426	20	388.8	24.6			Lacustrine sand
20	BH23	442423	785532	58	1382.4	40			Lacustrine sand
21	BH24	436488	790654	72					lapilli tuff
22	BH25	437578	788926	42					lapilli tuff
23	BH26	436484	790614	54	70	3			lapilli tuff
24	BH27	437542	789753	65					lapilli tuff
25	BH28	435064	790390	81					lapilli tuff
26	BH29	444223	779650	50	4809.6	150.3	0.2	7	pumaceous tuff & scoraceous basalt
27	BH30	445381	770562	50	453.6	11	3.54		sand & gravel with pumice
28	BH31	445027	770369	56	41.2	1.2	15	6.5	sand & gravel with pumice & tuff
29	BH32	444996	770976	62	1540	77	2.01		Sand with some gravel & weathered tuff
30	BH33			107	528.5	10.5	8.65		Sand & gravel, scoraceous basalt
31	BH34	444574	773563	50	880	18.7	7.34		sand
32	BH35	444086	772115	50	501	11.4	8		sand
33	BH36			100	411.8	4.7	1.2		sand with gravel
34	BH37			77					scoria
35	BH38			100					scoria

Table 4.1 Hydraulic Characteristics of wells in the area (Modified after Wondwosen Mekonnen 2005).

Neumann (1975) and Moench (1993) methods were used for the pumping analysis to determine the parameters. Eight wells from the lacustrine sediment were used for the interpretation of the assumption that the aquifer is unconfined and of infinite aerial extent, thickness of the aquifer takes the saturated thickness.

In general, the study area has no clear regional trend in hydraulic conductivity. In addition to the pumping test data, which doesn't represent the whole area but only the floor with available data, time-draw down plots of existing data was used to define the nature of the aquifer. In some areas where there is no sufficient data geology, structures, well logs and hydrological components such as surface water features are used to support the results from the methods used.

Except in some areas with confining layers of clay and ash deposits the general aquifer system of the catchment is unconfined. There are also some local multi-layered aquifer systems with variable permeability which is the nature of the lacustrine sediment in the area, and it is composed of clay, sand to gravel, ash, pumice, tuff, and volcanic fragments of rhyolites, ignimbrites and scoraceous basalt (Wondwosen Mekonnen, 2005).

Hydraulic conductivity and transmissivity assessment of the study area is done by Wondwosen Mekonnen and he has divided it into six zones, where the recent highly fractured scoraceous basalt associated with permeable lacustrine sediments of medium grained sand and volcanic necks of the scoria are grouped under a zone with hydraulic conductivity greater than 50 m/day. It is highly fractured zone and has limited aerial extent.

The second highly permeable zone of the study area has value ranging from 10-50 m/day. This zone encompasses thick lacustrine sediments and recent alluvium deposited on the floor and near the caldera rim, fractured ignimbrite found south east of the lake at the foot of the caldera is also grouped here.

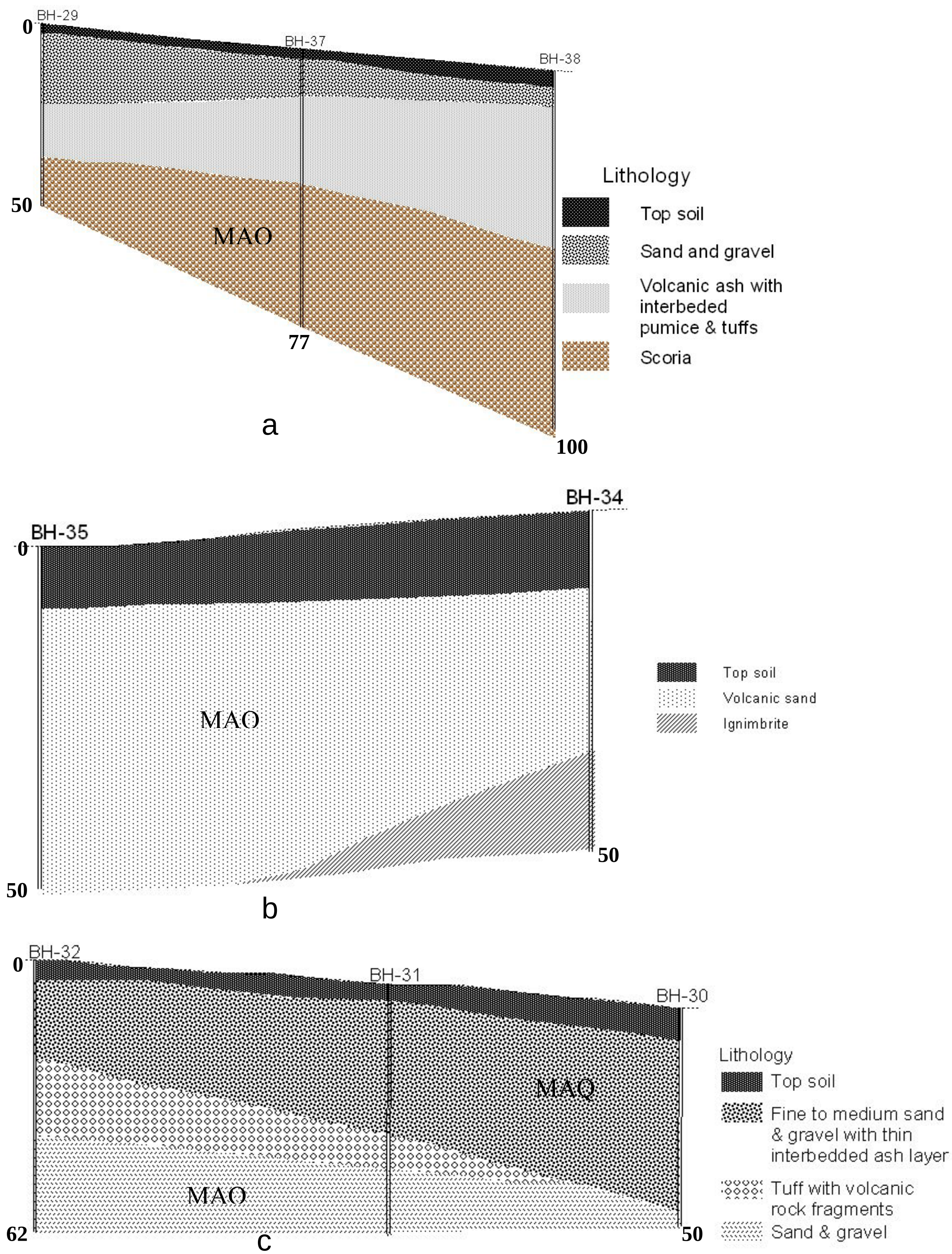

Fig. 4.2 Vertical distributions of aquifers correlated by neighboring wells (a, east of the Lake; b, south east of the Lake; c, further south near the caldera wall), MAQ-main aquifer. (modified after Wondwosen Mekonnen 2005)

The relatively thin lacustrine sediments found in the northern and western part of the lake have hydraulic conductivity ranging from 5 to 10 m/day. The permeability is reduced by the presence of unwelded poorly sorted less permeable volcanoclastics, volcanic ashes and lapilli tuffs. Fractured ignimbrites of the caldera floor and the escarpment have value ranging from 1 to 5 m/day. They are associated with ignimbrites and tuffs of this group, less fractured recent basalts, hayaloclastites and pyroclastic deposits of the southwestern parts of the caldera rim.

The hydraulic conductivity estimated for the Old alkaline & Peralkaline rocks of the escarpment is 0.1 to 1 m/day containing unwelded to moderately welded fine to coarse tuff and pumaceous deposits of acidic volcanics, it is a recharge area and has deep water table.

Less than 0.1 m/day is estimated for the acidic volcanic plugs of the Corbetti Caldera, which has characteristic very low permeability. This also includes volcanic necks and domes of the old rhyolitic lava flows, lapilli tuffs and lava flows of the floor and caldera rims. The six zones of Hydraulic Conductivity used for the initial input of the numerical model are shown in Fig. 4.3. These values were adjusted during model calibration to get the best fit between observed and calculated head.

The vertical distributions of the hydrostratigraphic units of the study area are shown by the simplified cross-sections from neighboring well logs shown in figure 4.2 in cross-section “a” found east of Lake Awassa the main aquifer unit is Scoria. In cross-section “b” the main aquifer unit is Volcanic sand and in “c” it is Sand & gravel. Except local variation, the main aquifer of lacustrine sediment is volcanic sand and gravel. Locally aquifers of scoria and basalts are found.

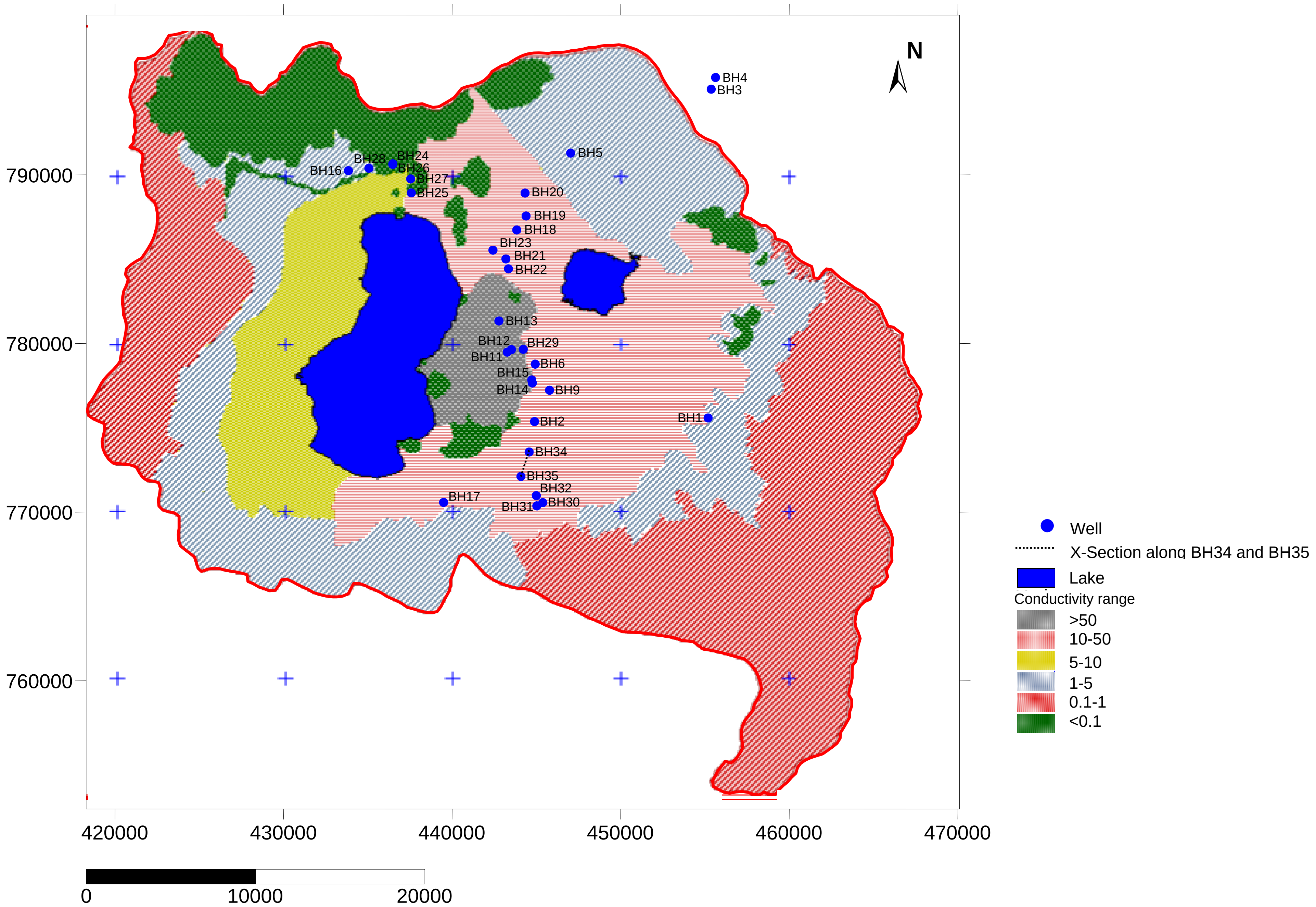

Fig. 4.3 Hydraulic conductivity range map, in m/day (modified after Wondwosen Mekonnen 2005)

4.4.2 Groundwater Levels and Movement

In general precipitation, evapotranspiration, and pumpage affect groundwater levels. In the study area water levels are generally highest in July, August and September when precipitation is greatest, evapotranspiration is lowest, and irrigation withdrawals are minimal; from November till February water levels are lowest when evapotranspiration and pumpage are greatest.

Average groundwater head distributions along with the direction of flow were estimated for the catchment from water level data of boreholes found in different parts of the catchment, which are also used for the calibration of the steady-state model. The general direction of groundwater movement throughout most of the catchment was from the margin of the caldera (recharge area) towards Lake Awassa (discharge area).

In the study area depth to the water table is highly variable; it ranges averagely from 18m in the Lacustrine Sediment to more than 100m in the lapilli tuff. Water level altitudes are highest in the southeastern part of the catchment, which is about 2580m above sea level. The high water levels may be the result of limited agricultural pumping and the low permeability of moderately welded coarse tuff in this area of the catchment.

The lowest water level altitude in the study area is around the northern part of the catchment and it is about 1660m above sea level, where small amount of groundwater flows into Ziway-Shalla Basin, north of Lake Awassa Basin. In the volcano-lacustrine sediments the water level gradient is fairly flat, where discharge occurs as base flow to streams or evapotranspiration from swampy areas around Lake Shallo, where groundwater is close to the surface or even above in some places.

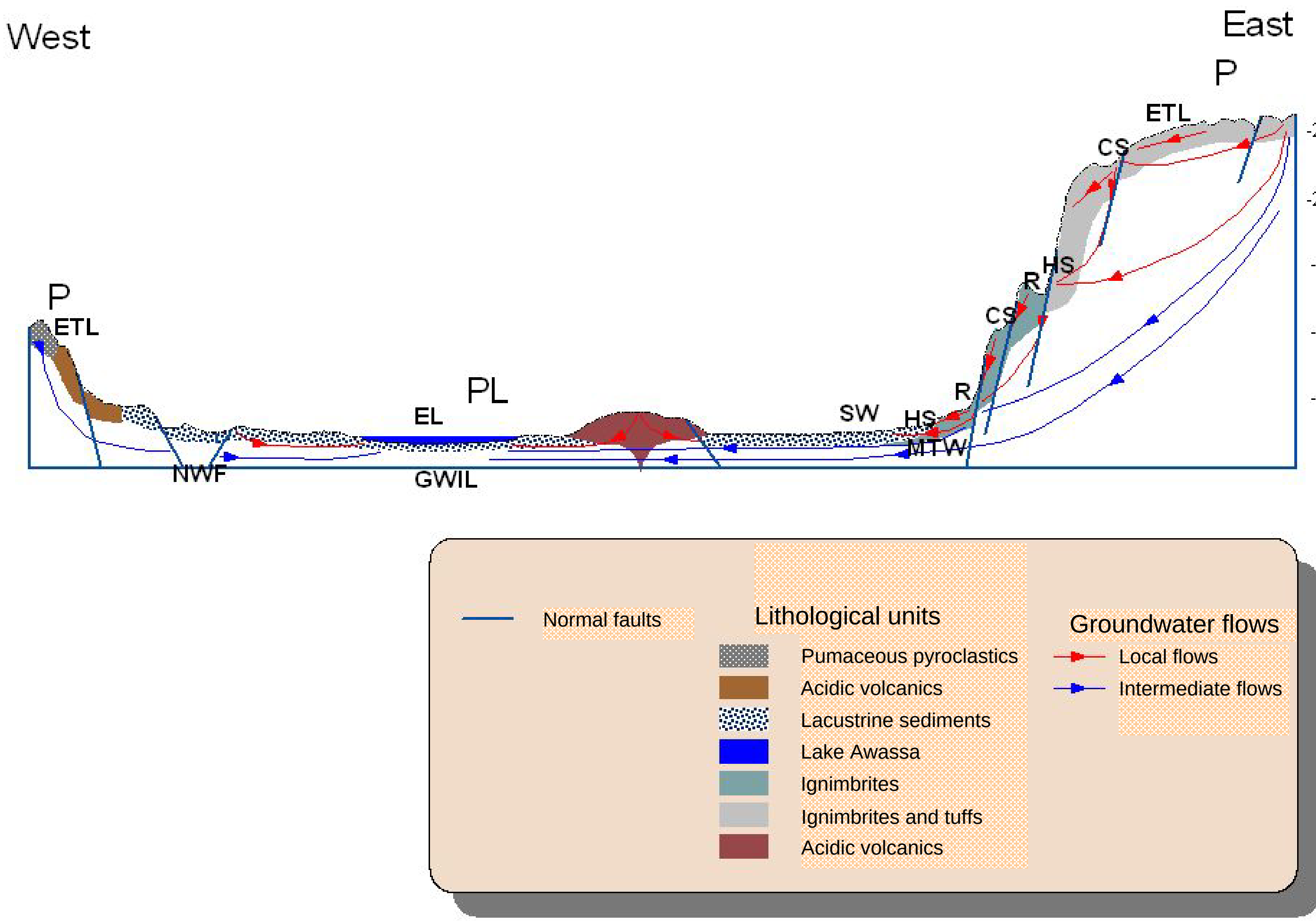

Fig. 4.4 The conceptual profile model showing the groundwater-surface water interactions in relation to groundwater flow (P, precipitation on the land; PL, precipitation on Lake surface; EL & ETL are evaporation from the Lake and land respectively; CS, cold springs; HS, hot springs; R, rivers; SW, swampy area (Shallo); MTW, mixing of thermal water; GWIL, groundwater inflows to the Lake; NWF, northward fault controlled flow; SP, seepage). Horizontal scale is approximately 46m. A-A' is shown in Fig. 4.5. (Modified after Wondwosen Mekonnen 2005)

Ground water moves from areas of high water-level altitudes to areas of low water-level altitudes; therefore, the general direction of ground-water flow can be inferred from contours of water level. Ground water flowed from areas of recharge along the caldera fronts and stream channels toward areas of discharge around Lake Awassa. In the northern part of the catchment, there was a small water-level gradient towards the north where some ground water flowed into the neighboring Ziway-Shalla Basin.

Hydrogeological study made by Tadesse Dessie and Zenaw Tessema (2003), revealed that the aerial distribution of electrical conductivity, temperature, calcium, nitrates and fluoride content of the lake and the groundwater showed that the groundwater at the northern, eastern and western side of the lake or the lacustrine sediment has greater concentration than the lake water. At the southern side of the lake and along Tikur Wuha River, the groundwater has lower concentrations, indicating that major groundwater inflow to the lake is from the southern side of the lake and along Tikur Wuha. Generally the electrical conductivity of Lake Awassa is less than the groundwater around the lake indicating that the main inflow to the lake is not groundwater, instead it is mainly surface water.

Spring waters on the eastern part of the lake and wells near the eastern lake shores have similar chemistry signifying groundwater flow to the lake in this direction. In the north Lake Awassa discharges to the groundwater which could be source of Chitu and Shalla thermal springs as it passes through the heating Corbetti Caldera. On average, the annual lake water outflow to groundwater has been calculated to be about 71.1 MCM per year, where as the total inflow to the lake is less than 3.2 MCM per year, which is insignificant when compared with total surface water inflow to the lake and total volume of the lake (cited in Tadesse Dessie and Zenaw Tessema 2003).

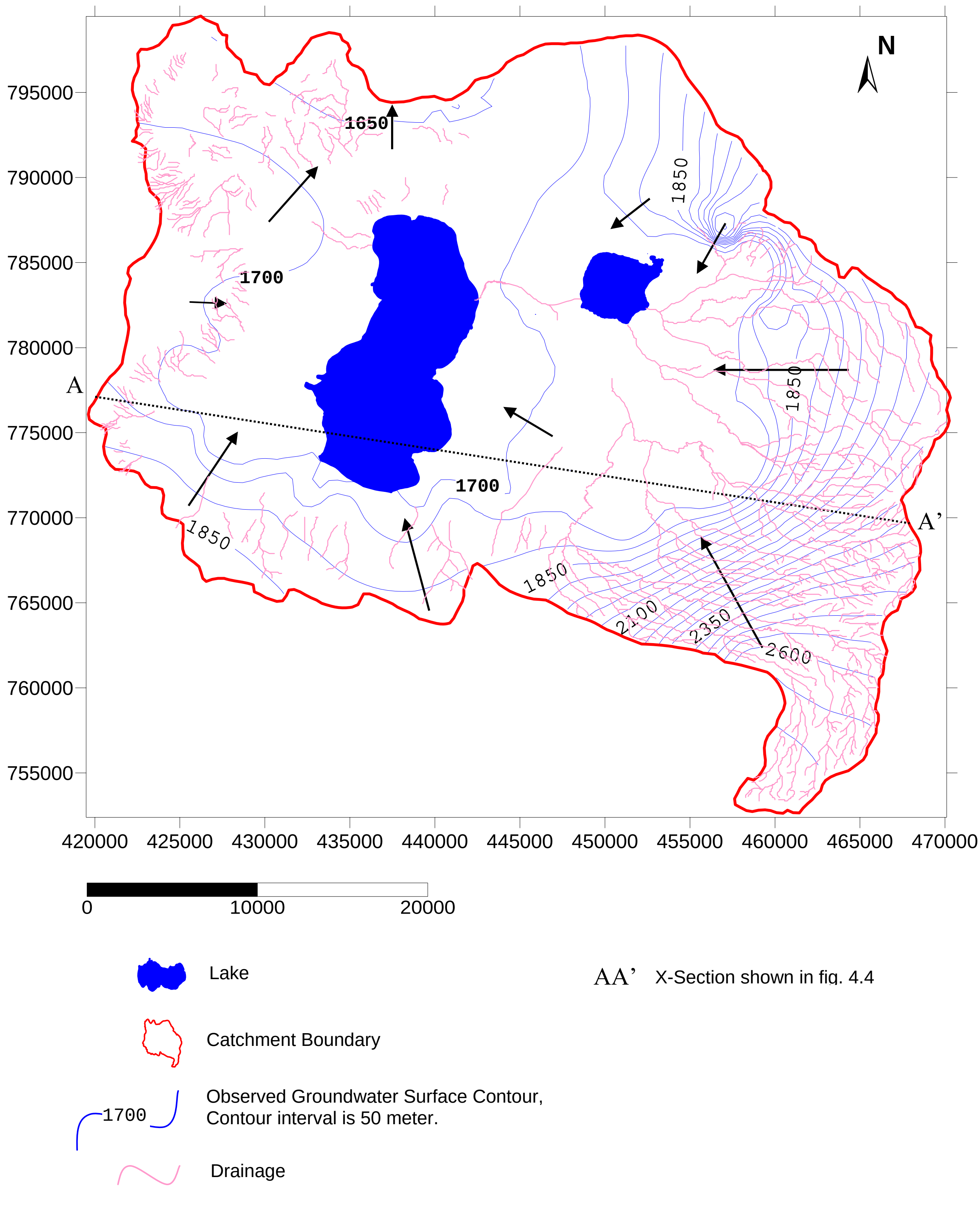

Fig. 4.5 Observed groundwater head distribution along with the direction of flow.

4.4.3 Groundwater Occurrence

The catchment has highly permeable lacustrine sediment, moderately permeable acidic volcanic (rhyolites, tuffs, pumice and obsidians) and low permeable ignimbrites and tuffs. High spatial variability in the permeability of volcanic rocks of the area is due to differences in the degree of fracturing. Acidic volcanics are highly permeable when sorted and ignimbrites are highly permeable when they are jointed, (W.W.D.S.E 2001).

Hydrogeological study conducted by Tadesse Dessie and Zenaw Tessema 2003, pointed out that Awassa Lake Catchment is classified qualitatively based on recharge, permeability, aquifer thickness, yield of springs and topography as very high, high, moderate, low and very low potential zones.

The very high potential aquifer encloses the area east of Wendogenet escarpment, where young alluvial sediment deposits overlay thick lacustrine sediment deposit. It is recharged mainly by overland flow from part of the Eastern Ethiopian Plateau, and partly from direct precipitation, perennial streams and springs from the eastern highland and recharge from irrigation.

Aquifers found in Awassa - Corbetti caldera zone have high to moderate potential constituting highly permeable sediment and unwelded coarse tuff. It has relatively higher aquifer thickness, deep water table and god water quality. This aquifer zone has limited recharge source that is recharge from Shemena escarpment and direct rainfall, during rainy season which is May to October.

The majority of Moderate Potential Aquifers constitute deeply buried fractured tertiary ignimbrite aquifer with plentiful good quality perennial springs supplying drinking water for surrounding villages and towns. Tuffs, basalts, scoria, and recent alluvium are other units of this group.

Low to moderate potential aquifers are found in the eastern highland containing mostly welded tuff. Very small amount of water infiltrates out of enormous rainfall where most of it goes as surface runoff to Awassa Caldera.

Low Potential Aquifers are those with thin layer of top clay soil and volcanic ash, it has very low permeability, very low recharge amount, very deep water table and poor water quality.

Pumice, tuff and other pyroclastics which have high permeability constitute Very Low Potential Aquifer due to the absence of confining layer which result in deep water table, this area gets lesser direct precipitation than other areas.

In the study area Acidic Volcanic Rocks such as Rhyolite, Trachyte and Obsidians are grouped under Aquicludes and are found in areas with hilly topography and poorly developed joints and fissures, which increase runoff instead infiltration.

4.4.4 Groundwater Recharge and Zonation

Recharge, which is water contributing to groundwater passing through water table, could be direct, indirect or localized based on the source and mechanism by which water reaches the water table. The amount and type of recharge depends on land use/land cover, topography, climate, drainage, geographic location, vegetation, structure, soil condition and other.

Generally the eastern part of the catchment gets better recharge than the western as a result of its higher rainfall amount and perennial streams from the eastern escarpment, in addition to these faults facilitate recharge to the aquifer. The floor of the catchment gets recharge from precipitation as direct recharge and as indirect from perennial rivers, mainly from Tikur Wuha River which is the only perennial river flowing to Lake Awassa.

Southeastern part of the catchment gets the highest recharge due to its high amount of rainfall, characteristic flat topped hill which facilitates infiltration instead of runoff, and its fracture and joints directing stream channels feeding the aquifer. Cold springs emanate from this area have a characteristics of low EC value and similar isotopic composition as the meteoric water. This implies fast infiltration and shallow circulation of groundwater, where the area gets substantial amount of direct recharge (Wondwosen Mekonnen, 2005).

Discharge areas of the catchment are manifested as swamps, depressions, and cold and hot springs, which are controlled by faults, are found largely in the eastern part of the study area. The swampy area around Lake Shallo is a typical discharge area in the catchment.

Previous hydrogeological study made by Wondwosen Mekonnen, shows qualitative recharge and discharge characterization based on recharge controlling factors, as a result zonation of recharge-discharge condition of the study area is given in figure 4.6, showing six different recharge-discharge zones of the catchment.

Escarpment and highland volcanic mountains of the eastern margin of the catchment gets large amount of recharge. Results from analysis of EC and isotopic composition of cold springs and meteoric water imply that there is fast infiltration and shallow circulation of groundwater as a result of the large amount of direct recharge. This is due to the characteristic features of the area, which are joint and fracture zones affecting this area, its high drainage density, high amount of rainfall and elevated altitude with flat topped hills, which favors infiltration over surface runoff.
The second group is caldera walls and the foot of escarpment and it has lower recharge relative to the highland due to reduced infiltration by the steep slope and undulating topography. It has fast and shallow circulating groundwater coming from direct recharge of this area and the highland. In this part of the

catchment recharge is mainly contributed from direct precipitation and perennial streams draining the eastern escarpment, faults of this area facilitate the recharge process. The eastern part gets higher amount of recharge than the western caldera rims and hills, which is characterized by intermediate direct recharge from depressions.

Volcanic domes and volcanic necks of the floor is another group of the zonation receiving localized recharge from precipitation through joints and depressions formed by faulted volcanic hill in the area. The absence of soil cover and the less permeable volcanic products of this group are the reason for lower amount of recharge compared to the other four recharge zones.

The last zone is The Floor of the Caldera with relatively lower amount of rainfall and characteristic evapotranspiration. Presence of lake, swamp and shallow groundwater table are lucid manifestation of discharge areas. It gets direct recharge from precipitation indirect recharge from Tikur Wuha River and associated open channels. The lacustrine sediment of this area facilitates the fast infiltration to the aquifer. Fig 4.6 shows initial recharge values for the numerical model estimated based on previous works.

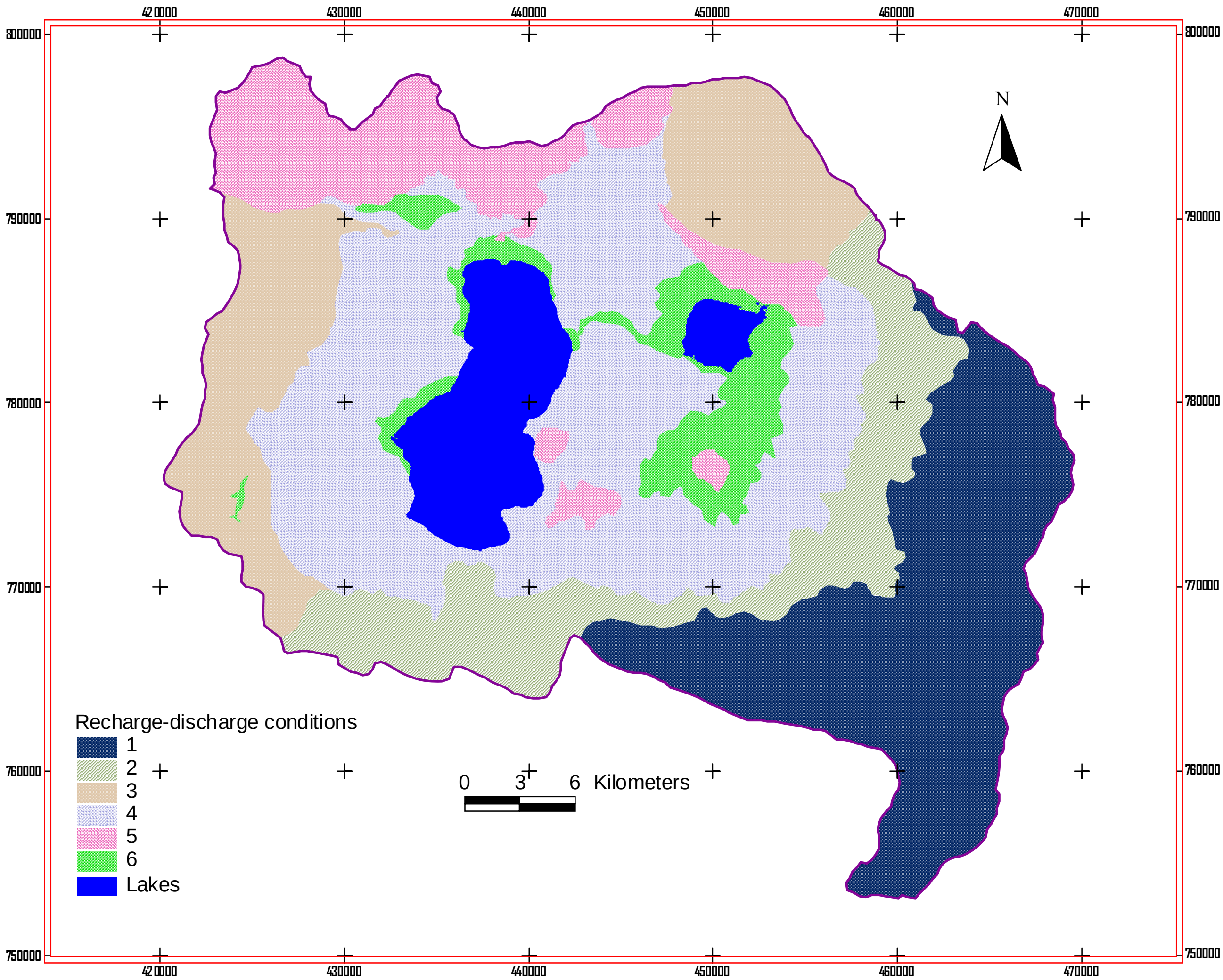

Fig. 4.6 A map showing zonation of recharge and discharge areas. (1-High direct recharge over the highland & escarpment (140 MCM/year), 2-moderate recharge with associated local discharge areas over the caldera rims (120 MCM/year), 3-intermediate recharge zone over caldera walls & volcanic hills (100 MCM/year), 4-the floor with localized direct recharge during high rainfall (80 MCM/year), 5-zones of local recharge areas over the volcanic domes & necks (60 MCM/year), 6-discharge areas) (Modified after Wondwosen Mekonnen 2005).

4.4.5 Groundwater Discharge

Discharge from the study area mainly occurs through well withdrawals and discharge to stream and springs. Discharge by evapotranspiration generally occurs in topographically low areas where groundwater table is intersected or close to the surface like the swamp around Lake Shallo. In the study area discharge to streams occurs as springs and seeps, there are several perennial springs with good discharge originating from the eastern highlands of the catchment and flowing to streams draining this part of the catchment. Well withdrawals are from domestic, stock wells and irrigation, which is the dominant development activity in the study area.

Synoptic measurements of stream flow under near base flow condition were conducted in the study area to obtain information describing aquifer discharge to streams, these measurements were taken during periods when direct runoff was not observed to occur and thus represent near base-flow conditions. Base flow separation made on Tikur Wuha River using mean monthly data from 1981 to 1998 show that annual base flow component of the Tikur Wuha River Discharge is 30.39MCM, which gives insight regarding the relative magnitude of groundwater discharge contributing to base flow (cited in Tadesse Dessie and Zenaw Tessema 2003).

In the study area there are several fault controlled hot and cold springs in the eastern, southeastern and southern parts of the catchment as shown in figure 4.7, these springs are fast, shallow circulating groundwater where the faults causes the westward flowing groundwater to emerge as spring flow. On the south eastern highland near the watershed boundary, there are some very low discharge cold springs in low depressions and open channels resulting when groundwater table and the surface coincide.

Locations of groundwater pumping sites and quantities of water withdrawn from these sites may affect substantially groundwater levels in the study area. Well withdrawals in the study area occur from irrigation, domestic, stock wells and industries. In the study area there are several wells that are not indicated here due to limitation in their location or pumping data, and some are not functional anymore.

In this study, there are about 80 water points with location and pumping data, and all are active including deep boreholes, machine drilled shallow wells, hand dug wells, protected springs (large, medium and Small), and ponds. The location of these water points is shown in figure 4.7.

4.5 Groundwater Quality

Normally, groundwater found in volcanic areas is of bicarbonate type having low total dissolved solids. In general, all the water types within the catchment show a relationship with that of the lake with regard to the major ions. All of the waters within the study area are sodium bicarbonate differing only in the degree of salinity. Water samples from the cold and hot springs, the rivers and groundwater show a relationship with correlation factors varying from 0.90 to 0.998, which shows that there is one homogenous water system in the lake catchment.

Deep aquifers may be affected by volcanic activity and recent tectonic movements, but surface waters are mostly affected by human activities. In the region agriculture is the main economic activity which is closely related to the use of fertilizers and pesticides to increase production. The application of these fertilizers and pesticides create favorable condition for contamination of surface water bodies. The lack of a well organized plan for treatment of urban, industrial and agricultural effluents is another potential source of water contamination. During the field work it has been observes that most of he effluents are discharged without treatment directly into the lake and rivers.

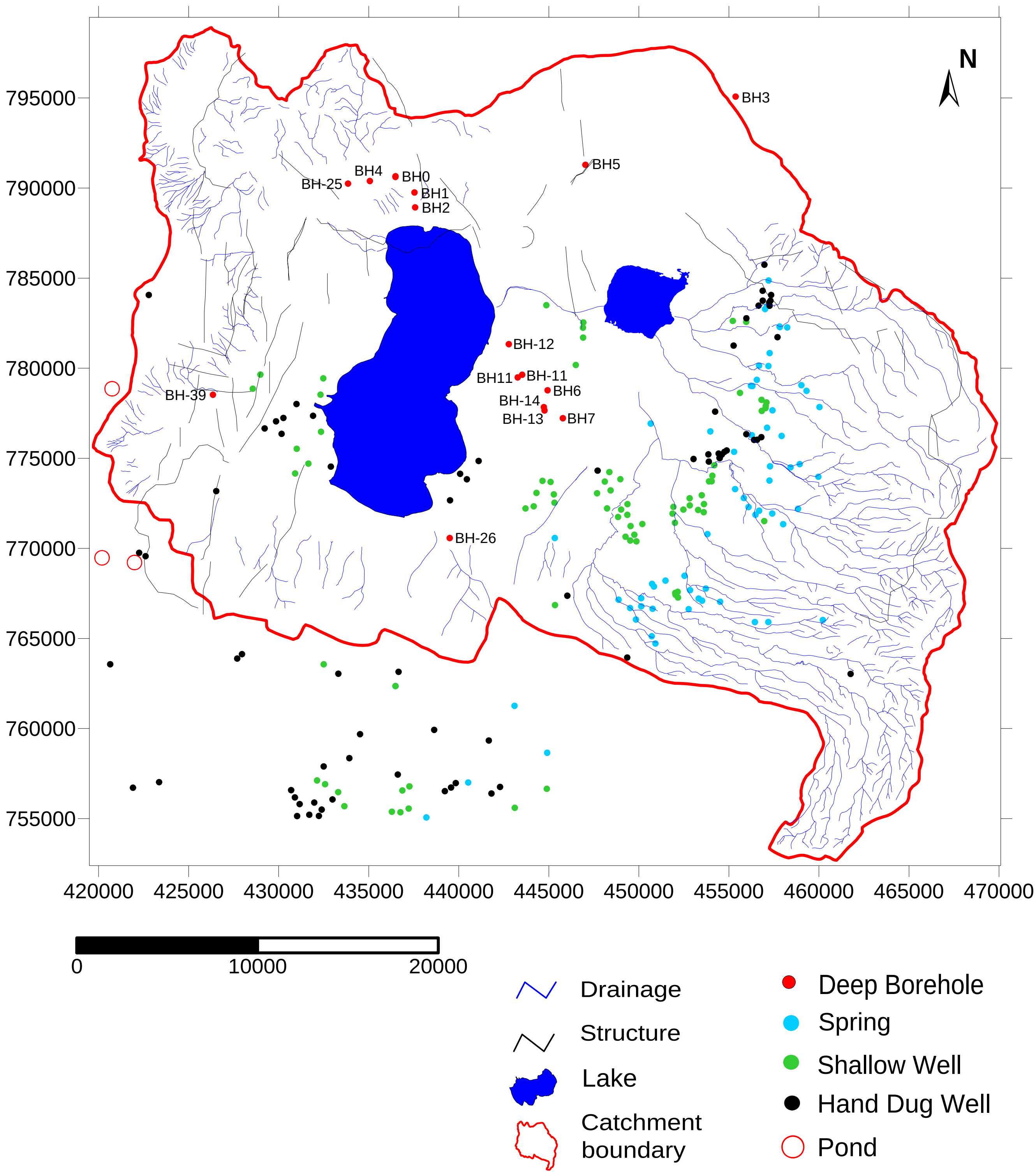

Fig 4.7 Water Points found within and around the study area.

4.6 Water Balance

In the steady-state water balance, inflows to and outflows from the aquifer system are identified and quantified on an average annual basis. The water balance described here includes the components simulated in the groundwater flow model; therefore, the direct runoff component of streamflow and evapotranspiration are not included.

Inflows include groundwater recharge from precipitation and groundwater recharge from Lake Awassa, outflow from the lake in the form of groundwater. Outflows include groundwater outflow from the aquifer to the perennial streams, groundwater outflow from the catchment to Ziway-Shalla Basin and discharge of groundwater by springs and wells.

Groundwater recharge from precipitation is the primary source of water to the aquifer. Precipitation recharge is the component of precipitation that infiltrates the land surface and reaches the water table. Precipitation recharge rates vary temporally and spatially with climatic conditions, land-surface permeability and slope, vegetation and soil saturation. Precipitation recharge rates, which can be estimated with a number of methods, were compiled from literature sources for the water balance. From base flow separation; the annual recharge to Lake Awassa Catchment is 63.7 MCM per year, which is 5 % of the annual rainfall and the other inflow to the aquifer is from the lake which is 71.5 MCM per year on average condition (cited in Tadesse Dessie and Zenaw Tessema, 2003). Therefore total groundwater inflow to the aquifer will be 135.2 MCM per year.

The primary outflow from the aquifer is groundwater outflow to streams as base flow. Discharge rates measured during the field work in April (cited in Tadesse Dessie and Zenaw Tessema, 2003) were taken as base flow in the water balance due to the presence of no direct runoff in this month, therefore the water in the stream comes from the aquifer as base flow. The total groundwater outflow to the perennial rivers as base flow is 111 MCM per year. Groundwater outflow through wells and springs is another way of groundwater withdrawal and equals to 3.03 MCM per year, which increase the total outflow to 114.03 MCM per year.

The remaining, 21.17 MCM per year, could be part of groundwater outflow from the catchment to neighboring catchments through deeper routes or fault zones, the magnitude of these flows could not be quantified, however, they are likely to be small relative to the total water balance.

4.7 Model Input Data Processing

In addition to the data collected from the field, the model is constructed using information gathered from different sources and formats, so a process of checking, selection, format conversion and organization had to be carried out to prepare for the model input. The relatively great numbers of investigations that have been carried out regarding the lake and its catchment have been spread among a great number of different organizations, and sometimes it is difficult to gather and organize the existing information needed for the new research activity.

Some of the important steps in data processing are removing wells where levels might be erroneously measured because of problems with the datum and organizing all necessary information in tables and maps in a format that is acceptable by the modeling software. Geographic Information System (GIS) was used to get a better general picture of the study area and assist in making some important decisions, like boundary condition.

The image used in the work was color composite Landsat TM of the Main Ethiopian Rift of the year 2000 with resolution of 14.25 meters. The original image covered a large area than the desired so a sub-area had to be selected which is important in increasing the computing and processing speed of the computer and to easily manipulate the sub-area. The image of the area of interest is then exported from Global Mapper to Surfer using JPG Export Option with UTM export bound of the study area (UTM: 419485-470099E and 752392-799477N). The image is then georeferenced using Base Properties in Surfer by simply giving the UTM values of xMin, xMax, yMin and yMax of the exported jpg image which is 419485, 470099, 752392 and 799477 respectively.

The other important feature of the new image was its usefulness in constructing and validating the conceptual model of the catchment. Different maps of segment, polygon and point were overlaid for checking location and distribution of observation wells, model boundaries, water point alignment with respect to structures, model boundaries and for other analysis. Correct zones of groundwater abstraction can also be selected using this image. Generally, the image of the study area was used as background during the construction of the numerical model and in different variations of the conceptual model for the period of calibration process.

.

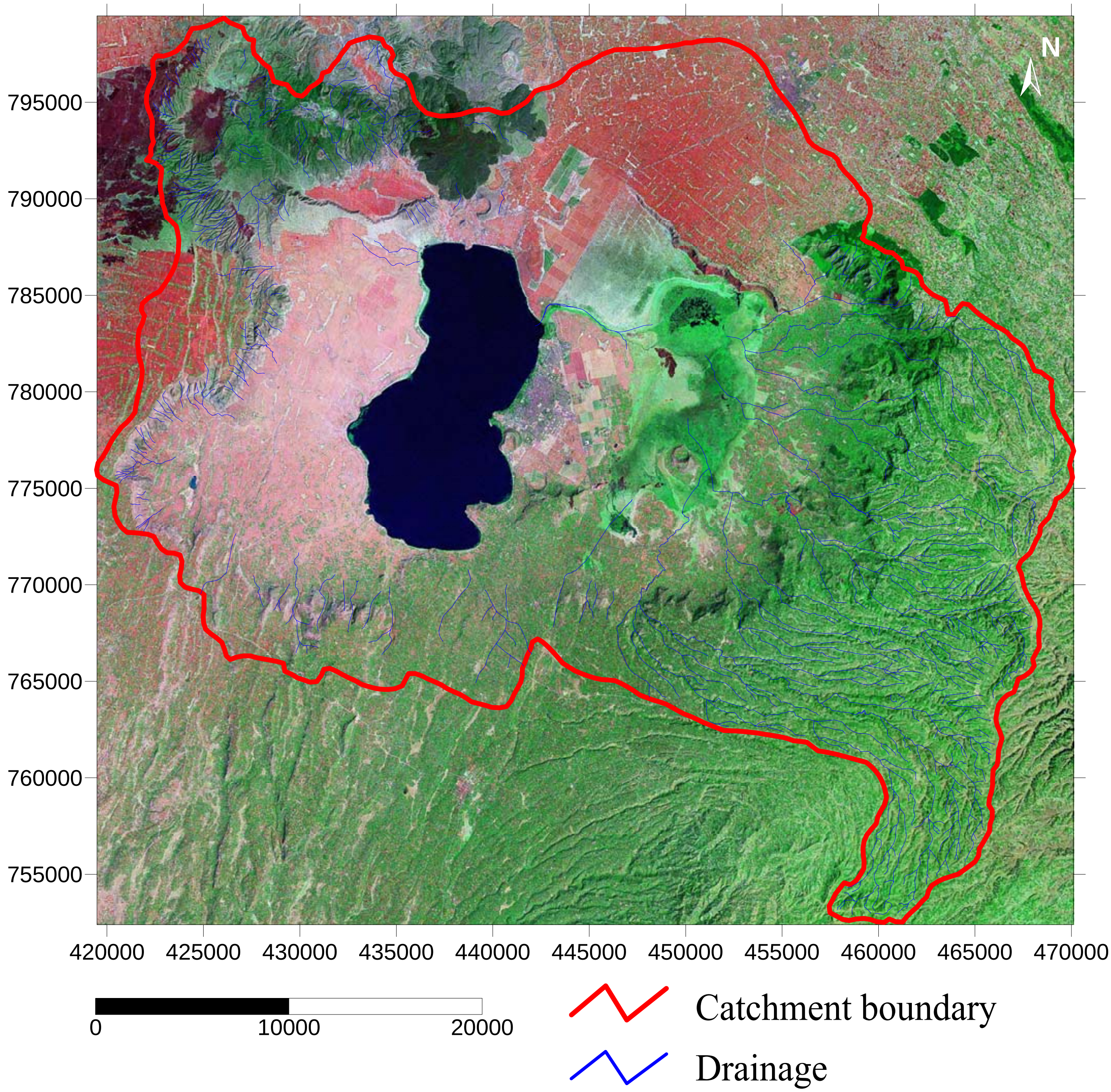

Fig. 4.8 Color composite Landsat TM image of the study area.

CHAPTER FIVE

Numerical Model

5.1 Introduction

Groundwater flow and head distribution across Lake Awassa Basin was simulated using the U.S. Geological Survey modular three-dimensional finite-difference groundwater flow model MODFLOW-2000 (Harbaugh and others, 2000). MODFLOW is a versatile finite-difference modeling program used to construct numerical flow models of specific areas. A MODFLOW model can simulate groundwater levels and fluxes on the basis of the ability of the aquifer system to transmit water (transmissivity), the portion of total porosity filled with mobile water (effective porosity), the applied hydrologic stresses (recharge and discharge), geometry and boundary conditions.

Groundwater levels were calculated at discrete points by solving simultaneous equations that approximate the partial differential equation for groundwater flow. The discrete points are the result of discretization of the model area into a series of rectangular model cells with the points (or nodes) located at the center of model cells. Steady-state simulation was performed because the purpose of the model is to simulate the ultimate effect on the flow system resulting from changes, could be recharge or discharge, in mean-annual basis, and not to determine how quickly the system responds to these changes.

The objective of constructing a numerical groundwater flow model of the Lake Awassa basin was to gain a better understanding of the aquifer system and to develop a tool for evaluating aquifer responses to various water management alternatives. The model, however, is only an approximation of the aquifer system being simulated and, therefore, cannot exactly duplicate or represent the actual system. Because model development requires the use of data, assumptions, and simplifications to approximate the system, the model is only as accurate as the assumptions and data used to develop the model.

5.2 Governing Equations

Based on Darcy's law and the conservation of mass (McDonald and Harbaugh, 1988), the movement of groundwater through porous media is described by the following partial differential equation:

$$\frac{\partial}{\partial x}\left[K_{xx}\frac{\partial h}{\partial x}\right]+\frac{\partial}{\partial y}\left[K_{yy}\frac{\partial h}{\partial y}\right]+\frac{\partial}{\partial z}\left[K_{zz}\frac{\partial h}{\partial z}\right]-W=S_s\frac{\partial h}{\partial t} \qquad (1)$$

Where:

K_{xx}, K_{yy}, and K_{zz}	are values of hydraulic conductivity in the x, y and z directions along Cartesian Coordinate Axes, which are assumed to align with principal directions of hydraulic conductivity (LT^{-1}),
h	is hydraulic head (L),
W	is a volumetric flux per unit volume and represents sinks and/or sources (T^{-1}),
S_s	is the specific storage of the porous material (L^{-1}), and
t	is time (T).

Equation (1) describes the distribution of hydraulic head and flow throughout a continuous region. Derivations of equation (1) can be found in Freeze and Cherry (1979) and Anderson and Woessner (1992).

In order to simulate the unconfined aquifer of Lake Awassa Catchment equation (2) is used which is the Boussinesq Equation.

$$\frac{\partial}{\partial x}\left[K_x h \frac{\partial h}{\partial x}\right] + \frac{\partial}{\partial y}\left[K_y h \frac{\partial h}{\partial y}\right] = S_y \frac{\partial h}{\partial t} - W \quad (2)$$

It is assumed that $T_x = K_x h$ and $T_y = K_y h$, where h is the saturated thickness, and S_y is the specific yield. Available data are limited to horizontal properties in aquifers and no relation can be established regarding the anisotropy of units. Thus, for this study, a hydraulic property within the layer is assumed isotropic. Consequently K_x and K_y are considered to be equal at any given location and K_x and K_y are replaced in this discussion by the single term K to describe horizontal hydraulic conductivity. Since the study is on a Steady State condition there is no change in head with time, therefore, this part of the right hand side of equation (2) becomes zero and it can be re-written as:

$$\frac{\partial}{\partial x}\left[K_x h \frac{\partial h}{\partial x}\right] + \frac{\partial}{\partial y}\left[K_y h \frac{\partial h}{\partial y}\right] + W = 0 \qquad (3)$$

Because of its continuity in space and time, generally equation (3) cannot be solved analytically for practical applications involving complex systems as Lake Awassa Basin. As a result, numerical methods are employed where a set of spatially and temporally discrete points replace the continuous system described by equation (3) in a process of discretization. Equation (3) is then replaced by a set of simultaneous algebraic equations that describe the distribution of hydraulic head at each point, and flow through the system in response to this head distribution. These simultaneous equations are set up in matrix form and then solved. There exist several techniques to solve the set of simultaneous equations. In this model, the Preconditioned Conjugate Gradient method of Hill (1990) was used as a solver. Discussions of the finite-difference method, which is the numerical technique used in this study, can be found in Anderson and Woessner (1992).

5.3 Spatial Discretization

The numerical method applied to use equation (3) requires that the modeled domain be divided into discrete volumes, called cells. The three-dimensional array of cells is known as the model grid. The center of each cell defines the point for which hydraulic head is determined and it is taken to represent the average head within the cell.

The model area corresponding to the study area of 1376km^2 and it was selected on the basis of preliminary numerical modeling. Extent of the modeled area is 50 km easting by 46 km northing and contains the entire study area shown in figure 2.1. The model uses a uniform grid size of 200 m by 200 m and contains 57,500 cells, 1 layer, 250 columns and 230 rows. The southwest corner of the model grid is located at UTM: 419923 Easting and 752854 Northing. The irregular shape of the study area reduced the number of active cells in the model to 34277. The regular grid spacing facilitated data input from a Geographic Information System (GIS) and analysis of model output by the GIS, and the grid size minimized errors in flow-path analysis that would be caused by a large grid size (Pollock, 1994; Zheng, 1994). Figure 6.1 shows the model grid containing cells representing lateral boundary conditions (no-flow and general head boundary), flow packages (river and well package), active, inactive and constant head representing the two lakes.

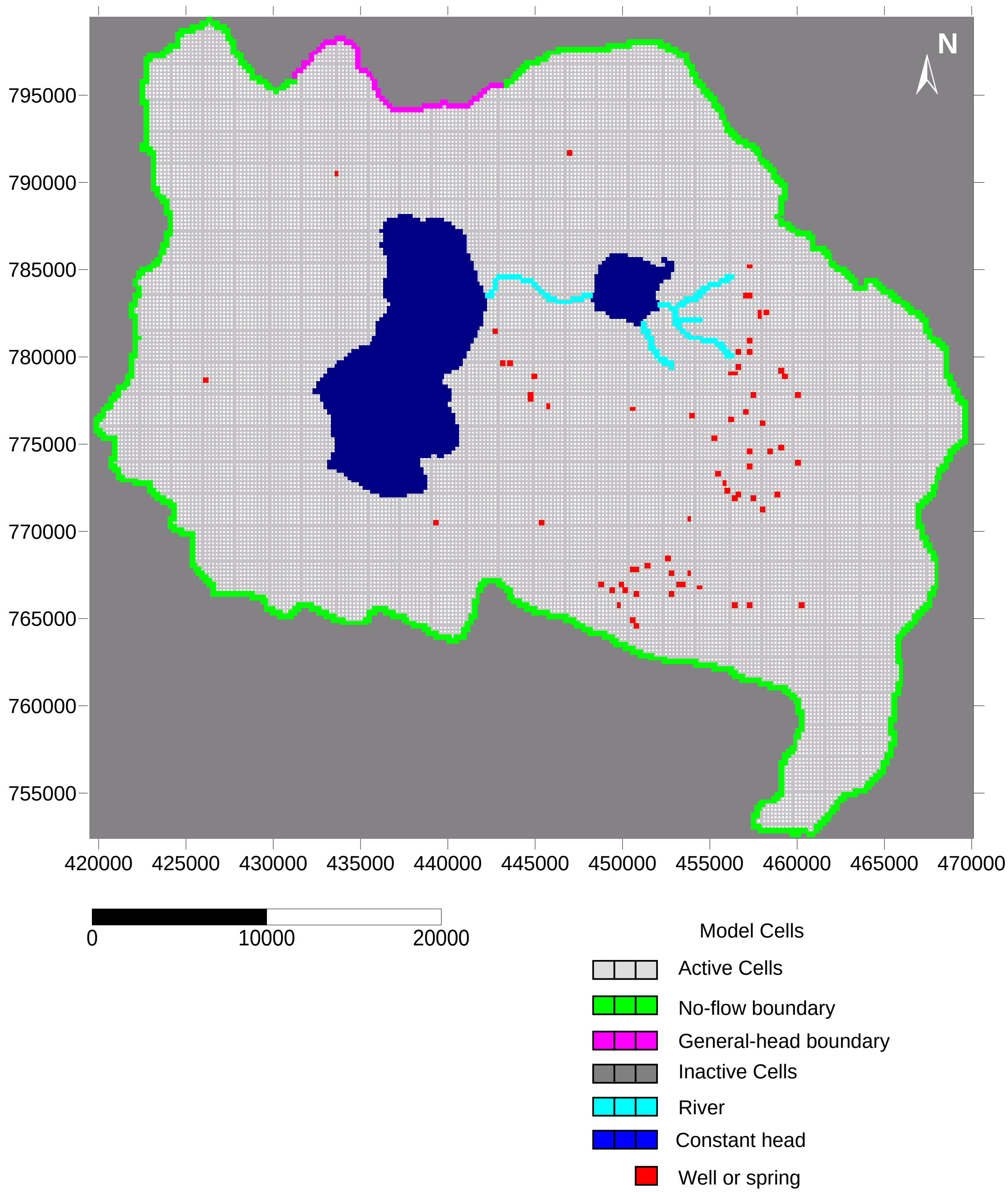

Fig.5.1 Model grid and lateral boundary conditions.

The model has a variable thickness where the upper boundary of the model is the water table whereas the bottom corresponds to the top of the bedrock. Thicknesses were assigned ranging from 80m, around the lacustrine sediments, to more than 200m, to areas near the model boundary where data on bedrock depth are sparse. The thickness of the layer is adequate to account for the anticipated range of water level variation within the aquifer during groundwater flow simulation which was modeled using unconfined aquifer hydraulic properties.

Because the finite-difference model grid must be rectangular, certain cells passing the catchment boundary may represent areas outside the modeled area with different kinds of shape. Such cells are considered inactive and the ground-water flow equation is not solved for them even though part of them, less than 50% of the cell size, is within the catchment boundary.

5.4 Boundary Conditions

In Lake Awassa basin, hydrologic and geologic boundaries control the ground water flow system. Boundary conditions define the geographic extent of the flow system as well as the movement of ground water into and out of the system, such as flow to or from streams.

Three types of boundary conditions were used to define the ground-water flow system in the Lake Awassa Basin: no-flow boundaries, specified-flux boundaries and head-dependent flux boundaries. Geologic or hydrologic barriers to ground-water flow were simulated using no-flow boundaries. In the study area, the contact between the permeable groundwater flow system and nearly impermeable bedrock is an example of a no-flow boundary. Known or estimated hydrologic fluxes, such as recharge and well discharge, are represented using specified-flux boundaries. A head-dependent flux boundary is one across which ground water moves at a rate proportional to the hydraulic-head gradient between the boundary and the ground-water system. Streams are usually represented as head-dependent flux boundaries because the movement of ground water to or from a stream is proportional to the difference between the head in the aquifer and the stage of the stream. Groundwater flow across catchment boundary is similar in concept to streams.

Boundaries in the Lake Awassa Basin regional groundwater flow model are divided into two broad categories. The first group includes boundaries related to the geographic extent of the regional aquifer system, such as contacts with effectively impermeable bed rock units. The second group includes boundaries within the model extent related to hydrologic processes or features, such as stream systems.

5.4.1 Geographic Boundaries

The geographic boundaries of the Lake Awassa Basin regional groundwater model were chosen to correspond as closely as possible with natural hydrologic boundaries across which groundwater flow can be assumed negligible, such as groundwater divides, or can be reasonably estimated. In the study area major topographic divides are often considered no-flow boundaries because topographic divides are typically coincident with ground water divides. Groundwater on either side of a groundwater-divide flows away from the divide and not across it, so the divide itself acts as a no-flow boundary. Topographic divides often coincide with groundwater divides because upland areas commonly have larger amounts of precipitation and recharge than surrounding areas, so the water table surface develops a coincident high elevation region from which groundwater flow diverges.

The lateral boundaries of the Lake Awassa Basin flow model are generally represented as no-flow boundaries, with the exception of one area, northern part of the catchment, where it is represented as head-dependent flux boundary due to the out going groundwater to the adjacent Ziway-Shalla Lake Catchment. Estimation equal to 12,345m^2/day for the outgoing groundwater was made by Tenalem Ayenew (1998). Annual groundwater outflow from the catchment to neighboring catchment was estimated to be around 313.9MCM, Yemane Gebreegziabher (2004).

The lower boundary of the model corresponds to the contact of the permeable rocks with underlying impermeable rock units and this lower boundary of the model is simulated as a no-flow boundary.

5.4.2 Hydrologic-Process Boundaries

The second broad categories of boundaries in the model of Lake Awassa Basin are those related to hydrologic processes including recharge, ground-water flow to and from streams, pumpage and groundwater outflow to the adjacent Ziway-Shalla Basin.

Groundwater recharge represents a specified-flux boundary condition. Recharge to the groundwater system was given by considering sources of groundwater from infiltration of precipitation and deep percolation of applied irrigation water. It is simulated as a specified flux to the uppermost layer of the model using five different zones based on the previously developed conceptual model. The first zone in the conceptual model that is high direct recharge over the highland & escarpment is given initial value of 140 MCM/year. Zone of moderate recharge with associated local discharge areas over the caldera rims is given initial value of 120 MCM/year. The third zone which is intermediate recharge zone over caldera walls & volcanic hills is given 100 MCM/year. The remaining two zones which are the floor with localized direct recharge during high rainfall and zones of local recharge areas over the volcanic domes & necks are given initial values of 80 MCM/year and 60 MCM/year respectively. During model calibration these recharge values were adjusted.

The movement of ground water to and from perennial rivers is another important boundary condition. The flux of water between the ground-water system and rivers is, in part, dependent on the hydraulic head in the ground-water system and is simulated as a head-dependent flux boundary. Cells in the model that correspond to the locations of perennial streams (fig 6.1) are mathematically represented in a manner that allows ground water to move between the aquifer and stream with a direction and magnitude that depends on the head relations. Streams were simulated using River Package, which is used to simulate the flow of water between an aquifer and an overlying source reservoir which is usually a river or a lake.

In a model cell containing river parameters, the rate of leakage between the river and the aquifer (Q_{riv}) is calculated from;

$$Q_{riv} = C_{riv} \cdot (h_{riv} - h) \qquad h > B_{riv}$$

Where

h_{riv} is head in the river

h is the head in the aquifer directly below the river

B_{riv} bottom of the streambed

C_{riv} is the streambed conductance which accounts for the length (L) and width (W_{riv}) of the river channel within the cell, the thickness of the riverbed sediments (M_{riv}), and their vertical hydraulic conductivity (K_{riv}), where

$$C_{riv} = \frac{K_{riv} \; L \; W_{riv}}{M_{riv}}$$

When the water table falls below the bottom of the streambed (B_{riv}), leakage stabilizes and the leakage rate through the riverbed (Q_{RIV}) is given by

$$Q_{riv} = C_{riv} \cdot (h_{riv} - B_{riv}) \qquad h \leq B_{riv}$$

Cells in the model representing stream-aquifer relations (River cells) are shown in figure 6.1. These include Tikur Wuha River and most perennial tributaries. The movement of ground water to or from streams is a function of the head in the stream, h_{riv}, also known as stream stage. Stream stage is the elevation of the water surface in the stream, and a single value must be chosen to represent the stream across the entire cell. Stream stages used in this simulation were determined by picking an approximate median stream elevation within the cell based on the observed field value, Digital Elevation Model (DEM) derived from a 90m-resolution Shuttle Radar Terrain Model (SRTM) image and 1:50,000-scale topographic maps.

The streambed conductance, C_{riv}, controls the rate at which water moves to or from a stream in response to a given head gradient. Direct measurements of streambed conductance are rare and these terms are usually derived empirically during model calibration. Streambed conductance terms were initially calculated for Tikur Wuha River using a streambed thickness of 1.2 m, stream widths of 10 m, and a vertical hydraulic conductivity of 30 m/day. For Wesha, Werka, Wetera, Lango and Gomesho Rivers a streambed thickness of 1 m, stream widths of 7 m, and a vertical hydraulic conductivity of 25 m/day were used. The hydraulic-conductivity value was then adjusted during model calibration.

The General-head boundary package was used to simulate underflow from the catchment to the neighboring Ziway-Shalla Basin. A general-head boundary simulates a source of water outside the model area that either supplies water to, or receives water from, adjacent cells in proportion to the hydraulic-head differences between the source and model cell.

The exchange rate of water between the model cell and the outside source or sink is given by the equation

$$Q = C\ (HB - h)$$

Where

Q is the rate of flow into or out of the model cell [L^3/T],

C is the conductance between the external source or sink and the model cell [L^2/T],

HB is the head assigned to the external source or sink [L], and

h is the hydraulic head within the model cell [L].

Values of C were initially calculated using the equation;

$$C = K \cdot L$$

Where

K is the hydraulic conductivity between the model cell and the boundary head [L/T], and

L is the length of the general-head boundary within a cell

The initial values of C, ranging from 500–1,200 m^2/day, were distributed across the model cells adjacent to the general-head boundary. The boundary head in the adjacent catchment was assigned an initial head that was slightly less than the water table altitude of the model cells around the general-head boundary. The final values of C and head in the adjacent catchment, determined during model calibration are 1,000m^3/d (showing high conductance due to conduting structures) and 1640m respectively. The total groundwater outflow across the boundary is 115724m^3/d (4.2×10^7 m^3/year), higher than the estimate made by Tenalem Ayenew (1998) and lower than estimate made by Yemane Gebreegziabher (2004).

The final hydrologic process boundary condition in this discussion is groundwater pumpage, which is simulated as a specified flux. In the study area there are irrigation, public supply and individual domestic wells pumping from the aquifer. Specified fluxes are removed from cells corresponding to the geographic locations of the wells and springs. The geographic distribution of pumping wells and discharge by springs in the model is shown in figure 4.6.

5.5 Initial Conditions

Initial conditions are boundary conditions in time since it refer to head distribution everywhere in the system at the beginning of the simulation. If the field-measured head values were used as initial conditions, the model response in the early time steps would reflect not only the model stress under study but also the adjustment of model head values to offset the lack of correspondence between model hydrologic inputs and parameters and the initial head values, Franke et al. (1987).

In the model, user specified initial head distribution obtained from the first steady-state simulation was used as initial and prescribed hydraulic head for the model, where the first steady-state simulation uses initial and prescribed hydraulic head by subtracting 10 m from Top of Layer of the model obtained from a 90m-resolution Shuttle Radar Terrain Model (SRTM) image, using Global Mapper and Surfer.

5.6 Hydraulic Properties

Groundwater flow within the model layer was assumed to be horizontal. Hydraulic conductivity and transmissivity are properties that, in conjunction with the horizontal hydraulic gradient, control horizontal flow of groundwater in the aquifer. Hydraulic conductivity is a measure of the water transmitting properties of aquifer material; coarse and/or well-sorted material has a higher hydraulic conductivity than fine and/or poorly sorted material. Transmissivity is the product of hydraulic conductivity and saturated thickness and represents the water-transmitting properties of the saturated section of the aquifer.

Previously published values were used as general indicators for hydraulic conductivity values and distributions; however, model calibration carried the most weight in determining the final values and distributions. Hydraulic conductivity values and the spatial distribution of zones were varied by trial and error to obtain an optimum fit to observed hydraulic heads. Greater discretization of zones could have improved the fit by adjusting hydraulic conductivities near individual wells or very small groups of wells; however, the data did not support this degree of heterogeneity. Therefore, the calibration accuracy obtained using the larger zones shown in figure 6.2 was considered sufficient to fulfill the objectives of this study.

In addition to the trial-and-error methods used, zone delineation for hydraulic properties was determined by considering potential structural features and geology to achieve best possible fit to observed data. Initially, based on the conceptual model, six major zones of horizontal hydraulic conductivity has been placed throughout the model area, which were determined on the bases of existing pumping test data, lithology acquired by means of well logs, hydrogeologic and geologic map, which was given priority. The initial estimate of hydraulic conductivity, which was determined by taking the average value of the ranges given by the conceptual model, varies from 0.05 to 100 m/d. These horizontal hydraulic conductivity values were adjusted during model calibration. The presence of structures makes the resulting horizontal hydraulic conductivity and transmissivity data spatially variable in the study area.

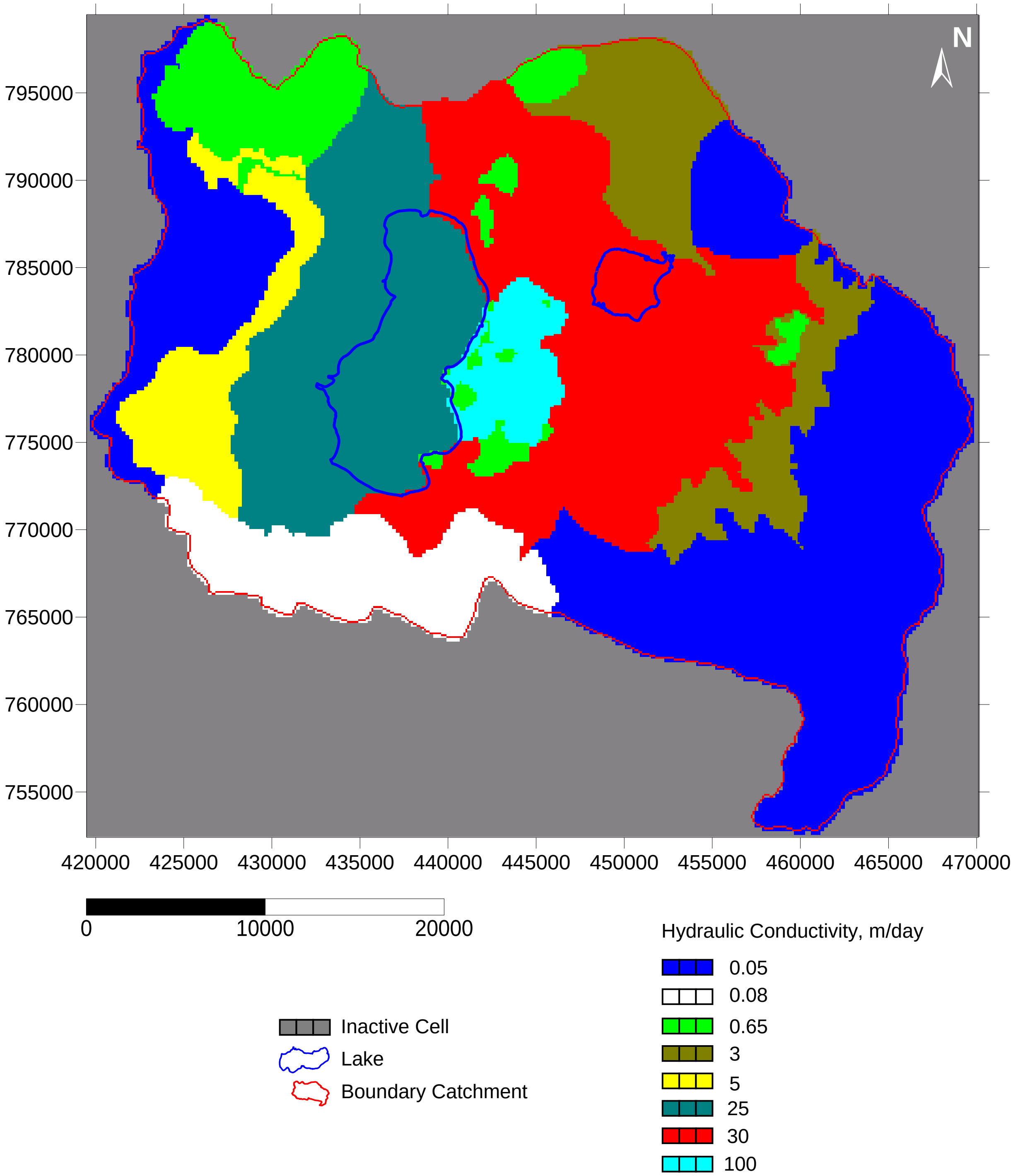

Fig. 5.2 Adjusted hydraulic conductivity zonation and values, in meter per day.

These six zones were used as a starting point for the delineation of sub zones when necessary. Using trial and error model calibration, sub zone delineation and estimated values were determined within reasonable limits estimated during the conceptual model. Since it is unconfined aquifer, the model was allowed to calculate changes in the transmissivity as the saturated thickness changes in the aquifer. The Effective porosity was set to 0.25, a default effective porosity value in MODFLOW.

The final estimates of horizontal hydraulic-conductivity value for the model ranges from 0.05 m/day to 100 m/day and the values and zonation is shown in figure 6.2. The spatial distribution of horizontal hydraulic conductivity estimated by Wondwosen Mekonnen (2005), figure 4.2, is in general agreement with that shown in figure 6.2. Generally, the hydraulic-conductivity is highest (100 m/day) near the center of the basin, where younger lacustrine sediments makes up a greater part of the aquifer.

5.7 Stresses

5.7.1 Recharge

Hydraulic heads in the groundwater flow system respond to stresses on the system, which correspond to recharge and discharge. Recharge to the model consisted of infiltration from direct precipitation, stream infiltration draining the eastern escarpment and artificial recharge of irrigation-return flow. Recharge was applied to the active model area as a spatially varying, specified flux to the highest active cell. In general, precipitation recharge varies spatially with land-surface permeability, which is a function of soil characteristics and land use, and spatial distribution and intensity of rainfall.

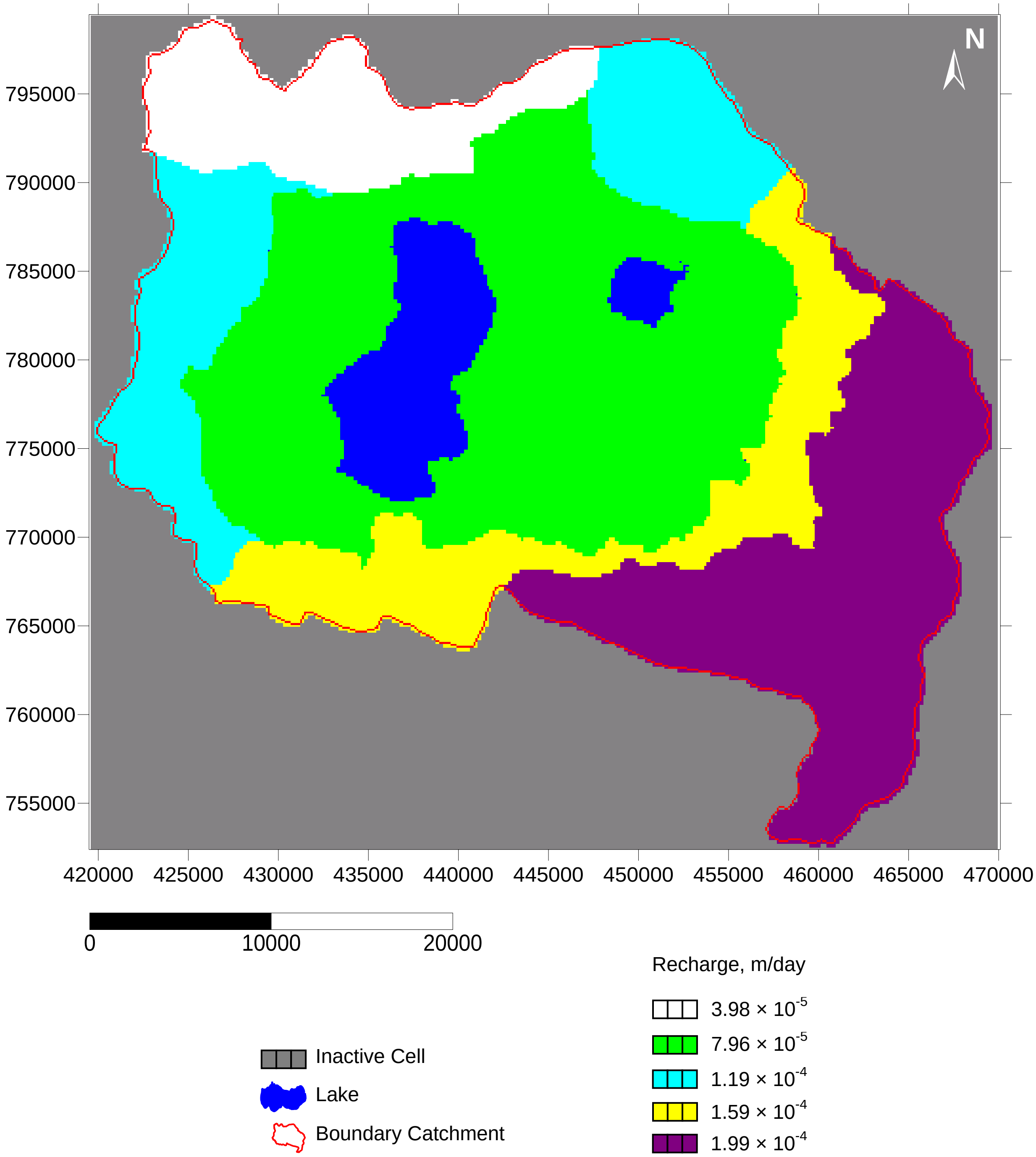

Fig. 5.3 Simulated recharge zonation and values, in meter per day.

Five recharge categories were defined with thirteen types of land use (Bare land, Cultivated land, Dense bushy woodland, water, Open bush land, Open bushy woodland & cultivated land, Open bushy woodland, Open grassland, Open shrub land, Open grassland & open shrub land, Shrubby grassland, Swampy grassland and Urban built-up), and different variables, such as hydro-metrological, geologic and hydrogeologic condition were used to develop a range of recharge rates for the study area. The initial recharge categories and associated rates were based on previous study made by Wondwosen Mekonnen (2005) and ranged from 1.195×10^{-4} m^2/day, for zones of local recharge areas over the volcanic domes & necks, to 2.787×10^{-4} m^2/day, for zone of high direct recharge over the highland & escarpment in the conceptual model. These recharge ranges were lowered to 3.98×10^{-5} m^2/day and 1.99×10^{-4} m^2/day respectively during the steady-state model calibration to get the best fit between simulated and observed hydraulic heads. The aerial distribution of simulated recharge is presented in figure 6.3.

5.7.2 Discharges

In the study area, discharge from groundwater systems includes groundwater pumpage, groundwater outflow to the adjacent Ziway-Shalla Basin and discharge to stream and springs. In the model, different MODFLOW-2000 packages were used to simulate these discharge components.

Discharge to streams were represented using the river package in MODFLOW-2000 and was used to simulate the hydraulic connection between groundwater and surface water by allowing streams to gain or lose water, based on the difference between the surrounding hydraulic head and stream stage, through riverbed material of a specified hydraulic conductance (McDonald and Harbaugh, 1988). Estimated riverbed conductance was based on model calibration. Model cells were designated as river cells along major streams and tributaries where the groundwater table intersected the land surface (figure 6.4).

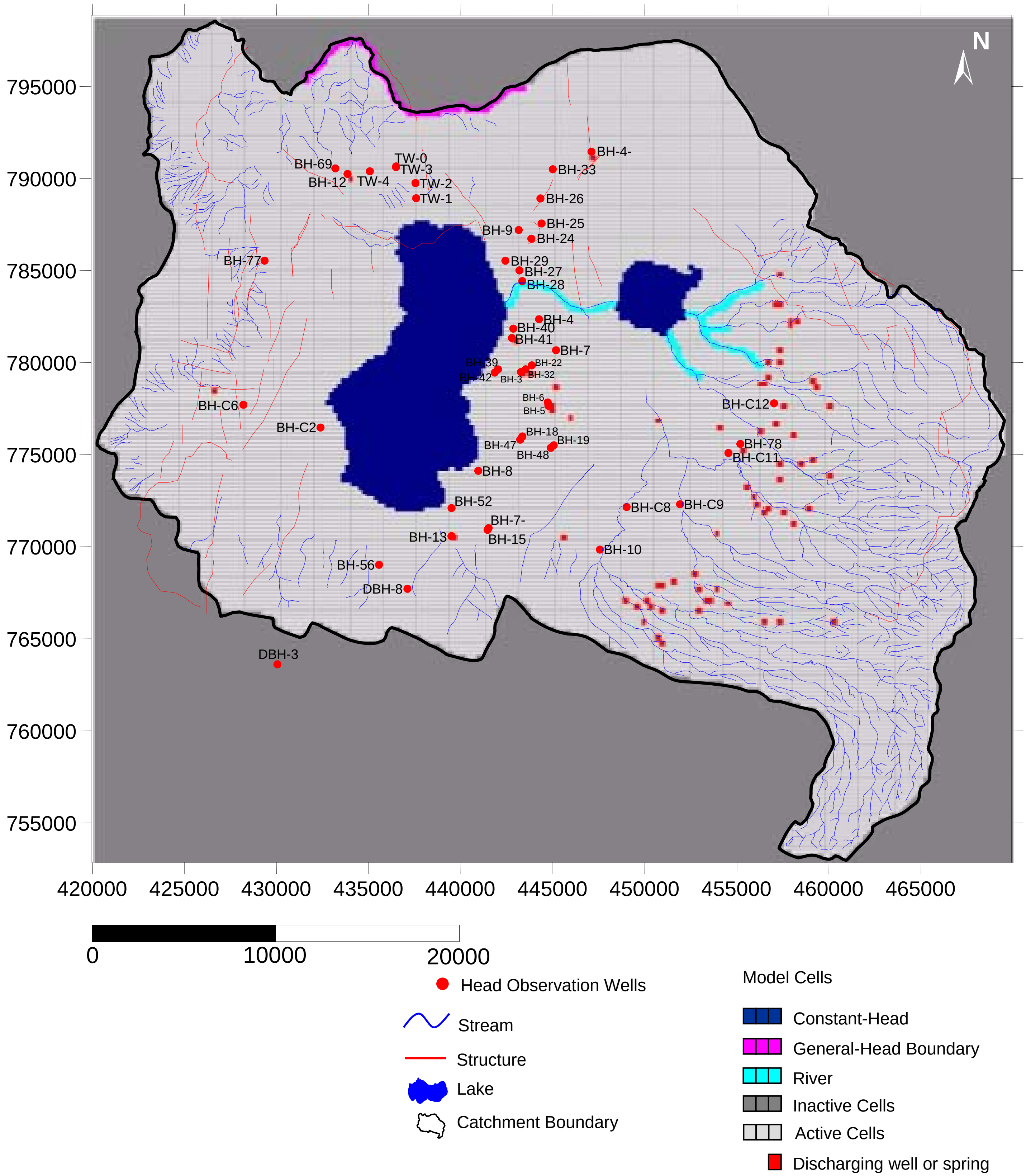

Fig. 5.4 A map showing discharge (Stream, Well & spring, General-head boundary), Head observation wells, Drainage and Structure.

In the study area, pumping wells and groundwater withdrawals from high yielding springs (such as Loke cold spring supplying water to Awassa town and surrounding areas with a yield of 20 l/sec), were simulated with the Well Package for MODFLOW-2000.

From previous studies and from groundwater table map of the study area, there is an indication of groundwater outflow towards northward to Lake Shalla, which was simulated using a general-head boundary at the northern periphery of the model. The final values of conductance, obtained from steady state calibration, between the external sink and the model cell, and head in the adjacent catchment are 1,000m^3/d and 1640m respectively, which result in a groundwater outflow equal to 115724m^3/d across the general-head boundary.

Withdrawals from pumping wells and high yielding springs were simulated as specified flows from the aquifer. Because there was limited well-construction data available, all wells were assumed to be fully penetrating in the layer.

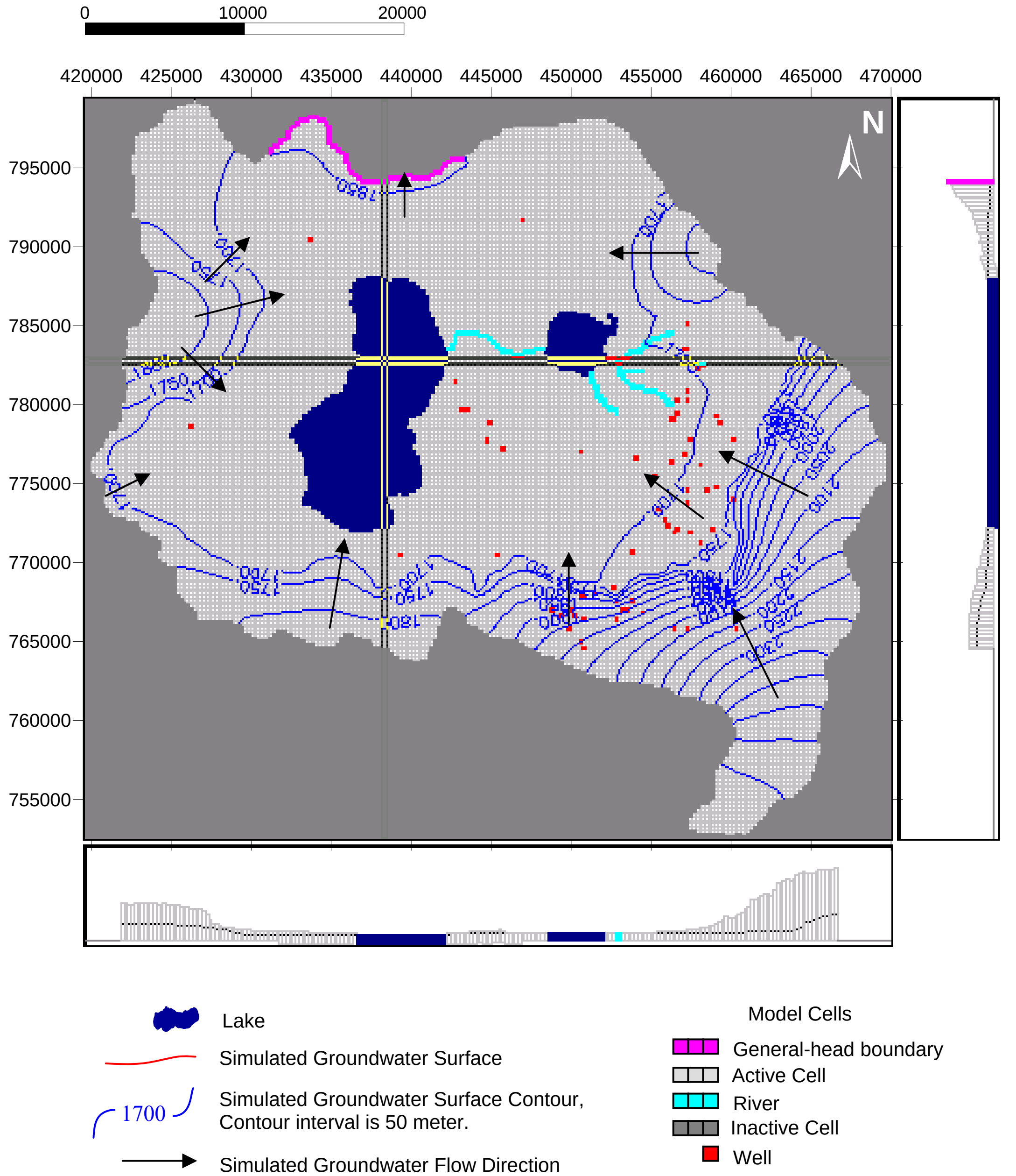

Fig. 5.5 Model-calculated steady-state water table, flow direction and X – section along Row-82 and Column-93.

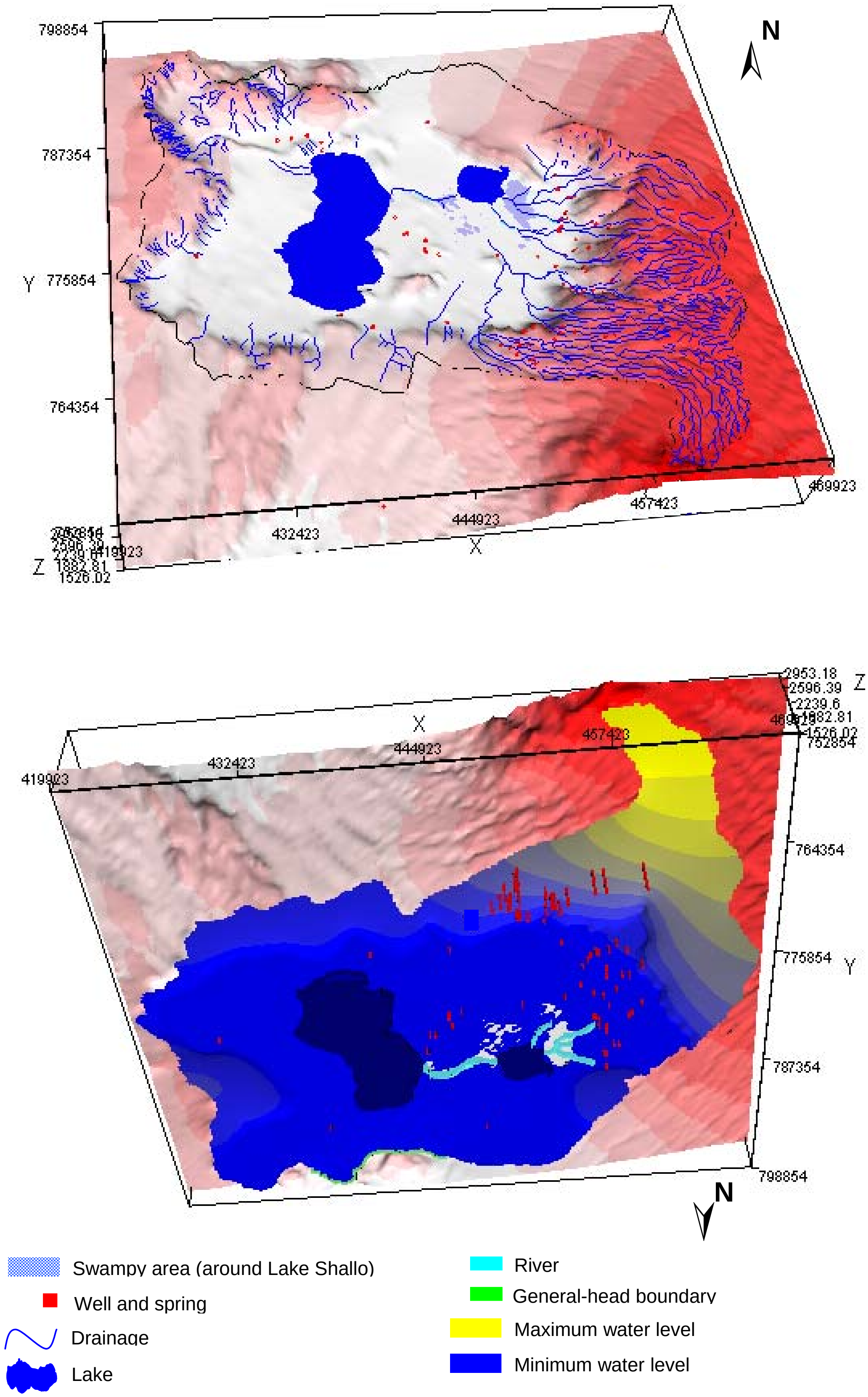

Fig.5.6 3D-View of top and bottom of the catchment

CHAPTER SIX

Calibration and Sensitivity Analysis

6.1 Model Calibration

Model calibration is the process whereby model parameter structure and parameter values are adjusted and refined to provide the best match between measured and simulated values of hydraulic heads and flows. The model is calibrated by a trial-and-error process in which model parameters are adjusted within reasonable limits from one simulation to the next to achieve the best model fit. Model fit is commonly evaluated by visual comparison of simulated and measured heads and flows or by listing measured and simulated heads together with their differences and some type of average of the differences, which is then used to quantify the average error in the calibration. The objective of calibration is to minimize this average error which is called calibration criterion.

The trial-and-error method provided satisfactory results for the steady state calibration and met the overall goals of the study. The Lake Awassa Basin regional steady-state groundwater model was calibrated to average conditions from 2004 to 2006. This period was chosen because much of the data collection for the study occurred during this time. Water level measurements for 49 wells that were used for estimation of groundwater level of the aquifer were considered for calibration of the steady state model. These head observations were not evenly distributed throughout the model domain but were clustered in the central part of the study area that is on the Volcano-Lacustrine Sediment (fig.6.4). The time of measurements of some wells were somewhat uncertain, as a result, head data were examined carefully and anomalous values due to measurement or location errors were removed from the calibration data set before the final 49 wells were selected.

Prior to the calibration of the model, there were criteria established to assess the simulation results in relation to measured data. The first calibration criterion for the simulation was that the simulated groundwater surface and hydraulic gradient generally match those of the estimated one, which were done by comparison of the two.

A second calibration criterion takes account of matching more than 95 percent of all wells to within ±10 meter of the observed hydraulic heads. This second criterion was considered satisfactory because 10 meter is about 0.95 percent of the difference between the maximum (which is 2664m in the southeastern part of the catchment) and minimum (which is 1617m in the northern part of the study area where groundwater goes out of the catchment to the adjacent Ziway-Shalla catchment) hydraulic heads of the estimated average groundwater surface in the model area.

To provide an overall indication of the quality of the calibration, summary statistics on the difference between simulated and measured water levels were calculated after model calibration. The root mean squared error (RMSE) and the mean error (ME) are common ways to express the average difference between simulated and measured water levels (Anderson and Woessner, 1991).

Steady-state flow conditions exist when inflow is equal to outflow, and aquifer storage does not change with time .Hydraulic heads for steady-state conditions are sensitive to the amount of water that recharges to and discharges from the groundwater system; the hydraulic conductivity of the aquifer system; the conductance across the faults and structures that are common in the basin and aquifer thickness.

Therefore, the steady-state simulation consisted of modifying the initial estimates of hydraulic conductivity, the quantity and distribution of recharge, fault parameters (hydraulic characteristics), boundary conditions and aquifer thickness to match observed water levels. Modification of these parameters were done (1) by matching simulated results to the conceptual model of the groundwater level and flow system, including distributions of recharge and discharge areas, and directions of flow; (2) by being faithful to the hydrogeologic and overall geologic understanding of the study area; and (3) by maintaining reasonable values of hydraulic properties as defined by field data.

The values of effective porosity were not changed from the initial values during the model calibration process because reasonable changes in these values had negligible affect on model results. Pumpage rates were derived independently and were considered reasonably reliable; as a result values were not changed during calibration.

Based on the calibration criteria set for the model, where the first one is simulated groundwater surface and hydraulic gradient generally match those of the estimated one. Comparison between contour maps of measured and simulated heads (figure 7.2) were done to get some idea on the spatial distribution of error in the calibration. The simulated water level gradient of the southeast part of the catchment is less than the measured gradient. In this part of the catchment, the difference between the measured and simulated water level contours is due to lack of available water level data and due to interpolation error of the measured gradient. In general the simulated groundwater surface is similar to the estimated average groundwater surface in comparison to both hydraulic heads and gradients, which approves fulfillment of the first criterion.

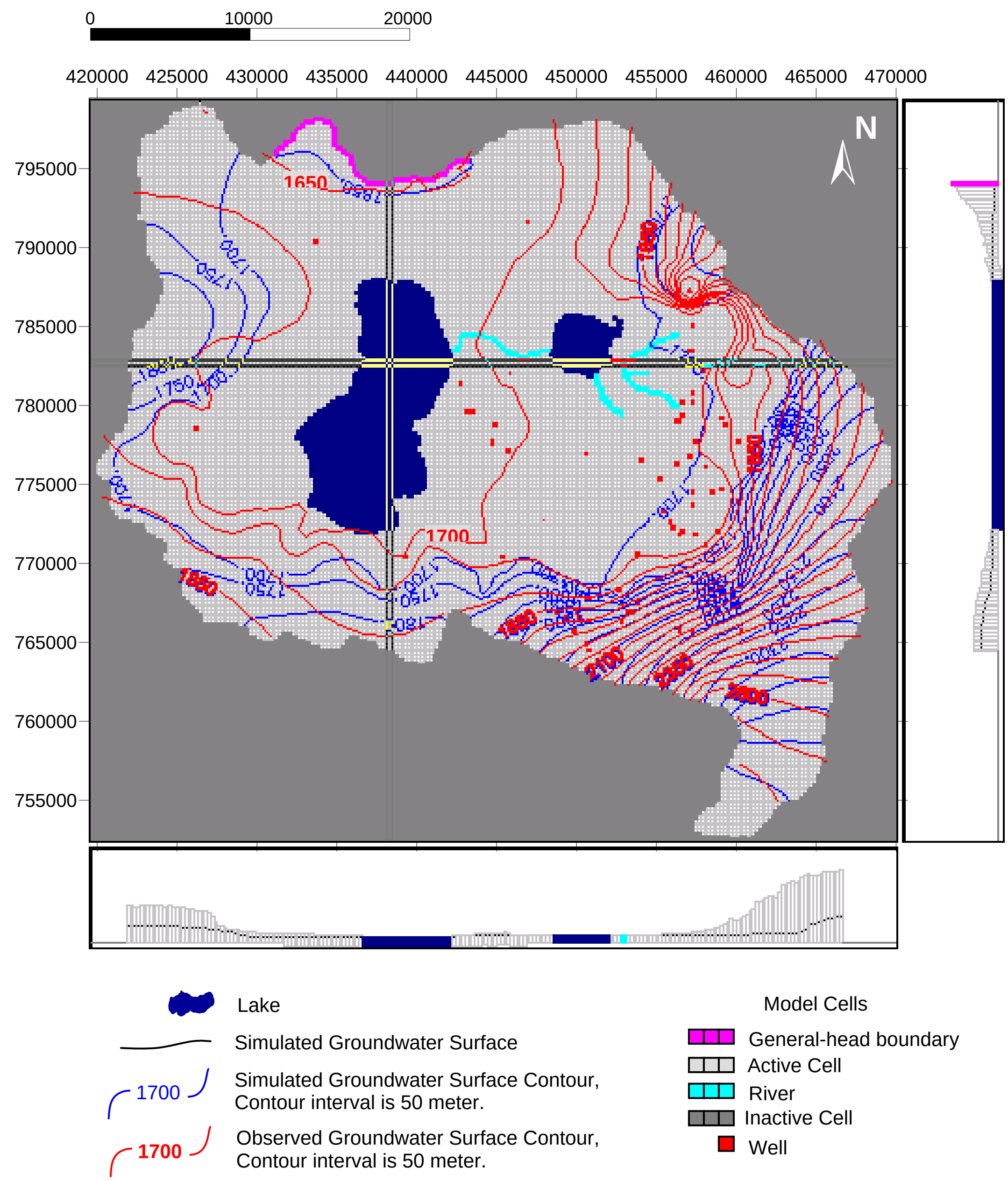

Fig. 6.1 Model-calculated and observed steady-state water table, and X – section along Row-82 and Column-93.

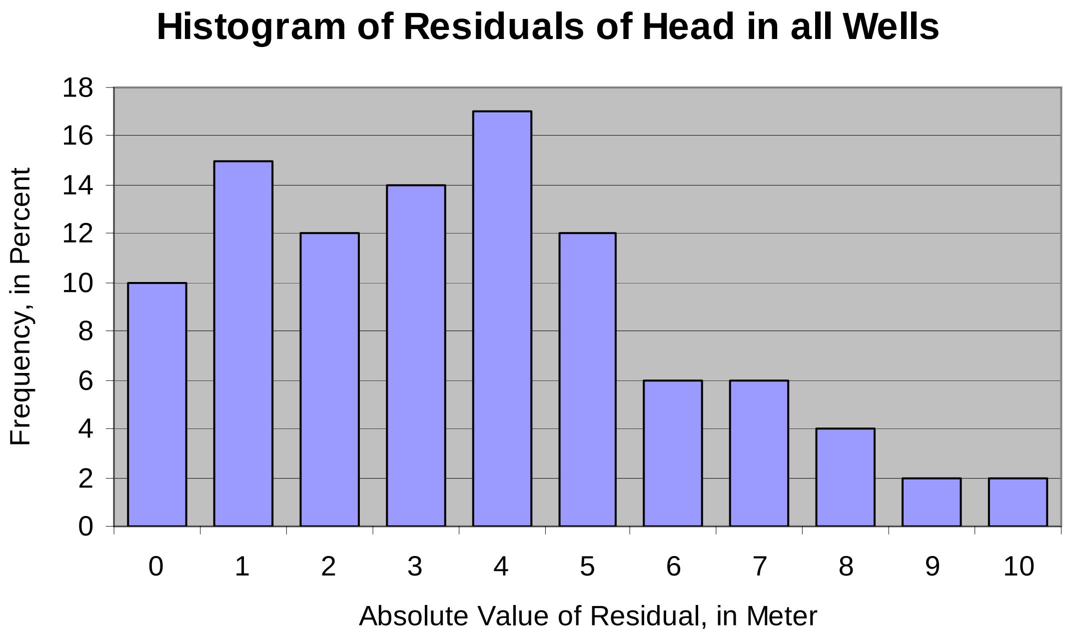

Fig.6.2 Histogram of residuals of estimated average observed and steady-state simulated hydraulic head in all wells.

The second calibration criterion is matching more than 95 percent of all wells to within ±10 meter of the observed hydraulic heads. Simulated hydraulic heads were within ±10 meter of the observed hydraulic heads for all the wells used in the calibration. A histogram shows the distribution of the difference between the observed and simulated hydraulic heads (residuals) (Figure 7.3). Out of the 100 percent of the wells (all the 49 wells), 80 percent of the wells have simulated hydraulic heads within ±5 meter of the observed hydraulic heads, whereas the remaining 16 and 4 percent of the 49 wells have simulated hydraulic heads between ±5 and ±8, and ±8 and ±10 meters of the observed hydraulic heads respectively. The fit was considerably better for wells found east of Lake Awassa and lesser for those found west of Lake Awassa. Observation well data were weighted more heavily in calibration because of a higher degree of confidence in that data. Table 7.1 shows the 49 wells with their simulated and observed groundwater altitudes and their difference.

		Groundwater altitude, in meters			
No.	Observation name	Calculated	Observed	Residual	Residual Square
1	BH-3	1684.5	1689	4.5	20.25
2	BH-4	1687.7	1688	0.3	0.09
3	BH-5	1685.5	1684	-1.5	2.25
4	BH-6	1685.5	1684	-1.5	2.25
5	BH-7	1687	1689	2	4
6	BH-9	1683.7	1693	9.3	86.49
7	BH-12	1671.8	1662	-9.8	96.04
8	BH-13	1682.1	1684	1.9	3.61
9	BH-15	1689.8	1694	4.2	17.64
10	BH-24	1684.5	1684	-0.5	0.25
11	BH-25	1683.5	1680	-3.5	12.25
12	BH-26	1681.3	1688	6.7	44.89
13	BH-27	1686.7	1682	-4.7	22.09
14	BH-28	1689.1	1681	-8.1	65.61
15	BH-29	1683.7	1683	-0.7	0.49
16	BH-32	1684.8	1690	5.2	27.04
17	BH-33	1676.4	1681	4.6	21.16
18	BH-39	1684.2	1686	1.8	3.24
19	BH-40	1686	1682	-4	16
20	BH-41	1686	1686	0	0
21	BH-42	1683.4	1687	3.6	12.96
22	BH-47	1685	1686	1	1
23	BH-48	1685.7	1682	-3.7	13.69
24	BH-52	1681.3	1684	2.7	7.29
25	BH-56	1751.4	1756	4.6	21.16
26	BH-69	1672	1673	1	1
27	BH-77	1753.5	1760	6.5	42.25
28	BH-78	1697.8	1694	-3.8	14.44
29	TW-0	1667.7	1671	3.3	10.89
30	TW-1	1675.7	1677	1.3	1.69
31	TW-2	1671.7	1677	5.3	28.09
32	TW-3	1668	1671	3	9
33	TW-4	1670.1	1663	-7.1	50.41
34	BH-C6	1683.1	1680	-3.1	9.61
35	BH-C3	1681.5	1687	5.5	30.25
36	BH-C2	1680.5	1685	4.5	20.25
37	DBH-8	1773.7	1777	3.3	10.89
38	BH-26-	1682.1	1684	1.9	3.61
39	BH-8	1681.1	1684	2.9	8.41
40	BH-7-	1688	1696	8	64
41	BH-18	1684.9	1686	1.1	1.21
42	BH-22	1685.8	1693	7.2	51.84
43	BH-19	1685.7	1682	-3.7	13.69
44	BH-4-	1677.9	1680	2.1	4.41
45	BH-10	1724.4	1727	2.6	6.76
46	BH-C8	1692	1698	6	36
47	BH-C9	1694.4	1694	-0.4	0.16
48	BH-C11	1697.5	1698	0.5	0.25
49	BH-C12	1698.9	1705	6.1	37.21

Table 6.1 Model-calculated steady-state water levels and observed water levels for all wells.

In addition to the above criteria, the quality of the calibration is evaluated by calculating summary statistics on the difference between simulated and measured water levels. The root mean square error (RMSE) or standard deviation, which is the average of the squares differences in measured and simulated heads, for all wells was 4.42 meter. The mean error, which is the mean difference between measured and simulated heads, was 1.4 meter, which indicates a model bias toward underestimating head values. Table 6.1 shows the root mean square error (RMSE) and mean error (ME) of calibration results. A linear regression analysis of simulated and observed hydraulic heads for all wells (Figure 7.4) yielded a coefficient of correlation and variance equal to 0.98 and 19.5 respectively.

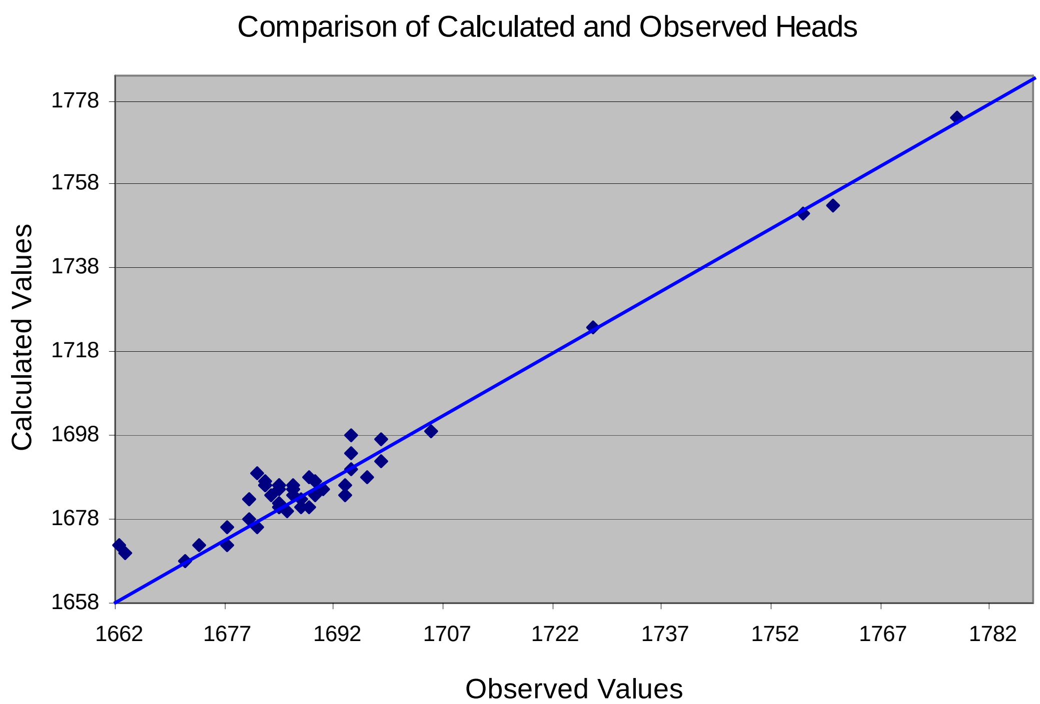

Fig.6.3 Linear regression of observed and simulated hydraulic heads for all wells.

Most of the wells diverging from the observed heads, as shown on the linear regression, are found around the eastern escarpment and highland where there is no sufficient data on the observed groundwater surface. There are also some wells diverging from the observed value around Tikur Wuha River which could be the influence of the river on the calculated head during the steady state model calibration.

Using the calibrated model, water budget of the whole model domain was calculated with a percent discrepancy of 0.04. It includes the following inflow components to the ground water flow system: (1) recharge from Constant Head Boundary, with a value of 21.2 MCM/year (5.8×10^4 m^3/day). (2) Groundwater recharge from precipitation, which is 55.5 MCM/year (1.5×10^5 m^3/day) and (3) Groundwater inflow from River Leakage with value equal to 151 MCM/year (4.1×10^5 m3/day). Total inflows were 227.7 MCM/year (6.2×10^5 m^3/day).

The simulated groundwater outflow from the system includes (1) Discharge to Constant Head Boundary, which is 138.7 MCM/year (3.8×10^5 m^3/day), (2) Groundwater outflow through River Leakage with value equal to 44.5 MCM/year (1.2×10^5 m^3/day), (3) Groundwater outflow by well pumpage with a value equal to 2.1 MCM/year (5.8×10^3 m^3/day) and groundwater outflow at the northern boundary of the model to the next catchment through Head dependent boundary which equals to 42.2 MCM/year (1.15×10^5 m^3/day). Generally, these values are somewhat different from the estimates made in the water balance of the conceptual model, which could be due to the larger aquifer thickness considered in the model and those parameters which are not considered in the model. Table 7.2 shows inflow and outflow components of the water balance and steady-state hydrologic budget of the study area calculated by the model.

Hydrologic budget component	Cubic meter per day(m^3/day)	Million cubic meter per year (MCM/year)
Inflow		
Recharge from precipitation	152086	55.5
Stream leakage to aquifer	413607	151
Inflow from Constant-head boundaries	58027	21.2
Total inflow	623720	227.7
Outflow		
Groundwater discharge to streams	121874	44.5
Pumpage and springs	5828	2.1
Outflow through General-head boundary	115724	42.2
Outflow to Constant-head boundaries	380054	138.7
Total outflow	623480	227.5
Budget error (inflow-outflow)	240	0.2
Percent discrepancy (%)	0.04	

Table 6.2 Model-calculated steady-state hydrologic budget

6.2 Model Sensitivity

Many assumptions and estimates are used in the design and construction of a groundwater flow model. To test the response of the calibrated model to a range of values for various input parameter, a sensitivity analysis is done. Sensitivity analysis can help determine which model parameters have the greatest effect on a model. Results of the analysis can guide future data collection efforts that will reduce model errors. It is done by varying the values of one input parameter while keeping all others constant.

Separate model simulations were made with varied input properties and the changes in simulated hydraulic head were recorded. The model is considered sensitive to a parameter when a change of the parameter value changes the distribution of simulated hydraulic head. When the model is sensitive to an input parameter, the value of that parameter within the model is more accurately determined during model calibration because small changes to the parameter value cause large changes in hydraulic head. When the model is insensitive to an input parameter, the value of that parameter within the model is more difficult to accurately determine from model calibration because large changes to the parameter do not cause large changes in hydraulic head.

Model sensitivity was determined for variations in hydraulic conductivity, pumpage and recharge. The results of the sensitivity analysis for this study were evaluated by calculating the Sum of Square Deviation between measured and simulated heads in the modeled area for a decrease or increase in percent, from the calibrated value, of that parameter. “Calibrated Model” at the center of the plot (Figure 7.1) represents the final model and the corresponding sum of square deviation, which is 958. The greater the deviations of the water level from its calibrated model value, the greater the sensitivity of the model to an increase (positive percent) or decrease (negative percent) for that parameter. To test the sensitivity of the above parameters, the calibrated values of each parameter were separately increased and decreased by 25, 50 and 75 percent and then simulated to see the resulting heads.

In the model, simulated water levels were most sensitive to the decrease in the recharge values, mainly beyond 50 percent. Compared to recharge, the mode is less sensitive to the decrease in hydraulic conductivity value. The model is relatively insensitive to changes in pumpage and increase in hydraulic conductivity and recharge.

Results of the sensitivity analysis show that small errors in estimating values of the aquifer properties to which the model is most sensitive, which in this case is recharge, can have a significant effect on the model simulation results. However, other properties such as pumpage can be varied in magnitude with little effect on the results.

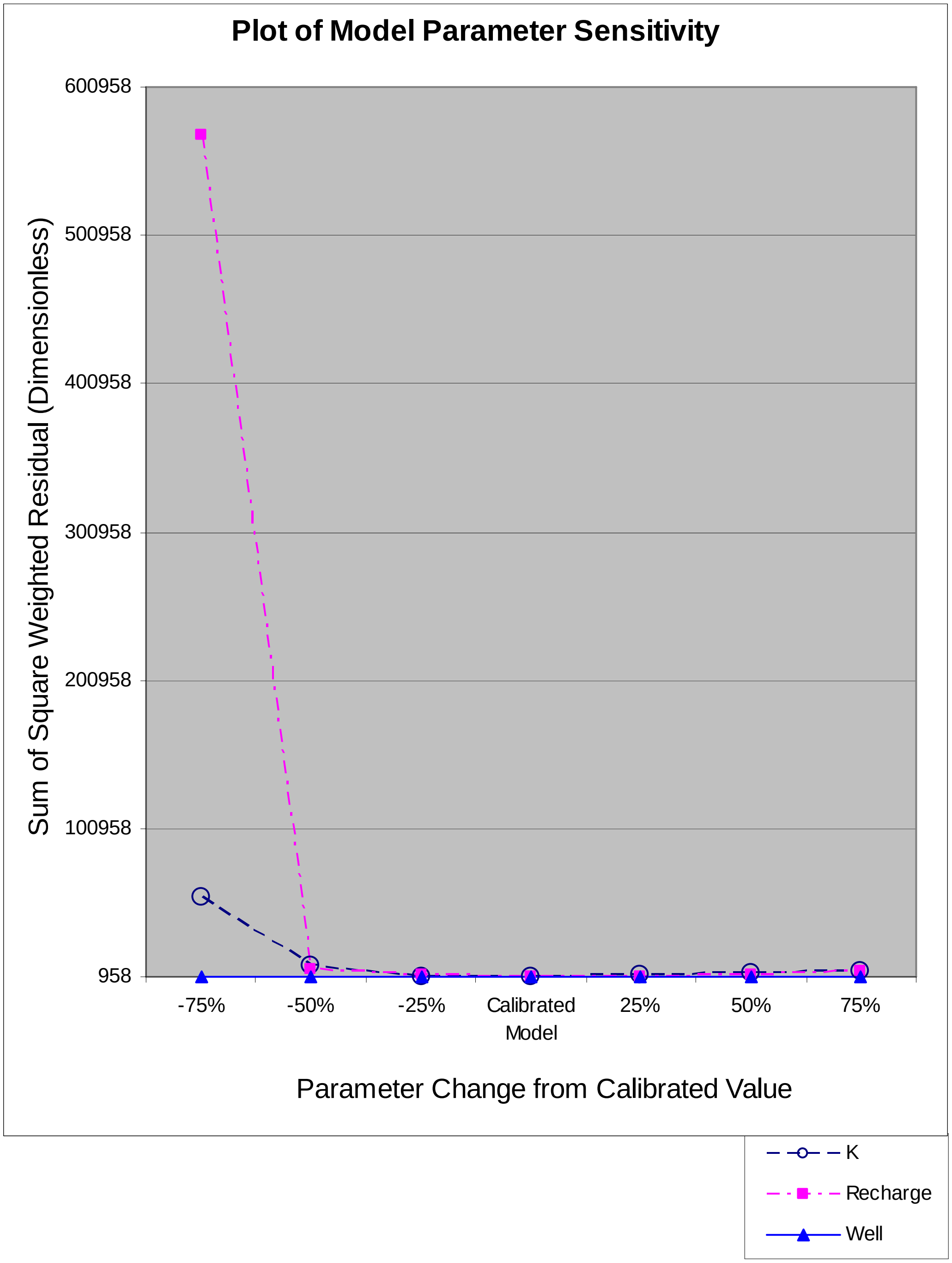

Fig. 6.4 Plot of model parameter sensitivity.

6.3 Scenario analysis

A calibrated flow model can be used as a tool to evaluate and compare the responses of an aquifer system to potential future stresses. Management actions involving changes in the quantity and distribution of pumpage or altered hydrologic conditions which could be drought conditions or conditions of altered recharge that may result, for example, from land-use changes can be simulated. The response of the aquifer-system can be compared to evaluate the effectiveness of these probable changes of stresses in such away that it satisfies management goals. Although water levels simulated for a given scenario may not accurately represent the values in the real system, the relative differences in water levels can be compared to provide useful information for planning and decision making. In this study, the model was used to simulate the aquifer-system response to increased withdrawals, decreased recharge and complete disappearance of Lake Shallo, for all scenarios, all model parameters were unchanged from those specified in the steady state simulation.

The first scenario, which is increment of pumpage by 50 percent, was selected to represent possible future changes in water use in the basin, or to investigate the effects of water-management practices that could mitigate potential adverse effects of increased water withdrawals. The heads calculated for this scenario shows a maximum decline of the water level by 0.36 meter and a minimum of 0.001 meter, where high yielding wells get the bigger decline of water level. The increase in pumpage decreases the groundwater outflow through river leakage and general-head boundary.

The second scenario simulated by the model is a decrease in recharge by 25 percent which could be the case if mild drought conditions were imposed on the aquifer system while water extraction is maintained at current rates. The decrease in recharge caused more inflow from constant-head boundaries as well as lower streamflow and groundwater discharge through the general-head boundary. Simulated drought condition showed a reduction of water level up to 18 meter and a minimum of 0.006. Large difference in water level occurs in the border of the caldera and the smaller differences result from wells found in the lacustrine sediment.

The third scenario is the removal of Lake Shallo, which is one of the two constant-heads in the model, from the model. This is in consideration of the disappearing Lake Shallo, which could be due to some climatological or landuse changes. The absence of this constant-head from the model causes an increase in water level particularly in wells found around this lake. The maximum increment is by 1.03 meter northwest of Lake Shallo and 0.002 meter the least increment in southeastern part of the catchment where some wells are not affected by this change. Simulation without Lake Shallo results in increased groundwater outflow to streams and adjacent Ziway-Shalla catchment through the general-head boundary. The increased water level and groundwater outflow to streams, resulting from disappearance of Lake Shallo, could be the cause to the increasing water level of Lake Awassa, which is fed by the perennial Tikur Wuha River.

Table 6.3 shows the resulting water balance from the three different scenarios with the steady state model calculated water balance. Values of the difference between the simulated water level in the scenarios and those specified in the steady state simulation are shown in Table 6.4.

Flow term	IN				OUT				IN-OUT			
	Calculated	Increased pumpage	Decreased recharge	Lake Shallo removal	Calculated	Increased pumpage	Decreased recharge	Lake Shallo removal	Calculated	Increased pumpage	Decreased recharge	Lake Shallo removal
Storage	0	0	0	0	0	0	0	0	0	0	0	0
Constant head	58027	58091	60884	57279	380054	378813	364884	261922	-322027	-320721	-304000	-204643
Wells	0	0	0	0	5828	8742	5828	5828	-5828	-8742	-5828	-5828
Drains	0	0	0	0	0	0	0	0	0	0	0	0
Recharge	152086	152086	114071	153611	0	0	0	0	152086	152086	114071	153611
ET	0	0	0	0	0	0	0	0	0	0	0	0
River leakage	413607	414546	423145	333983	121874	121260	113393	159934	291732	293286	309752	174049
Head dep bounds	0	0	0	0	115724	115670	113812	116948	-115724	-115670	-113812	-116948
Stream leakage	0	0	0	0	0	0	0	0	0	0	0	0
Interbed storage	0	0	0	0	0	0	0	0	0	0	0	0
Reserv. leakage	0	0	0	0	0	0	0	0	0	0	0	0
SUM	623720	624724	598100	544874	623480	624484	597916	544633	240	239	184	241
Discrepancy [%]	0.04	0.04	0.03	0.04								

Table 6.3 Water balance of the three scenarios and the steady state model in m^3/day.

				Difference Between Calibrated and Scenario Water Levels		
No.	Observation Name	Observed Value	Calibrated Value	Recharge Decrease by 25%	Pumpage Increase by 50 %	Removal of Lake Shallo
1	BH-3	1689	1684.5	0.217	0.277	-0.145
2	BH-4	1688	1687.7	0.071	0.017	-0.09
3	BH-5	1684	1685.5	0.329	0.073	-0.191
4	BH-6	1684	1685.5	0.319	0.069	-0.192
5	BH-7	1689	1687.0	0.161	0.034	-0.186
6	BH-9	1693	1683.7	0.164	0.006	-0.504
7	BH-12	1662	1671.8	0.469	0.03	-0.012
8	BH-13	1684	1682.1	0.41	0.072	-0.024
9	BH-15	1694	1689.8	1.943	0.051	-0.078
10	BH-24	1684	1684.5	0.147	0.005	-0.504
11	BH-25	1680	1683.5	0.205	0.008	-0.671
12	BH-26	1688	1681.3	0.289	0.011	-0.763
13	BH-27	1682	1686.7	0.034	0.001	-0.122
14	BH-28	1681	1689.1	0.006	0.001	-0.017
15	BH-29	1683	1683.7	0.035	0.001	-0.113
16	BH-32	1690	1684.8	0.219	0.36	-0.154
17	BH-33	1681	1676.4	0.443	0.021	-0.846
18	BH-39	1686	1684.2	0.164	0.038	-0.11
19	BH-40	1682	1686.0	0.078	0.024	-0.082
20	BH-41	1686	1686.0	0.098	0.034	-0.098
21	BH-42	1687	1683.4	0.152	0.033	-0.094
22	BH-47	1686	1685.0	0.35	0.056	-0.163
23	BH-48	1682	1685.7	0.443	0.062	-0.182
24	BH-52	1684	1681.3	0.214	0.021	-0.021
25	BH-56	1756	1751.4	14.281	0.011	-0.005
26	BH-69	1673	1672.0	0.566	0.022	-0.011
27	BH-77	1760	1753.5	15.096	0.009	-0.002
28	BH-78	1694	1697.8	1.986	0.142	-0.138
29	TW-0	1671	1667.7	0.208	0.007	-0.023
30	TW-1	1677	1675.7	0.079	0.002	-0.017
31	TW-2	1677	1671.7	0.128	0.004	-0.028
32	TW-3	1671	1667.9	0.208	0.007	-0.023
33	TW-4	1663	1670.1	0.323	0.013	-0.014
34	BH-C6	1680	1683.1	0.808	0.044	0
35	BH-C3	1687	1681.5	0.384	0.012	0
36	BH-C2	1685	1680.5	0.126	0.004	0
37	DBH-8	1777	1773.7	17.966	0.018	-0.009
38	BH-26-	1684	1682.1	0.41	0.072	-0.024
39	BH-8	1684	1681.1	0.134	0.013	-0.025
40	BH-7-	1696	1688.0	1.489	0.052	-0.083
41	BH-18	1686	1684.9	0.337	0.055	-0.16
42	BH-22	1693	1685.8	0.209	0.083	-0.164
43	BH-19	1682	1685.7	0.432	0.062	-0.184
44	BH-4-	1680	1677.9	0.658	0.049	-1.032
45	BH-10	1727	1724.4	8.62	0.156	-0.156
46	BH-C8	1698	1692.0	1.591	0.094	-0.22
47	BH-C9	1694	1694.4	1.947	0.108	-0.215
48	BH-C11	1698	1697.5	2.078	0.134	-0.158
49	BH-C12	1705	1698.9	1.491	0.103	-0.072

Table 6.4 Water level difference between simulated and those resulting from scenarios

6.4 Model Limitations

The steady-state flow model of the Lake Awassa Basin provides a regional-scale simulation of ground-water flow in the aquifer system of the study area. The model of the study area is a simplification of the “real world” ground-water system, which is the case of all groundwater-flow models, and has corresponding limitations in model precision and how the model can be used. For example, the MODFLOW model discretization or the node is 200 meter by 200 meter. As a result of this discretization, the conditions within the node, such as groundwater level and flow, are reduced to one average value for the entire node. Therefore, the model is not suitable for analysis of site-specific problems or issues. Hydrologic parameters and aquifer unit geometry in portions of the model area are not well known at this scale. For instance, aquifer thickness and hydraulic conductivity can change at intervals smaller than the current model resolution, especially where structures are extensive. Model uncertainty could also stem from random error in the field measurements used for model calibration, which is translated through model calibration to uncertainty in the calibrated parameter values.

Highly fractured and recent tectonic areas can have a widely variable hydraulic conductivity and although groundwater level and flow in these areas may be simulated indirectly, by increasing the hydraulic conductivity, the effects of these structures on the aquifer system may not be appropriately addressed with the models. Free flowing well and aquitard layers of clay and ash deposits exists on some parts of the area, thus reported water levels may not always be representative of the water levels of the regional aquifers simulated by the model. Calibration of the model possibly could be improved by breaking down further the spatial discretization of some parameters, such as hydraulic conductivity or recharge; however, without more field data, finer discretization was not justifiable. In this case, a simpler model adequately represented the system.

This numerical model is suitable as a tool to help understand the flow system, to confirm that previous estimates of aquifer properties are reasonable, and to estimate aquifer properties in areas without data. Limitations of the model should be taken into account when applying the model to water management. With additional data, further refinement of the model would be possible, which could improve the accuracy of model prediction of the effects of additional stresses on the system, such as increased withdrawals or drought.

CHAPTER SEVEN

Conclusion

The modeled aquifer is important water resource in the study area and is used extensively for irrigation, municipal, and domestic water supplies. A continued or increased withdrawal from the aquifer has the potential to affect water levels in this aquifer. A water resource tool is needed to evaluate management and environmental issues associated with the aquifer, such as planning for source-water protection, describing potential impacts of contamination, and estimating sustainable aquifer withdrawals. This thesis describes a conceptual model of groundwater flow in the aquifer and documents the development and calibration of a numerical model to simulate groundwater flow. Data for a two year period (from 2004 to 2006) and other source without specified time were analyzed for the conceptual model. Regional steady-state groundwater model was calibrated to average conditions from 2004 to 2006.

Arial recharge to the Lake Awassa basin aquifer occurs from precipitation and small quantity comes from Lake Awassa. Ground water from aerial recharge moves from areas of higher altitude toward streams that gain flow from the aquifer. Discharge from the aquifer occurs through discharge to perennial streams, well withdrawals and springs, and groundwater outflow from the catchment to the next Ziway-Shalla Basin. On a basin-wide basis, ground water evapotranspiration is likely to be small relative to the total water balance because the areas where it can occur is small; therefore it is not considered in the model.

In the study area, stream flow measurements under near base flow condition were conducted to obtain information describing streamflow gains. These measurements were taken during periods when direct runoff was not observed to occur and thus represent near base-flow conditions. Base flow separation made on Tikur Wuha River using mean monthly data from 1981 to 1998 show that annual base flow component of the Tikur Wuha River Discharge is 30.39MCM, which gives insight regarding the relative magnitude of groundwater discharge contributing to base flow.

Well withdrawals in the study area occur from irrigation, domestic, stock wells and industries and equals to 3.03 MCM per year. In the study area there are about 80 water points with location and pumping data, and all are active including deep boreholes, machine drilled shallow wells, hand dug wells, protected springs (large, medium and Small), and ponds. Groundwater outflow to the adjacent Ziway-Shalla catchment across the general-head boundary is 115724m^3/d (4.2×10^7 m^3/year), higher than the estimate made by Tenalem Ayenew (1998) and lower than estimate made by Yemane Gebreegziabher (2004).

Estimated horizontal hydraulic conductivity used for the numerical model ranged from 0.05 to 100 m/d, which were adjusted during model calibration. The initial recharge rates were given in five different zones ranging from 1.195×10^{-4} m^2/day to 2.787×10^{-4} m^2/day. Discharge rates in million cubic meters per year (MCM/year) for the steady-state simulation were 111 for base flow including Tikur Wuha River and 3.03 for outflow through wells and springs. Outflow to the neighboring catchment is simulated using general-head boundary.

Model calibration was accomplished by varying the model parameters within plausible ranges to produce the best fit between simulated and observed hydraulic heads in the Lake Awassa Basin. Steady state simulations representing average conditions over the two year analysis period were analyzed to determine the optimum combination of model parameters. Water level measurements for 49 wells that were used for estimation of groundwater level of the aquifer were considered for calibration of the steady state model.

Calibration criteria for the steady state simulation included: (1) generally matching the simulated groundwater surfaces and hydraulic gradients to those of the estimated one, and (2) matching hydraulic heads at 95 percent of the wells to within ±10 meter of the observed hydraulic heads. Results of the steady state simulations were within the calibration criteria established to meet the objectives of the study. Summary statistics on the difference between simulated and measured water levels show root mean square error (RMSE) of 4.42 meter and mean error of 1.4 meter, which indicates a model bias toward underestimating head values. A coefficient of correlation and variance equals to 0.98 and 19.5 respectively.

A sensitivity analysis was used to examine the response of the numerical model calibrated to steady state conditions to changes in model parameters including horizontal hydraulic conductivity, recharge, and pumpage, which were increased and decreased for the sensitivity analysis. The model was most sensitive to recharge and relatively less sensitive to horizontal hydraulic conductivity. Three scenarios including increased withdrawals by 50% result in decreased water level and groundwater outflow through river leakage and general-head boundary. Decrease in recharge by 25% caused more inflow from constant-head boundaries as well as lower streamflow and groundwater discharge through the general-head boundary and decrease water level up to 18 meter and a minimum of 0.006. Simulation without Lake Shallo results in increased groundwater level and groundwater outflow to streams and adjacent Ziway-Shalla catchment through the general-head boundary.

CHAPTER EIGHT

Recommendations

The Lake Awassa Basin groundwater flow model could be improved with additional hydrologic and geologic research, data collection and interpretation, and the use of additional MODFLOW options and packages. As new data become available, the model could be updated and recalibrated. The following is a list of research, data collection needs, and MODFLOW options that could enable refinements, and in turn increase the utility of the groundwater flow model.

- Within the study area, there are no observation wells (non-pumping wells) that are continuously monitored and evenly distributed in the catchment. Monitoring of water levels, especially in the rims of the caldera, would provide insight and valuable calibration points for future refinement of the model.

- The hydraulic relation between the perennial rivers and the groundwater system is not understood completely. For example, the present simulated flows assume that river sediments are uniform in all parts of the river, but the river actually consists of a variety of main channel and backwater sediments from the eastern highlands. Knowledge of the sediment hydraulic properties could allow a better estimation of the distribution of groundwater discharge into or from the river, and a more refined simulation of the groundwater-surface water interaction that results from existing and that could result from future high-capacity water withdrawals. Similarly, data are lacking for some river bottom thickness and river width. Furthermore, the model could be improved by additional data on the spatial distribution and flow duration of important streams in the area. More detailed study of the relation between selected streams and the groundwater system would be needed if the groundwater flow model is to approximate smaller-scale stream gains and losses accurately. Such a study could provide better estimates of hydraulic parameters of streambeds.

- The presence of some layers of clay and ash deposits in some parts of the study area, and the existence of highly fractured and recent tectonic areas can have a widely variable hydraulic conductivity within a short distance. As a result, there is a mixture of over- and under-simulated water levels that are often adjacent to each other. Moreover, hydrogeologic data, including measured water levels, are sparse in many areas, making interpretations using the model results difficult. A more comprehensive interpretation of the groundwater flow system in the catchment could be attained as new data become available.

- Many springs in the basin are not simulated explicitly because of the regional nature of the model. Thus, the relation of the springs to the groundwater flow system is poorly understood. An understanding of the spatial and temporal sources of water to springs could be gained by additional field investigation and modeling.

- The distribution and rate of recharge and effects of development on recharge are poorly understood, so further work on recharge would give better result. The boundary conditions should be better exploited since the area is highly affected by structures, especially in the southern part of the catchment.

- To increase the utility of the model, several features could be added. Climatic variations such as drought and significant recharge events can be simulated if the model is run in transient mode. The addition of MODFLOW packages such as Stream Routing would improve the calibration procedure and explicitly couple the groundwater to the surface water systems

Reference

Andrew J. Long, Larry D. Putnam, and Janet M. Carter (2003), Simulated Ground-Water Flow in the Ogallala and Arikaree Aquifers, Rosebud Indian Reservation Area, South Dakota, Water-Resources Investigations Report 03-4043.

B.D. Smerdon, K.J. Devito, C.A. Mendoza, (2005), Interaction of groundwater and shallow lakes on outwash sediments in the sub-humid Boreal Plains of Canada, Journal of Hydrology 314 (2005) 246–262.

Barry S. Smith (2005), Simulated Changes in Water Levels Caused by Potential Changes in Pumping from Shallow Aquifers of Virginia Beach, Virginia, Scientific Investigations Report 2005-5067.

Bernard N. Lenz, David A. Saad, and Faith A. Fitzpatrick (2003), Simulation of Ground-Water Flow and Rainfall Runoff with Emphasis on the Effects of Land Cover, Whittlesey Creek, Bayfield County, Wisconsin, Water-Resources Investigations Report 03–4130.

Brian P. Kelly (2004), Simulation of Ground-Water Flow, Contributing Recharge Areas, and Ground-Water Travel Time in the Missouri River Alluvial Aquifer near Ft. Leavenworth, Kansas, Scientific Investigations Report 2004–5215.

Carl S. Carlson and Forest P. Lyford (2005), Simulated Ground-Water Flow for a Pond-Dominated Aquifer System near Great Sandy Bottom Pond, Pembroke, Massachusetts, Scientific Investigations Report 2004-5269.

Caroline, L. T., Jean, J. T., Elisabet, G., Yves, T., Kiram, E. L., Jean, P. R., Marc, M., Francoise, G., Raymond, B., Michel, D., Bernard, G., Vincent, J., Endale Tamirat, Mohammed Ummer, Koen, M., Balemwal Atnafu, Tesfaye Cherenet, David, W., and Maurice, T. (1999) The Ziway-Shalla Lake basin system, MER, influence of volcanism, tectonics and climatic forcing on basin formation and sedimentation, Paleogeog,, Paleoclimatology, 150, 135-177.

Charles Berenbrock (2005), Simulation of Hydraulic Characteristics in the White Sturgeon Spawning Habitat of the Kootenai River near Bonners Ferry, Idaho, Scientific Investigations Report 2005–5110.

Charles Berenbrock and James P. Bennett (2005), Simulation of Flow and Sediment Transport in the White Sturgeon Spawning Habitat of the Kootenai River near Bonners Ferry, Idaho, Scientific Investigations Report 2005-5173.

D. Matthew Ely and Sue C. Kahle (2004), Conceptual Model and Numerical Simulation of the Ground-Water-Flow System in the Unconsolidated Deposits of the Colville River Watershed, Stevens County, Washington, Scientific Investigations Report 2004–5237.

Daryll A. Pope and Martha K. Watt (2004), Simulation of Ground-Water Flow in the Potomac-Raritan-Magothy Aquifer System, Pennsauken Township and Vicinity, New Jersey, U.S. Geological Survey Scientific-Investigations Report 2004-5025.

David A. Leighton and Steven P. Phillips (2003), Simulation of Ground-Water Flow and Land Subsidence in the Antelope Valley Ground-Water Basin, California, Water-Resources Investigations Report 03-4016.

David S. Brown and Timothy H. Raines (2002), Simulation of Flow and Effects of Best-Management Practices in the Upper Seco Creek Basin, South-Central Texas, Water-Resources Investigations Report 02–4249.

Dessie Nadaw (1997) Hydrogeology of Awassa area, Unpub. M. Sc. Thesis, AAU, Addis Ababa, 106pp.

Dorothy F. Payne, Malek Abu Rumman, and John S. Clarke (2005), Simulation of Ground-Water Flow in Coastal Georgia and Adjacent Parts of South Carolina and Florida— Predevelopment, 1980, and 2000, Scientific Investigations Report 2005-5089, Version 1.1.

Douglas K. Maurer (2002), Ground-Water Flow and Numerical Simulation of Recharge from Streamflow Infiltration near Pine Nut Creek, Douglas County, Nevada, Water-Resources Investigations Report 02–4145.

Ebinger, C., Yemane, T., Gidey Woldegebriel, Aronson, J. L. and Walter, R. C. (1993) Late Eocene-Recent volcanism and faulting in the southern MER, J. Geol. Soc. London, 150, 99-108.

Ethiopian Mapping Agency (1975) 1:50000 topographic maps, Addis Ababa, Ethiopia.

Ethiopian Mapping Agensy (1988) National Atlas of Ethiopia, Addis Ababa, Ethiopia.

Fetter, C. W. (1994) Applied hydrogeology, Mir publishing com., 691pp.

Frederick J. Tenbus and William B. Fleck (2001), Simulation of Ground-Water Flow and Transport of Chlorinated Hydrocarbons at Graces Quarters, Aberdeen Proving Ground, Maryland, Water-Resources Investigations Report 01-4106.

Freeze, R. A. and Cherry, J. A. (1997) Groundwater, Prentice-hall, Englewood Cliffs, N. J., USA, 604pp.

Gary J. Barton, Richard R. McDonald, Jonathan M. Nelson, andRandal L. Dinehart (2005), Simulation of Flow and Sediment Mobility Using a Multidimensional Flow Model for the White Sturgeon Critical-Habitat Reach, Kootenai River near Bonners Ferry, Idaho, Scientific Investigations Report 2005-5230.

Gidey Woldegebreil (1987) Volcanotectonic histery of the Central sector of the MER: A geochronological, geochemical and petrological approach, Unpub. Ph. D. Thesis, Clevland, Ohio, Case Western Reserve University, 410pp.

Gidey, Woldegebreil, Aronson, J. L. and Walter, R. C. (1990) Geology, Geochronology and Rift basin development in the Central sector of the MER, Geol. Soc. Am. Bul., 102, 439-458.

Hila Abboa, Uri Shavit, Doron Markel, Alon Rimmer (2003), A numerical study on the influence of fractured regions on lake/groundwater interaction; the Lake Kinneret (Sea of Galilee) case, Journal of Hydrology 283 (2003) 225–243.

J.F. Ruhl, and T.K. Cowdery (2004), Regional Ground-Water-Flow Models of Surficial Sand and Gravel Aquifers Along the Mississippi River Between Brainerd and St. Cloud, Central Minnesota, Scientific Investigation Report 2004-5087.

J.W. Grubbs (1995), Evaluation of Ground-Water Flow and Hydrologic Budget for Lake Five-O, A Seepage Lake in Northwestern Florida, Water-Resources Investigations Report 94-4145.

Janet M. Carter, Daniel G. Driscoll and Ghaith R. Hamade (2001), Estimated Recharge to the Madison and Minnelusa Aquifers in the Black Hills Area, South Dakota and Wyoming, Water Years 1931-98, Water-Resources Investigations Report 00-4278.

Jill N.Densmore (2003), Simulation of Ground-Water Flow in the Irwin Basin Aquifer System, Fort Irwin National Training Center, California, Water-Resources Investigations Report 02-4264.

John P. Hoffmann and S.A. Leake (2005), Simulated Water-Level Responses, Ground-Water Fluxes, and Storage Changes for Recharge Scenarios along Rillito Creek, Tucson, Arizona, Scientific Investigations Report 2004–5286.

John T. Atkins Jr., Jeffrey B. Wiley, and Katherine S. Paybins (2005), Calibration Parameters Used to Simulate Streamflow from Application of the Hydrologic Simulation Program-FORTRAN Model (HSPF) to Mountainous Basins Containing Coal Mines in West Virginia, Scientific Investigations Report 2005–5099.

John W. Fulton, Edward H. Koerkle, Steven D. McAuley, Scott A. Hoffman, and Linda F. Zarr (2005), Hydrogeologic Setting and Conceptual Hydrologic Model of the Spring Creek Basin, Centre County, Pennsylvania, Scientific Investigations Report 2005-5091.

Kari A. Winfield (2005), Development of Property-Transfer Models for Estimating the Hydraulic Properties of Deep Sediments at the Idaho National Engineering and Environmental Laboratory, Idaho, Scientific Investigations Report 2005-5114.

Leslie A. Desimone, Donald A. Walter, John R. Eggleston, and Mark T. Nimiroski (2002), Simulation of Ground-Water Flow and Evaluation of Water-Management Alternatives in the Upper Charles River Basin, Eastern Massachusetts, Water-Resources Investigations Report 02-4234.

Louis C. Murray, Jr. and Keith J. Halford (1999), Simulated Effects of Projected Ground-Water Withdrawals in the Floridan Aquifer System, Greater Orlando Metropolitan Area, East-Central Florida, Water-Resources Investigations Report 99-4058.

Lulseged Ayalew, Yamagishi, H. and Reik, G. (2004) Ground cracks in Ethiopian Rift Valley: Facts and uncertainities, URL: www.Sc.niigata-u.ac.jp/environment/as.html.

Lynette E. Brooks and James L. Mason (2005), Hydrology and Simulation of Ground-Water Flow in Cedar Valley, Iron County, Utah, Scientific Investigations Report 2005-5170.

Marijke van Heeswijk and Daniel T. Smith (2002), Simulation of the Ground-Water Flow System at Naval Submarine Base Bangor and Vicinity, Kitsap County, Washington, Water-Resources Investigations Report 02-4261.

Marshall W. Gannett and Kenneth E. Lite JR.(2004), Simulation of Regional Ground-Water Flow in the Upper Deschutes Basin, Oregon, Water-Resources Investigations Report 03-4195.

Mary P. Anderson and William W. Woessner (1992), Applied Groundwater Modeling, Simulation of Flow and Advective Transport, Academic Press, Inc. 381pp.

Melinda J. Chapman, Richard E. Bolich, and Brad A. Huffman (2005), Hydrogeologic Setting, Ground-Water Flow, and Ground-Water Quality at the Lake Wheeler Road Research Station, Scientific Investigations Report 2005–5166.

Mohr, P. (1960) Report on geological excursion through Southern Ethiopia, Bul. Geophy. Obser., AAU, 2, 9-19.

Mohr, P. (1967) Major volcano-tectonic lineament in the Ethiopian Rift system, Nature, 213, 664-665.

Mohr, P. (1968) Transcurrent faulting in the Ethiopian Rift system, Nature, 218, 938-941.

Mohr, P. (1987) Patterns of faulting in the Ethiopian Rift valley, Tectonophysics, 143, 169-179.

Mohr, P. A., Mitchel, J. G. & Raynolds, R. G. (1980) Quaternary volcanism and faulting at O'a caldera, Central Ethiopian Rift, Bul.geophy. obs., Addis Ababa, 3, 9-20.

Perry M. Jones (2005), Simulated Effects of Water-Level Changes in the Mississippi River and Pokegama Reservoir on Ground-Water Levels, Grand Rapids Area, Minnesota, Scientific Investigations Report 2005–5139.

Randall J. Hunt1, David A. Saad1, and Dawn M. Chapel (2003), Numerical Simulation of Ground-Water Flow in La Crosse County, Wisconsin, and into Nearby Pools of the Mississippi River, Water-Resources Investigations Report 03–4154.

Rochelle A. Nustad and Jerad D. Bales (2005), Simulation of Conservative-Constituent Transport in the Red River of the North Basin, North Dakota and Minnesota,2003-04, Scientific Investigations Report 2005–5273.

Rodney A. Sheets and Karen E. Bossenbroek (2005), Ground-Water Flow Directions and Estimation of Aquifer Hydraulic Properties in the Lower Great Miami River Buried Valley Aquifer System, Hamilton Area, Ohio, Scientific Investigations Report 2005-5013.

S. S. Sumioka and H. H. Bauer (2003), Estimating Ground-Water Recharge from Precipitation on Whidbey and Camano Islands, Island County, Washington, Water Years 1998 and 1999, Water-Resources Investigations Report 03-4101.

Scot K. Izuka and Delwyn S. Oki (2002), Numerical Simulation of Ground-Water Withdrawals in the Southern Lihue Basin, Kauai, Hawaii, Water-Resources Investigations Report 01-4200.

Susan S. Hutson, Eric W. Strom, David E. Burt, and Michael J. Mallory (2000), Simulation of Projected Water Demand and Ground-Water Levels in the Coffee Sand and Eutaw-McShan Aquifers in Union County, Mississippi, 2010 through 2050, Water-Resources Investigations Report 00-4268.

Tadesse Dessie and Zenaw Tessema (2003) Hydrogeology and Engineering geology of Awassa Lake catchment, Unpub. Report, Geological Survey of Ethiopia, Addis Ababa.
Tamiru Alemayehu (2003) Controls on the occurrence of cold and thermal springs in central Ethiopia, African Geoscience Review, Vol. 10, 3, 245-251.

Tenalem Ayenew (1998) The hydrogeological system of the Lake district basin, Ethiopia, Unpub. Ph.D. Thesis, ITC, Enschede, The Netherlands, 259pp.

Tenalem Ayenew (2001) Surface kinetic temperature mapping using satellite spectral data in Central Main Ethiopian Rift and adjacent Highlands, Sinet: Ethio. J. Sc., 24(2), 51-68.

Tenalem Ayenew (2003) Environmental isotope based integrated hydrogeological study of some Ethiopian Rift Lakes, Jour. of Radioanalytical and Nuclear chemistry, Vol. 257, 1, 11-16.

Tenalem, A. and Tamiru, A. (2001) Principles of hydrogeology, Department of Earth Sciences, AAU, Addis Ababa.

Tesfaye Cherenet (1982) Hydrogeology of Lakes region, Ethiopia (Lake Ziway, Langano, Abiyata, Shalla and Awassa), Unpub. Report, Ethiopian Institute of Geological Survey, 97pp.

Tesfaye Korme, Chorowicz, J., Collette, B. and Bonavia, F. F. (1997) Volcanic vents rooted on extension fractures and their geodynamic implications in the Ethiopian Rift, Jour. of Vol. & Geotherm. Res., 79, 205-222.

Thomas E. Reilly (2001), System and Boundary Conceptualization in Ground-Water Flow Simulation, Book 3 Applications of Hydraulics Chapter B8.

Timothy H. Raines and Roger M. Miranda (2002), Simulation of Flow and Water Quality of the Arroyo Colorado, Texas, Water-Resources Investigations Report 02–4110.

Water Works Design & Supervision Enterprise (1999) The study of Awassa Lake level rise, Interim Report, Addis Ababa, Vol. I-III , 265pp.

Yemane Gebreegziabher (2004) Assessment of the Water Balance of Lake Awassa Catchment, Ethiopia, Unpub, M.Sc. Thesis, ITC, Enschede, The Netherlands, 103pp.

Zemenu Geremew (2000) Engineering geology of Awassa area, Unpub. M. Sc. Thesis, Department of Earth Sciences, AAU, 132pp.

Appendix

Appendix I Summary of initial meteorological data

Year	Jan	Feb	Mar	Apr	May	Jun	Jul	Aug	Sep	Oct	Nov	Dec
1972	x	x	x	x	x	x	70.6	143.4	123.7	17.4	8.5	31.1
1973	17.9	7.4	x	65.9	148.2	83.4	116.4	181.5	82	33.9	0.7	6.2
1974	7.7	28.3	97.9	6.8	106.5	118.3	210	159.3	163.9	37.5	0	3.3
1975	10.2	36.5	34.2	103.6	98.4	88.4	175	119.7	107.8	46.7	5.7	0
1976	6.5	33	78	42.1	171	70.4	161.2	134.2	112.6	79.1	47.1	18.2
1977	87.1	53.2	37.9	94.7	113.6	108.1	123.5	120.7	130.4	222.9	122	12.1
1978	3.3	164.9	23.9	96.8	118.9	85.7	74.7	118.2	199.1	58.9	57.1	41.4
1979	65.9	37	53.3	99	121.5	66.6	126.3	136.4	158.8	86.1	0	27.3
1980	13.8	15.5	38.3	110.6	112.5	73.8	88.3	127.7	40.2	139.1	34	x
1981	x	25	198.7	135.9	48.3	127.2	132.9	155.9	157.3	52.4	7	x
1982	49.6	46.6	99.9	92.1	70.8	121.1	166.3	117.1	72.7	95.9	84.4	12.4
1983	60.5	47.9	56.3	186.2	239.4	76.1	102.8	125.9	153.9	90.6	14.2	6.4
1984	x	x	36.5	17.4	170.2	70.7	96.1	92.7	165.7	27.4	34.5	13.3
1985	9.2	x	75.7	201.9	93.3	106.9	146.1	80.7	116.4	50.2	12.8	8.3
1986	x	34.7	69.6	109.8	167.2	193	153.3	194.2	171.8	57.3	22.8	18.4
1987	0.1	11.8	151.4	127.8	230.8	58	97.3	108.1	68.8	100.1	0.4	4.1
1988	25.8	68.5	17.5	80.9	100.1	110.9	117.7	138.8	205	83.9	1.3	6.6
1989	38.8	49.9	62.8	191.8	95.2	123.8	78.1	86.4	166.3	44.7	22.3	50.2
1990	10.5	93.7	121.1	89.9	85.3	44.4	139.5	39.5	94.1	27.3	7.6	3.8
1991	12.3	90.6	87.4	48	129.5	116.7	109.2	90.6	104	21.6	12.2	44.8
1992	23.4	83.2	73	109	60.5	83	92.8	123.6	74.5	142.3	80.1	16.6
1993	101.6	109.1	22.3	104.9	165.3	46.7	54.7	130.8	47.8	130.8	10.5	3.9
1994	x	4.7	56.8	108.7	80.8	146.2	195.7	118.9	68.9	58.8	19.1	2.9
1995	0.8	21.4	61.8	156.1	43.6	118.7	175.7	134.7	166.8	22.3	18.3	84.2
1996	78.4	36.9	89.6	113.8	161.5	243.3	121.2	108.7	145	69.6	19.7	1.4
1997	23.4	1.7	75.1	125	73	111.2	98.6	113.9	118.9	157.1	132.2	24
1998	92	140	90.8	86.4	88.4	56	172.9	108.3	109.6	193.3	10.6	0
1999	19.8	0.4	105.5	27.1	64.7	99.8	135.1	83.8	115.4	120.4	20.1	16.8
2000	1.1	x	11	132	145.1	36.4	80	179.3	87.6	110.7	29	9.3
2001	1.8	39.9	122.7	67	233.7	137.5	93.5	131.7	89.7	80.2	2.6	21.3
2002	52.5	2.4	127.7	119.6	85.2	118.4	76.6	190.4	82.2	37.2	x	51.5
2003	30.4	2	78.2	179.1	40.4	110.5	74.5	76.1	85.7	56.4	6.2	51.8

Monthly rain fall data at Awassa station(mm)

Year	Jan	Feb	Mar	Apr	May	Jun	Jul	Aug	Sep	Oct	Nov	Dec
1975	9.4	9	8.2	6.2	7.2	6.5	3.8	3.4	4.9	7	9.3	9.8
1976	9.6	8.9	7.9	7.2	6.8	7.3	4.7	5.1	5.8	7.3	8.3	9.5
1977	7.4	8.4	7.8	6.4	6.9	5.9	4	5	5.3	5	8.5	9.6
1978	9.6	6.6	7	7.7	7.5	6.8	4	5.4	5.1	6.2	8.8	8.6
1979	6.5	8.1	7.4	7.5	6.9	7.4	5	6.1	5.6	7.2	9.7	9.1
1980	8.9	9.3	7.8	6.7	7.2	6.1	5.1	6.3	4.9	7.5	8.7	10
1981	9.6	8.9	5.8	5.6	7.6	7.9	4.6	5.5	4.6	7.8	9.6	9.5
1982	8.5	7.1	8.5	6.5	6.6	7	5	5	5.9	7.3	7.3	8.6
1983	9.2	8.2	8.1	6.3	6.6	7.2	5	3.7	5.3	8	8.7	8.6
1984	9.4	9.6	8.2	7.5	6.4	6.2	6	6.3	5.5	8.9	8.9	9.2
1985	9.3	8.6	8.2	5.7	6.9	7.7	4.8	5.3	5.7	7.1	8.6	9.5
1986	9.5	7.6	7.8	5.5	7.5	5.3	5.4	7	6.6	7.8	9.1	9.3
1987	x	8	x	7.3	6.3	7.2	7.1	6.6	6.2	x	9.7	10
1988	8.8	7.6	8.3	5.8	8.2	6.5	2.9	4.6	5.2	7.1	9.9	8
1989	8.5	8.4	7	5.9	7.9	7.1	3.8	5.9	5.2	x	8.5	7.6
1990	8.8	6	7.3	6.5	6.5	7.3	5.1	4.5	5.5	8	8.1	9.4
1991	8.4	7.3	7.1	7.5	7.4	6.5	3.7	4.1	5.8	7.6	8.2	8.2
1992	7.8	7.5	8.5	8.2	8.1	7.2	5.5	4.5	5.4	6.8	8.7	8.7

1993	7.7	7.2	9.2	6.4	6.8	6	4.3	5.4	x	x	x	x
1994	9.6	8.9	7.4	6.3	6.6	5.7	4	5.1	5.2	8.5	8.4	9.4
1995	9.7	7.6	7.3	5.9	7.9	7.7	4.1	4.8	6.4	2.9	9.5	8.5
1996	8.3	8.9	7.1	2.7	7.1	4.8	1.6	4.3	5.4	8	9.3	10.1
1997	X	10.4	8.3	6.4	6	6.8	5.5	6.6	7.1	7.1	6.8	8.6
1998	7.2	7.9	7.8	7.8	6.8	6.3	4.4	4.4	5.3	3.8	9.4	10
1999	9.4	9.7	6.7	6.9	7.5	7.1	4.6	5.9	6	5.1	8.6	9.9
2000	9.8	9.8	8.9	7	11.3	6.6	5.6	X	5.4	6.2	9.1	9.4
2001	8.8	9.1	6.5	6.9	7.5	5.8	5.5	5.2	5.8	6.8	9.1	9.7
2002	9	9.6	X	7.6	7.1	6.4	7.1	6.3	7.1	6.9	9.7	8.1
2003	9	9.5	8.3	6.8	7.8	4.5	7.3	5.3	x	x	x	x

Monthly sun shine hours data at Awassa station

Year	Jan	Feb	Mar	Apr	May	Jun	Jul	Aug	Sep	Oct	Nov	Dec
1973	x	1.5	1.7	1.6	1.5	1.6	1.5	1.4	1.1	1.1	1.3	1.5
1974	1.7	1.7	1.6	1.5	1.5	1.5	1.3	1.4	1.1	0.9	1.3	1.5
1975	1.4	1.6	1.5	1.4	1.4	1.6	1.3	1.4	1.1	1	1.2	1.5
1976	1.5	1.4	1.5	1.5	1.4	1.5	1.4	1.1	0.9	0.9	1	1.3
1977	1.4	1.4	1.5	1.4	1.4	1.3	x	x	1	0.9	1	x
1978	1.2	1.1	1.2	1.3	1.1	1.4	1.5	1.1	1	0.9	1	1.1
1979	1.2	1.1	1.2	1.2	1.2	1.4	1.1	1.1	1.4	0.9	1	1.1
1983	x	x	x	x	x	1.2	1.3	1.1	1	0.9	0.9	1.2
1984	1.4	1.5	1.5	1.4	1.4	1.6	1.6	1.1	1	1.1	1.1	1.4
1985	x	x	x	x	x	x	x	x	x	x	x	x
1990	1	1.1	0.9	0.9	1.1	1.4	1.3	1.1	0.9	0.8	x	0.9
1991	x	x	x	x	x	x	x	x	x	x	x	x
1992	x	x	x	x	x	x	x	x	x	x	x	x
1993	x	x	x	x	x	x	x	1.1	0.8	0.5	0.7	0.9
1994	1	1.1	1	0.8	0.8	1.1	0.8	1.4	0.7	0.5	1.2	0.9
1995	0.9	0.9	1	0.8	1.1	1.2	0.9	0.9	0.7	0.6	0.7	0.7
1996	0.8	0.8	0.8	0.8	0.7	1	1	0.7	0.7	0.5	0.6	0.7
1997	0.8	1	0.9	0.7	0.9	0.9	1.1	0.9	0.7	0.5	0.5	0.6
1998	0.6	0.6	0.6	0.7	0.8	1.1	1	1	0.7	0.5	0.5	0.8
1999	0.9	0.7	0.6	0.8	1	1.1	1	0.9	3.2	0.5	0.7	0.8
2000	0.9	1.1	0.8	0.8	0.7	1.2	1.2	0.9	0.7	0.6	0.6	0.7
2001	0.8	0.7	0.7	0.7	0.8	0.9	0.9	0.8	0.6	0.6	0.6	0.7
2002	0.7	0.8	0.6	0.7	1	1.1	1.1	0.8	0.7	0.6	0.8	0.8
2003	0.8	0.8	0.8	0.6	0.8	1	0.9	0.9	x	x	x	x

Monthly wind speed data at Awassa station(m/s) at 2m above the ground

Year	Jan	Feb	Mar	Apr	May	Jun	Jul	Aug	Sep	Oct	Nov	Dec
1986	230.5	211.7	240.9	176.6	113.2	140.2	124.4	146.9	162.6	172.4	192.5	188.1
1987	239.8	200.1	179.9	179.9	190.7	173.8	173.5	172.2	154.5	175.1	208.0	230.5
1988	212.9	203.3	243.2	192.1	206.3	171.4	110.2	146.6	140.2	164.5	273.5	193.0
1989	196.4	126.3	227.6	155.4	219.6	183.5	129.4	153.7	166.6	179.7	189.1	158.6
1990	180.5	143.6	167.2	173.9	187.0	187.7	149.7	143.2	158.4	198.6	198.5	224.2
1991	222.3	191.0	178.1	154.6	153.0	159.1	120.6	142.1	149.4	183.6	178.5	188.1
1992	152.5	120.9	254.4	216.2	182.0	185.6	178.4	160.7	135.3	155.5	177.6	184.4
1993	182.7	163.6	237.1	170.0	200.1	161.5	153.2	161.7	148.2	169.7	212.3	234.8
1994	250.1	242.9	235.3	195.1	179.7	179.7	121.6	141.5	162.4	206.1	231.3	248.9
1995	267.2	242.5	240.0	182.0	202.9	198.8	122.6	107.5	118.5	139.2	158.5	202.6
1996	148.1	183.0	159.1	140.3	129.4	109.4	108.3	118.0	103.2	149.9	164.8	176.5
1997	169.6	211.9	203.1	126.6	169.0	143.9	146.3	153.9	114.3	128.1	110.2	139.9
1998	207.6	129.8	149.3	152.5	143.5	141.2	113.8	103.8	110.7	93.4	144.9	170.3
1999	177.8	196.8	150.3	162.0	160.1	152.4	128.9	133.5	109.8	103.3	153.8	171.8
2000	201.5	201.8	205.2	158.2	131.2	142.4	127.6	117.1	113.0	113.9	139.0	158.8
2001	156.4	172.7	137.9	144.2	130.3	105.3	104.7	114.1	109.5	120.9	154.5	170.3
2002	153.8	164.2	149.6	144.7	136.5	131.5	147.3	103.8	111.5	136.4	183.6	138.5
2003	160.3	174.0	149.3	109.9	145.4	130.2	96.8	117.5	129.5	156.6	190.4	183.0

Monthly pan evaporation data at Awassa station(mm)

Year	Jan	Feb	Mar	Apr	May	Jun	Jul	Aug	Sep	Oct	Nov	Dec
1988	93	87	88	92	77	90	97	97	96	96	91	85
1989	84	82	86	97	95	99	93	93	97	95	84	96
1990	89	92	96	94	98	92	90	92	94	92	86	78
1991	81	90	92	94	95	x	94	94	97	94	84	86
1992	88	94	89	90	96	92	93	x	95	96	92	93
1993	93	94	89	94	95	93	91	89	95	96	90	82
1994	73	73	88	91	95	92	94	93	94	93	93	86
1995	76	82	92	95	96	93	93	93	97	93	92	91
1996	92	84	96	96	97	94	92	94	96	96	92	83
1997	87	70	82	95	97	93	91	88	92	92	91	87
1998	92	89	90	88	91	89	87	88	92	90	88	79
1999	81	70	91	91	94	90	91	92	95	94	87	85
2000	72	64	68	86	95	90	92	91	95	94	91	91
2001	78	81	88	92	93	92	92	93	95	93	83	x
2002	88	74	93	91	92	91	90	91	94	93	79	89
2003	86	82	83	90	93	x	x	x	x	x	x	x

Monthly relative humidity(%) at 06:00 at Awassa

1988	44	46	37	51	60	63	73	67	63	57	38	39
1989	44	46	37	59	55	66	68	63	65	49	42	58
1990	43	56	58	56	58	56	65	66	57	46	42	36
1991	40	51	55	49	59	65	71	64	61	44	38	41
1992	37	54	44	49	57	60	66	x	62	59	49	51
1993	55	59	37	55	62	67	65	63	61	56	41	39
1994	35	34	43	52	58	65	73	68	61	46	46	41
1995	36	49	50	60	56	60	68	68	64	51	43	47
1996	54	40	52	59	63	71	71	70	66	52	44	40
1997	47	33	43	60	57	65	67	60	57	55	56	49
1998	57	55	51	43	60	59	68	69	62	62	42	34
1999	39	30	53	45	56	60	71	62	59	64	42	40
2000	35	31	33	48	63	60	66	64	62	59	50	45
2001	46	44	56	53	62	64	68	67	61	54	40	x
2002	46	34	50	47	61	62	57	63	58	45	35	51
2003	47	36	44	56	56	x	x	x	x	x	x	x

Monthly relative humidity(%) at 12:00 at Awassa

1988	39	45	54	57	65	61	70	72	79	73	37	36
1989	34	40	51	66	55	63	67	65	79	61	47	52
1990	55	66	65	58	63	55	74	64	68	49	40	31
1991	32	44	57	59	63	61	69	67	75	49	34	39
1992	42	51	45	53	65	58	63	x	78	68	53	44
1993	50	54	37	66	66	63	63	64	71	71	42	33
1994	28	28	50	53	68	58	69	72	73	52	42	34
1995	28	36	51	66	64	60	66	65	72	56	40	47
1996	51	35	62	69	75	69	68	70	73	57	43	36
1997	41	22	39	68	63	66	65	66	70	68	62	47
1998	52	51	60	54	61	57	64	64	69	68	42	30
1999	32	22	54	54	60	59	64	65	71	66	42	36
2000	27	23	28	59	65	57	62	61	75	71	54	40
2001	35	35	62	64	64	65	64	66	73	67	35	x
2002	36	22	52	51	61	59	52	64	66	53	29	49
2003	38	31	50	60	56	x	x	x	x	x	x	x

Monthly relative humidity(%) at 18:00 at Awassa

Year	Jan	Feb	Mar	Apr	May	Jun	Jul	Aug	Sep	Oct	Nov	Dec
1988	29.2	29.6	31	28.4	27.5	24.9	22.8	23.8	24.8	25.9	27.9	27.8
1989	27.7	28	28.7	26.2	27.1	23.9	23.3	24.3	24.4		27.3	27.1
1990	28.6	27.7	27.5	27.8	27.2	26.1	24.4	24.4	25.8	28	29.5	29.2
1991	30.4	29	27.7	29.3	28	26.1	23.3	25.1	26	27.8	29.2	28.1
1992	29.4	28.5	30.5	29.8	27.5	26.3	24.3	23.8	24.9	25.8	27.1	28.5
1993	27.6	26.9	30.8	27	26.9	25.2	24.4	24.8	25.7	26.9	30.1	29.7
1994	30.5	32	30.9	29	26.7	24.7	23.5	25	26.2	28.3	28.3	29.3
1995	30.4	30.7	30	27.3	27.9	27	24.3	24.7	25.9	27.5	29.3	29.3
1996	28.3	30.8	29.4	27.7	26.8	23.8	23.8	24.3	25.2	27	28.1	28.6
1997	28.9	30.3	30.8	26.9	27.5	25.7	23.9	25.5	26.7	26.5	26.4	27.3
1998	27.7	28.7	29	29.7	27.3	26.3	24.3	23.6	25.4	25.3	27.5	28.1
1999	29.1	31.4	28.1	29.1	27.2	26.1	23.6	25	25.6	25	27.2	28
2000	29.5	30.7	31.8	28.8	26.1	25.7	24.7	24.8	25.1	25.6	27.2	28.3
2001	28.7	29.1	28.4	28.4	26.9	24.8	24.4	24.5	25.9	26.7	28.2	28.6
2002	28.2	30.9	28.8	28.6	27.1	25.7	25.6	25.4	26.1	28.3	29.8	28.9
2003	28.4	31.3	30.6	28.1	28.3	25.6	24.2	24.8	25.9	28.2	29.3	27.2

Monthly maximum temperature data at Awassa station(^{0}C)

1988	11.3	13.6	12.2	14.6	13.9	13.9	14.7	14.1	13.9	12.8	6.5	7.9
1989	9.5	10.7	12.7	13.5	12.4	13.1	14.1	13.4	12.9	x	9.7	13
1990	9	14.1	12.6	13.7	13.3	12.8	14.2	10.7	12.9	10.5	10.4	9
1991	11.9	12.5	13.4	12.8	14	15.3	14.3	13.7	12.9	9.5	9.4	9.6
1992	12.4	13.6	12.8	14.3	13.5	14	13.9	14.5	12.7	13.1	10.5	11
1993	12.1	12.3	9.7	14.1	14	14.2	13.9	13.7	12.9	13.2	9.3	9.2
1994	9.7	12	13	13.8	14.3	14.5	14.3	14.7	14	10.1	10	8.9
1995	9.8	12.7	13.6	14.9	13.1	13.6	14.2	14.5	13	12.3	8.4	10.6
1996	12.1	10.5	13	14	14.1	14.3	14.5	14.4	13.7	10.9	8.8	9.6
1997	12.4	10	13.3	13.9	13.2	13.6	14.2	14.2	13.2	13.6	13.8	14.4
1998	13.3	14.3	13.9	14.8	15.7	14.7	15.7	15.9	14.5	14.4	8.9	7.8
1999	10.2	9.9	13.8	12.5	13.6	14	14.2	13.7	13.8	14	9.3	9.3
2000	9.6	10.6	11.1	14.1	14	13.7	14.3	14	13.4	14	10.5	9.7
2001	11.5	11.1	13.7	14.4	14.1	15	14.7	15	13.1	13.8	10.3	10.9
2002	12.4	11.8	14	13.5	14.8	14.5	14.4	14.2	13.4	12.8	9.8	13.2
2003	11.8	11.6	13.2	14.3	14.2	14.3	14.5	14.5	14	11.9	11.2	10.4

Monthly minimum temperature data at Awassa station(^{0}C)

Appendix II Summary of initial hydrological data

year	Jan	Feb	Mar	Apr	May	Jun	Jul	Aug	Sep	Oct	Nov	Dec
1969	x	x	x	x	x	x	x	x	x	1.11	1.04	0.89
1970	0.78	0.69	0.70	0.73	0.74	0.73	0.72	0.81	1.08	1.37	1.41	1.26
1971	1.10	0.97	0.81	0.77	0.79	0.89	1.07	1.19	1.30	1.45	1.55	1.48
1972	1.38	1.32	1.26	1.25	1.36	1.43	1.48	1.62	1.83	1.95	1.86	1.71
1973	1.58	1.40	1.23	1.06	1.02	1.01	1.00	1.17	1.28	1.34	1.25	1.07
1974	0.78	0.69	0.70	0.73	0.74	0.73	0.72	0.81	1.08	1.37	1.41	1.26
1975	1.10	0.97	0.81	0.77	0.79	0.89	1.07	1.19	1.30	1.45	1.55	1.48
1976	1.38	1.32	1.26	1.25	1.36	1.43	1.48	1.62	1.83	1.95	1.86	1.71
1977	1.58	1.40	1.23	1.06	1.02	1.01	1.00	1.17	1.28	1.34	1.25	1.07
1978	1.59	1.47	1.45	1.37	1.38	1.42	1.45	1.62	1.88	2.17	2.22	2.14
1979	2.04	2.01	1.93	1.90	1.86	1.87	1.89	1.99	2.12	2.26	2.26	2.14
1980	2.04	2.01	1.93	1.90	1.86	1.87	1.89	1.99	2.12	2.26	2.26	2.14
1981	1.18	1.02	0.95	1.03	1.02	0.97	0.95	1.07	1.26	1.47	1.43	1.28
1982	1.15	1.04	0.96	0.89	0.85	0.81	0.87	0.94	0.99	1.09	1.19	1.18
1983	1.08	1.01	0.90	0.83	0.97	1.29	1.39	1.51	1.81	2.10	2.17	2.14
1984	1.98	1.78	1.61	1.47	1.39	1.41	1.39	1.40	1.45	1.48	1.39	1.23
1985	1.06	0.89	0.72	0.72	0.88	0.93	0.97	1.10	1.19	1.30	1.45	1.39
1986	1.10	0.92	0.83	0.78	0.76	0.90	1.09	1.28	1.46	1.70	1.74	1.61
1987	1.40	1.23	1.19	1.17	1.25	1.62	1.72	1.75	1.81	1.89	1.88	1.73
1988	1.57	x	1.32	1.20	1.19	1.17	1.22	1.48	1.86	2.24	2.36	2.20
1989	2.06	1.96	1.85	1.83	1.82	1.93	1.96	1.96	2.02	2.17	2.17	2.11
1990	2.02	1.96	1.98	2.07	2.13	2.10	2.08	2.11	2.11	2.18	2.10	1.92

1991	1.77	1.65	1.60	1.56	1.57	1.57	1.59	1.62	1.67	1.71	1.60	1.47
1992	1.32	1.27	1.18	1.10	x	x	1.14	1.25	1.48	1.80	2.01	2.00
1993	1.92	1.93	1.83	1.74	1.82	1.93	1.97	2.03	2.09	2.22	2.34	2.23
1994	2.06	1.89	1.76	1.67	1.70	1.69	1.78	2.08	2.30	2.37	2.30	2.14
1995	1.95	1.81	1.72	1.71	1.73	1.67	1.68	1.73	1.94	2.02	1.94	1.81
1996	1.72	1.58	1.49	1.49	1.60	1.91	2.27	2.54	2.82	3.06	3.05	2.90
1997	2.74	2.58	2.41	2.38	2.37	2.36	2.46	2.57	2.62	2.75	3.02	3.13
1998	3.10	3.08	3.12	3.05	3.06	3.07	3.09	3.21	3.31	3.58	3.80	3.70
1999	3.53	3.36	3.27	3.17	3.08	3.01	2.99	3.05	3.05	3.22	3.29	3.17
2000	x	x	x	x	2.58	2.47	2.40	2.38	2.44	2.62	2.71	x
2001	x	x	x	2.22	2.26	2.40	2.52	2.65	2.85	3.02	3.09	3.01
2002	2.88	2.71	2.64	2.63	2.60	2.59	2.55	2.63	2.74	2.73	2.61	2.46
2003	2.35	2.21	2.09	2.04	2.12	x	x	x	x	x	x	x

Mean monthly water level of Awassa Lake(m)

year		**Jan**	**Feb**	**Mar**	**Apr**	**May**	**Jun**	**Jul**	**Aug**	**Sep**	**Oct**	**Nov**	**Dec**
1985	I	0.217	0.140	0.078	0.016	1.432	1.857	1.130	1.725	4.730	4.420	1.087	0.331
	II	0.280	0.154	0.126	0.027	2.860	3.300	2.060	2.170	7.560	7.240	1.430	0.461
	III	0.154	0.126	0.029	0.005	0.004	0.413	0.200	1.280	1.900	1.600	0.743	0.200
1986	I	x	0.160	0.199	0.319	0.995	5.400	4.850	5.200	4.000	5.050	x	x
	II	x	0.186	0.271	0.512	2.200	7.800	5.270	5.860	6.060	6.940	x	x
	III	x	0.142	0.160	0.214	0.526	2.460	4.430	3.300	2.740	2.780	x	x
1987	I	0.381	0.207	0.340	1.095	3.483	4.300	1.973	1.399	2.742	2.556	1.504	0.788
	II	0.499	0.238	0.643	1.660	6.370	6.560	2.310	2.030	3.440	3.030	2.000	1.030
	III	0.246	0.193	0.207	0.643	1.720	2.000	1.540	1.050	2.030	2.030	1.050	0.597
1988	I	0.513	0.397	0.424	0.435	0.594	1.141	2.682	5.347	6.423	5.613	3.603	1.817
	II	0.582	0.436	0.499	0.540	0.674	1.570	4.660	5.790	7.010	7.010	4.900	2.390
	III	0.448	0.358	0.358	0.347	0.473	0.401	1.570	4.900	5.790	4.900	2.500	1.600
1989	I	1.374	1.107	0.971	1.050	1.395	2.853	2.239	2.358	3.660	4.477	2.592	1.663
	II	1.570	1.230	1.010	1.280	1.960	3.890	2.620	2.950	4.660	4.960	3.790	1.840
	III	1.260	1.010	0.945	0.674	0.707	2.030	1.930	1.900	2.240	3.890	1.870	1.570
1990	I	1.457	1.356	2.902	5.300	3.507	1.917	1.852	2.632	2.869	5.915	4.339	1.133
	II	1.570	1.540	4.430	5.930	4.660	2.500	2.950	2.780	4.380	7.170	7.170	1.300
	III	1.280	1.230	1.600	4.490	2.540	1.090	0.905	2.580	2.500	4.540	1.350	0.965
1991	I	0.847	0.607	0.452	1.225	3.521	1.334	2.503	3.700	4.527	5.182	3.438	1.971
	II	0.965	0.707	0.526	3.080	4.660	2.130	3.400	4.100	4.100	5.520	5.020	2.310
	III	0.707	0.526	0.337	0.246	2.310	0.945	0.867	3.400	4.840	4.900	2.310	1.430
1992	I	0.778	0.305	0.233	0.319	1.140	1.645	2.165	2.969	6.501	8.050	5.610	1.864
	II	1.430	0.358	0.254	0.401	2.280	2.170	2.620	4.660	7.240	8.660	8.740	2.820
	III	0.358	0.254	0.207	0.262	0.242	1.260	1.600	2.170	4.660	7.320	2.860	1.280
1993	I	1.090	0.766	0.504	0.420	1.420	3.630	4.450	4.300	5.020	5.900	4.540	3.840
	II	1.260	0.925	0.612	0.582	2.350	4.320	5.080	4.900	5.590	6.200	5.590	4.780
	III	0.925	0.627	0.424	0.358	0.582	2.390	3.790	3.940	4.260	5.590	3.740	2.860
1994	I	2.180	x	0.336	0.625	1.000	1.680	2.820	5.530	6.110	4.040	2.830	2.210
	II	2.860	x	0.448	0.829	1.330	2.170	3.790	6.420	6.780	4.660	3.490	2.420
	III	1.380	x	0.271	0.473	0.643	1.330	2.200	3.890	4.720	3.490	2.420	1.960
1995	I	1.740	1.440	0.411	0.959	x	2.460	2.830	3.630	4.440	4.780	6.020	6.860
	II	1.930	1.540	0.965	1.720	x	3.490	3.490	4.160	4.660	5.400	6.710	7.320
	III	1.540	1.030	0.238	0.317	x	1.680	2.500	2.780	4.210	4.210	5.580	5.930
1996	I	x	x	x	1.710	x	6.870	5.900	5.870	6.210	7.670	6.290	4.800
	II	x	x	x	1.930	x	8.480	8.220	6.780	6.780	8.740	7.480	5.660
	III	x	x	x	1.410	x	5.270	4.050	4.320	5.520	6.420	5.720	3.890
1997	I	3.290	2.580	2.150	1.719	2.200	2.359	2.030	2.306	2.546	3.948	5.028	6.032
	II	3.840	2.660	2.500	2.200	2.460	2.600	2.540	2.660	2.820	4.720	5.790	6.200
	III	2.660	2.500	1.720	1.540	2.100	2.130	1.780	1.870	2.310	2.620	4.260	5.790
1998	I	6.876	6.629	3.979	1.738	3.490	7.113	7.222	5.700	5.980	8.009	x	x
	II	7.480	7.560	5.520	2.460	5.660	7.970	8.050	5.990	6.860	8.220	x	x
	III	6.270	5.660	1.840	1.380	2.540	5.720	6.060	5.270	5.270	6.710	x	x